Synthetic efforts towards an analog of the SPM PD1$_{\text{n-3 DPA}}$

Daniel Haga Hasselstrøm

Dissertation for the degree of Master of Pharmacy

Department of Pharmaceutical Chemistry

School of Pharmacy

Faculty of Mathematics and Natural Sciences

UNIVERSITY OF OSLO

May 2016

Synthetic efforts towards an analog of the SPM PD1$_{n-3 \text{ DPA}}$

Daniel Haga Hasselstrøm

Dissertation for the degree of Master of Pharmacy at

Department of Pharmaceutical Chemistry
School of Pharmacy
Faculty of Mathematics and Natural Sciences

UNIVERSITY OF OSLO

May 2016

Supervisors

Trond Vidar Hansen

Anders Vik

Marius Aursnes

2016

Synthetic efforts towards an analog of the SPM PD1$_{\text{n-3 DPA}}$

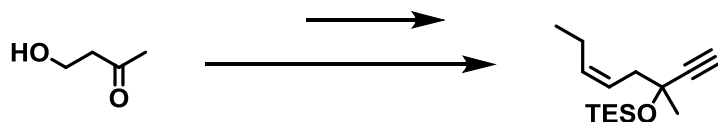Daniel Haga Hasselstrøm

Acknowledgements

Abstract

Chronic inflammation is involved in a number of severe diseases, including cancer, asthma, cardiovascular diseases, Alzheimer's and Parkinson's diseases. A series of oxygenated derivatives of polyunsaturated fatty acids such as eicosapentaenoic acid, docosahexaenoic acid and n-3 docosapentaenoic acid have been found to play an essential role in the inflammatory process. These derivatives have been coined specialized pro-resolving mediators because of their potent capabilities of resolving inflammation, a trait that enables them to be used as pharmaceuticals for the prevention and treatment of several diseases in which the inflammatory process is involved.

Protectin $D1_{\text{n-3 DPA}}$ is a pro-resolving mediator derived from n-3 docosapentaenoic acid, which exhibits very potent anti-inflammatory and pro-resolving actions. Because of its chemical instability and short metabolic half-life *in vivo* though, its applications as a potential drug are severely limited. It is thought that structural modifications of the compound may lead to new analogs with increased chemical and metabolic stability, while still retaining the desirable biological activities.

The synthetic efforts discussed in this thesis resulted in the successful synthesis of one analog of protectin $D1_{\text{n-3 DPA}}$. Remaining work includes a final step in order to prepare the other desired analog discussed in this thesis. Biological studies of the prepared analog will be performed in order to evaluate its anti-inflammatory and pro-resolving actions.

Graphical abstract

The ω-fragment

The middle fragment
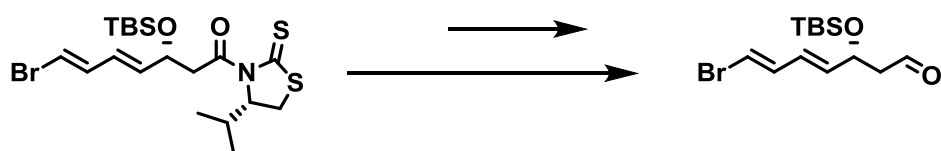
The α-fragment
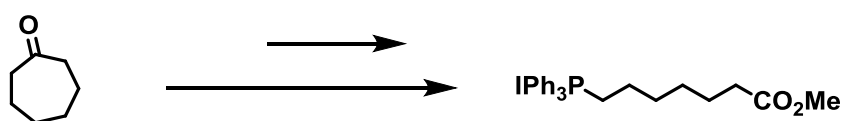
Assembly of the fragments

1)   IPh₃P⌒⌒CO₂Me   **+**   Br⌒ TBSO ⌒CHO

OTBS

Br⌒⌒⌒CO₂Me

2) OTBS
Br⌒⌒⌒CO₂Me   **+**   TESO⌒⌒≡

OH

HO⌒⌒C≡C⌒⌒ MeO₂C⌒⌒ - - - → OH HO₂C⌒⌒ OH

VIII
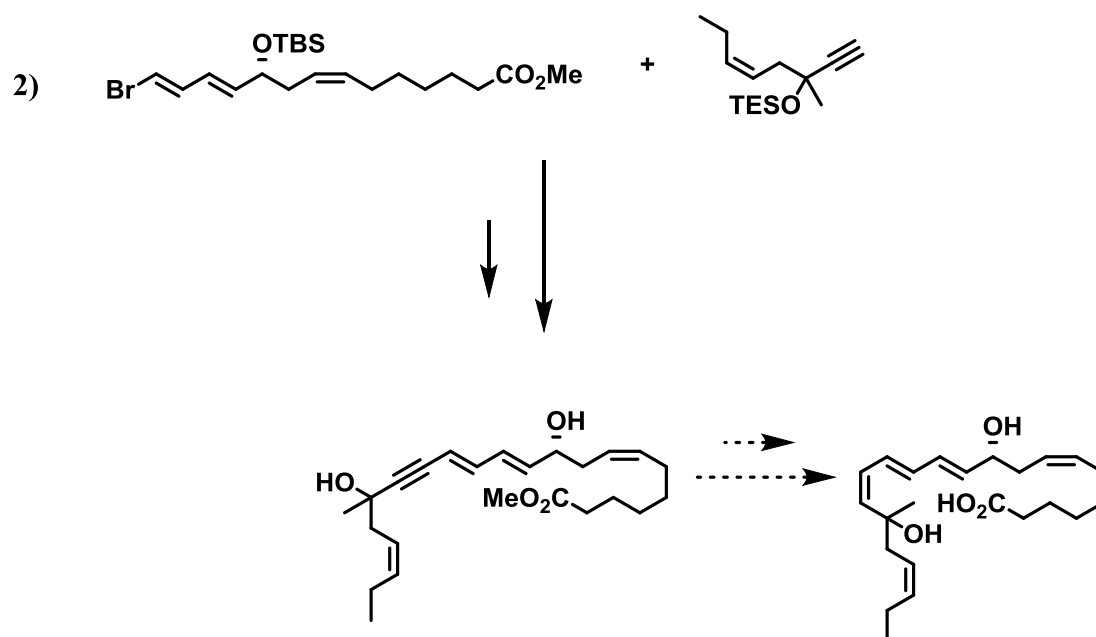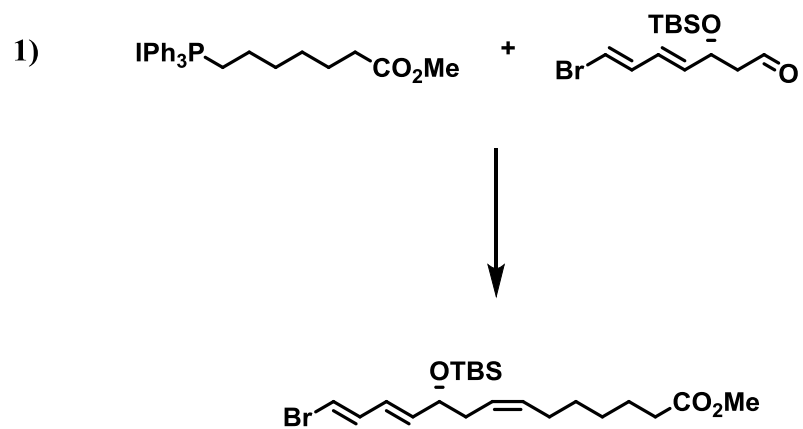
List of abbreviations

AA   Arachidonic acid ((5Z,8Z,11Z,14Z)-eicosatetraenoic acid)

CAM   Cerium Ammonium Molybdate

COX   Cyclooxygenase enzyme

DHA   Docosahexaenoic acid ((4Z,7Z,10Z,13Z,16Z,19Z)-docosahexaenoic acid)

DIBAL-H   Diisobutyl aluminium hydride

n-3 DPA   Docosapentaenoic acid ((7Z,10Z,13Z,16Z,19Z)-docosapentaenoic acid)

DMSO   Dimethyl sulfoxide

EPA   Eicosapentaenoic acid ((5Z,8Z,11Z,14Z,17Z)-eicosapentaenoic acid

GPCR   G-protein coupled receptor

HMPA   Hexamethylphosphoramide

KHMDS   Potassium *bis*(trimethylsilyl)amide

LO   Lipoxygenase enzyme

LT   Leukotriene

LX   Lipoxin

MaR1   Maresin 1

*m*CPBA   *meta*-Chloroperbenzoic acid

NaHMDS   Sodium *bis*(trimethylsilyl)amide

PCTR   Protectin conjugates in tissue regeneration

PD1   Protectin D1

$PD1_{\text{n-3 DPA}}$ Protectin $D1_{\text{n-3 docosapentaenoic acid}}$

PG	Prostaglandin
PMN	Polymorphonuclear neutrophil
PPAR	Peroxisome proliferator-activated receptor
PUFA	Polyunsaturated fatty acid
RvD	Resolvin of the D-series
RvE	Resolvin of the E-series
SPM	Specialized pro-resolving mediator
TBAF	Tetrabutylammonium fluoride
TBS	*tert*-Butyldimethylsilyl
TES	Triethylsilyl
THF	Tetrahydrofuran

Table of contents

1　Introduction

1.1　Background

1.1.1 ω-3 PUFAs and health

Polyunsaturated fatty acids (PUFAs) of the ω-3 group, such as eicosapentaenoic acid (**1**, EPA) and docosahexaenoic acid (**2**, DHA) are essential fatty acids that our human body cannot biosynthesize itself, but has to be provided by dietary consumption.[1] Their structures are depicted in Figure 1. These PUFAs are abundantly found in oily fish such as salmon and mackerel, and are widely used as dietary supplements.[2]

EPA (**1**)　　　　　　　　　　　DHA (**2**)

Figure 1. Structures of the ω-3 PUFAs EPA (**1**) and DHA (**2**)

For a long time an association has been observed between regular consumption of such ω-3 PUFAs and prophylactic and therapeutic effects in several health disorders.[3] This association is especially pronounced for inflammation,[4] autoimmune diseases,[4] cardiovascular diseases,[5,6] neurodegenerative diseases like Parkinson's and Alzheimer's diseases,[7] type-2 diabetes[8] and several forms of cancer.[9]

The Norwegian pharmaceutical company Pronova Biopharma, now part of the chemical producer BASF,[10] specializes in research, development and production of drugs derived from marine ω-3 PUFAs. They have developed the drug Omacor®, with the active pharmaceutical ingredients (APIs) being the ethyl esters of EPA (**1**) and DHA (**2**). Omacor® has shown to be effective in reducing serum levels of triglyceride and very-low-density lipoprotein. High levels of these are associated with increased risk of developing cardiovascular disease, and Omacor® is approved for the treatment of high levels of triglycerides (hyperglyceridemia), and for secondary prevention after myocardial infarction.[11]

Until recently, no molecular basis for the mechanism of action of ω-3 PUFAs had been established. Recent efforts by Serhan and collaborators have provided compelling evidence for the existence of metabolites of these PUFAs[12-15] that were found to function as exceptionally potent mediators down-regulating the inflammatory process.[15]

1.1.2 Inflammation

Inflammation is an innate, protective host response to tissue damage or invasion by pathogens. It is primarily a beneficial response with the main purpose of eliminating pathogens and restoring the function and structure of the affected tissue.[16,17] There are five classical cardinal signs of inflammation: Pain, heat, redness, swelling and loss of function. These symptoms arise from chemotactic and vasodilating mediators in the affected tissue. The inflammatory response is categorized as either acute or chronic.[17]

Initiation of the acute inflammatory response involves phospholipase enzymes acting on phospholipids in cell membranes, releasing arachidonic acid (**3**, AA). This ω-6 PUFA is then converted into pro-inflammatory lipid mediators such as prostaglandins (PGs) and leukotrienes (LTs), see Figure 3. By acting on their respective G protein-coupled receptors (GPCRs) they promote vasodilation, opening of tight junctions in the endothelium and production of inflammatory chemokines and cytokines. These actions promote the recruitment of polymorphonuclear neutrophils (PMNs) to the affected tissue. These PMNs are capable of phagocytosis, ingesting microorganisms or particles. Recruitment of leukocytes and increased biosynthesis of LTs and PGs result in what is known as acute inflammation.[15,16]

Arachidonic acid (**3**)

Prostaglandin E$_2$ (**4**)   Prostaglandin D$_2$ (**5**)

Leukotriene C$_4$ (**6**)
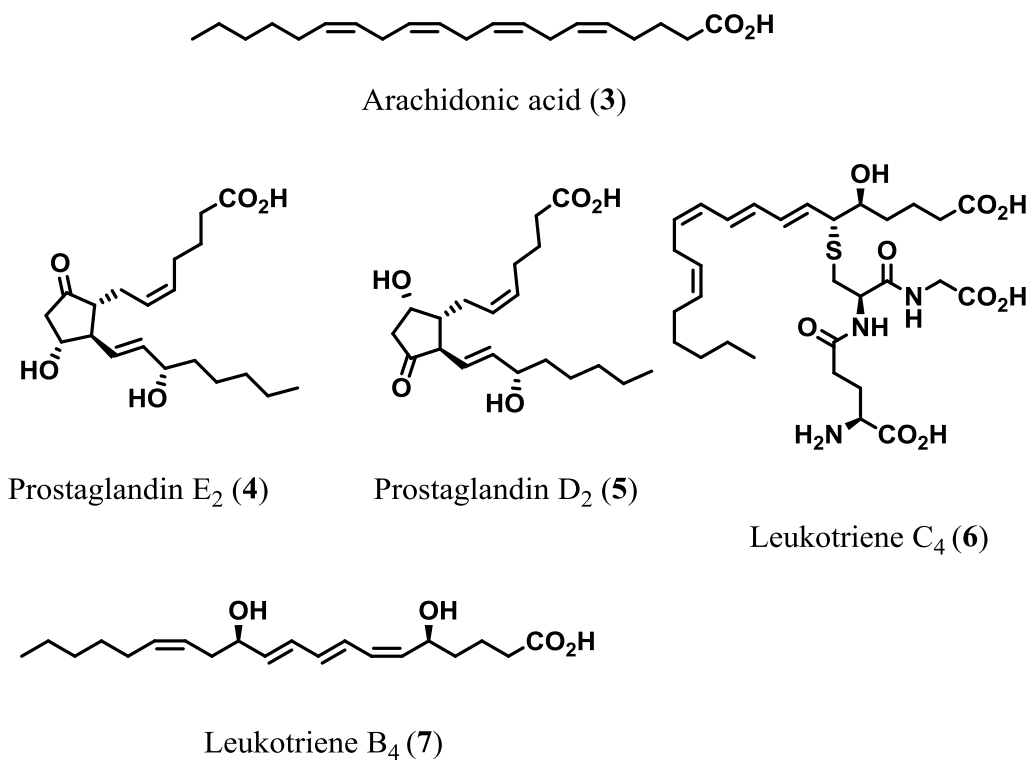
Leukotriene B$_4$ (**7**)

Figure 3. Structure of arachidonic acid (**3**) and some examples of prostaglandins and leukotrienes derived from it.

Although beneficial to host health if properly regulated, acute inflammation is not sustainable over long periods of time and has to be terminated. Termination of the inflammatory process is known as resolution of inflammation.[16,18] Resolving inflammation is of crucial importance for re-establishing homeostasis subsequent to injury or infection. If acute inflammation is not resolved, increasing levels of PMNs, LTs, PGs and debris lead to a condition of chronic inflammation.[15,17] This type of inflammation can ultimately lead to fibrosis of the affected tissue, and is linked to a number of chronic diseases such as asthma, diabetes, cardiovascular diseases, cancer, age-related macular degeneration, Alzheimer's and Parkinson's diseases.[17,19-21]

Resolution of inflammation is characterized by cessation of PMN-recruitment, reduction in the release of cytokines and chemokines, blocking the actions of PGs and LTs, and the recruitment of monocytes. These monocytes differentiate into macrophages, which remove cell debris, foreign material and apoptotic PMNs by a process called efferocytosis.[15,16]

Until recently, resolution of inflammation was hypothesized to be a passive process. There is now strong evidence supporting the notion that resolution is actually an active process,[22] initiated by several classes of compounds, including proteins, peptides, acetylcholine and other neuropeptides, adenosine and gaseous mediators like CO and H_2S.[18] Recent efforts by the Serhan group at Harvard Medical School have shown that resolution is also initiated by a lipid mediator class switching from pro-inflammatory PGs and LTs to a novel class of compounds called SPMs.[14,23] They will be discussed in more details later. An overview of the acute inflammatory process and resolution of inflammation is portrayed in Figure 4.
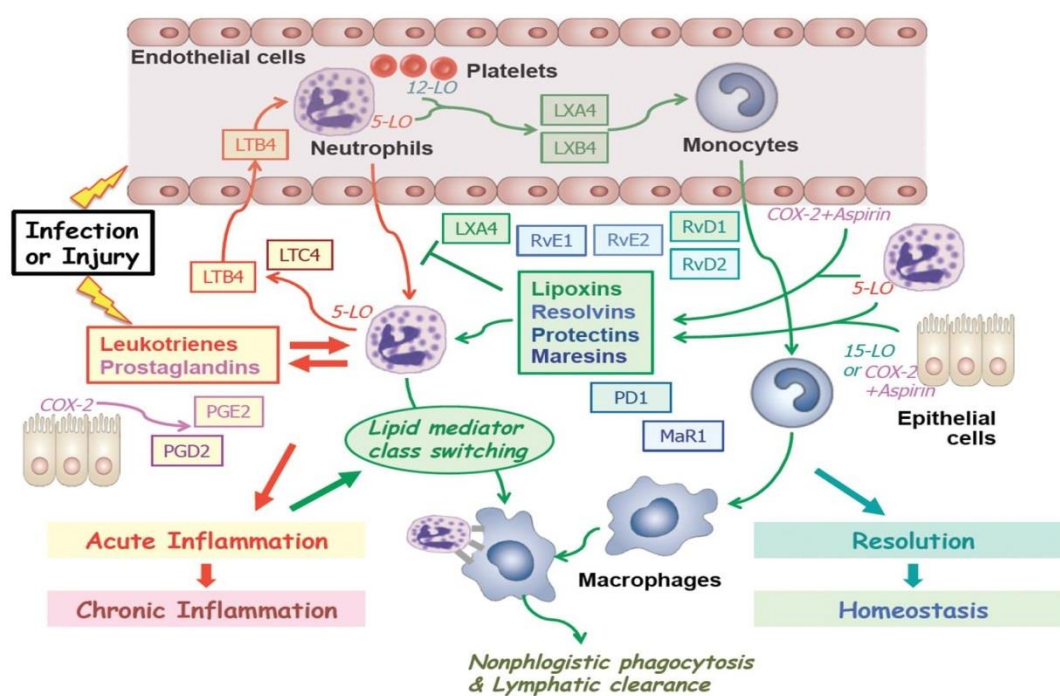
Figure 4. Initiation of the acute inflammatory process, and the role of specialized, oxygenated lipid mediators in resolution inflammation Adapted from reference.[15]

1.1.3 Oxygenases

Arachidonic acid (AA, **3**) is as mentioned an important precursor for key pro-inflammatory mediators. AA is converted to these mediators through the initiation of several biosynthetic pathways involving several different oxygenase enzymes, a class of enzymes which catalyse oxidation of their substrates. [15]

The enzymes responsible for the conversion of AA (**3**) into prostaglandins are called cyclooxygenases (COX).[24] The isoform COX-2 is of particular importance, since an active process of inflammation induces this particular isoform of the enzyme. COX-2 catalyses the generation of an intermediate PGH_2, which is further transformed into prostaglandin E_2 and D_2 (PGE_2 (**4**) and PGD_2 (**5**)). Formation of leukotrienes from AA is mediated through another group of oxygenases which are named lipoxygenases (LO), specifically 5-LO.[15,24] There are several important lipoxygenases involved in the inflammatory process, and they are named after which position of AA they transfer oxygen to.[24] Great efforts have been made in developing drugs which target pro-inflammatory pathways and receptors. Several pharmaceuticals such as COX-inhibitors,[25-27] LT antagonists[28] and LO inhibitors[29] (Figure 5) have been developed and are currently in clinical use against an array of inflammatory diseases.

Ibuprofen (**8**)   Acetylsalicylic acid (**9**)

Celecoxib (**10**)

Montelukast (**11**)   Zileuton (**12**)
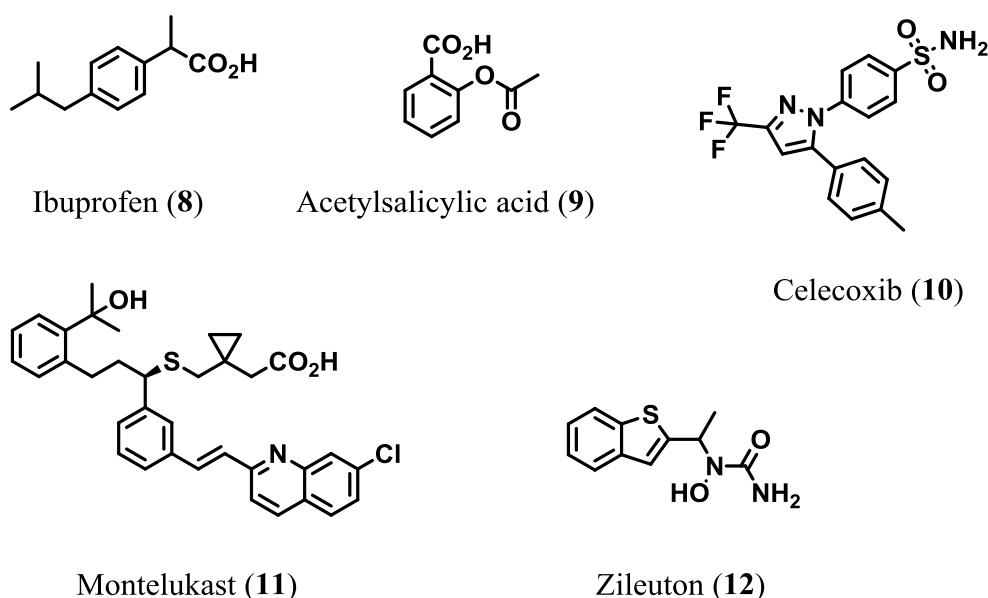
Figure 5. The non-selective COX-inhibitors ibuprofen (**8**) and acetylsalicylic acid (**9**), the selective COX-2 inhibitor celecoxib (**10**), the LT-antagonist montelukast (**11**) and the 5-LO inhibitor zileuton (**12**).

In addition to its important involvement in the biosynthesis of pro-inflammatory mediators, AA is a known precursor of lipid mediators which promote resolution of inflammation. This group is formed through the enzymatic actions of LOs, and have been named lipoxins (LXs).[30] The lipoxins will be discussed in more detail in section 1.1.4. Figure 6 portrays a schematic outline of the oxygenase-driven biosynthetic pathways from AA.

Arachidonic acid (AA)

COX-2   5-LO   12/15-LO

PGH$_2$ **LTA$_4$**   **15S-HETE**

15-LO   5-LO

PGD$_2$ **PGE$_2$**   **LTB$_4$**   **LTC$_4$**   **LXA$_4$**
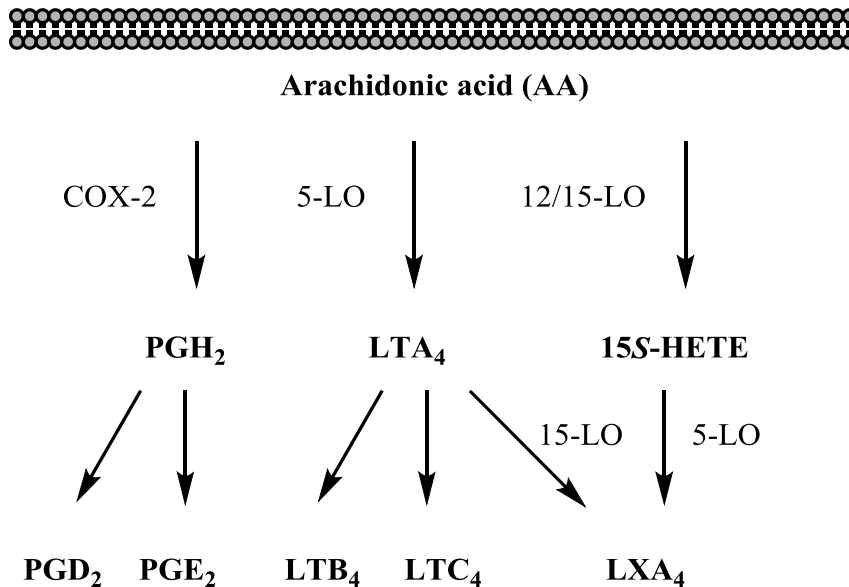
Figure 6. Biosynthetic cascade of selected lipid mediators derived from arachidonic acid through different oxygenase enzymes.

Arachidonic acid (**3**) is thus clearly capable of forming both anti-inflammatory and pro-resolving lipid mediators through the enzymatic actions of different oxygenases. Recent endeavours by Serhan and collaborators have revealed that biosynthetic pathways that follow the same principles and usually the same enzymes also exist for the ω-3 PUFAs, such as DHA, EPA and n-3 DPA. The new resulting lipid mediators formed from these PUFAs show potent pro-resolving and tissue-protective properties. Together with the lipoxins, the name specialized pro-resolving mediators (SPMs) has been given to these mediators.[14,15,23,30-32]

1.1.4 Specialized pro-resolving mediators (SPMs)

As mentioned, Serhan and co-workers discovered a novel class of oxygenated PUFAs with anti-inflammatory and pro-resolving abilities.[15] These compounds were coined specialized pro-resolving mediators (SPMs), and include the resolvins, the protectins and the maresins. The resolvins derived from the ω-3 polyunsaturated fatty acid EPA are named resolvins (Rv) of the E-series (RvE), while those derived from DHA are named resolvins of the D-series (RvD). Other SPMs derived from DHA are the maresins and protectins.[15] Even more recent studies have revealed the existence of novel mediators derived from n-3 docosapentaenoic

acid (n-3 DPA) as well, including members of the maresin, resolvin and protectin classes. Their biological activities have been partly investigated *in vitro* and *in vivo*, and found to be comparable to those of their DHA-derived counterparts with regard to anti-inflammatory and pro-resolving potential.[32] At large, the newly discovered SPMs have been revealed to be very potent, showing pro-resolving biological actions in the nanomolar and even picomolar range, in several *in vitro* cell types and *in vivo* animal studies against numerous inflammatory diseases.[13] SPMs mediate their biological actions through agonism on several newly discovered GPCRs, such as ChemR23 and GPR32, the known lipoxin receptor ALX, as well as antagonism on the leukotriene B$_4$ receptor BLT1.[15] The biosynthesis, metabolism and biological actions of the different groups of SPMs have been investigated, and these studies will be discussed below. As the protectins, especially those derived from n-3 DPA, are of special importance for this master's thesis; they are to be discussed in detail in section 1.1.5.

E-series resolvins

So far, six RvEs have been identified (RvE1-6).[14] The biosynthesis of RvE1 (**13**) and RvE2 (**14**) begins with the enzymatic actions of cytochrome P450 enzymes or acetylated COX-2 on EPA (**1**), see Figure 7. In the presence of aspirin, the COX-2 enzyme becomes acetylated, thus altering its enzymatic activity. These pathways both generate an 18*R*-hydroperoxide intermediate, called 18*R*-HpEPE (**15**), which in turn is reduced by a peroxidase into the alcohol 18*R*-HEPE (**16**). 5-LO then catalyzes another lipoxygenation in order to produce a 5-hydroperoxide (**17**). Transformation to the epoxide (**18**) followed by enzymatic hydrolysis generates resolvin E1 (**13**), while a peroxidase catalyzes the reduction of the hydroperoxide into resolvin E2 (**14**).[15]
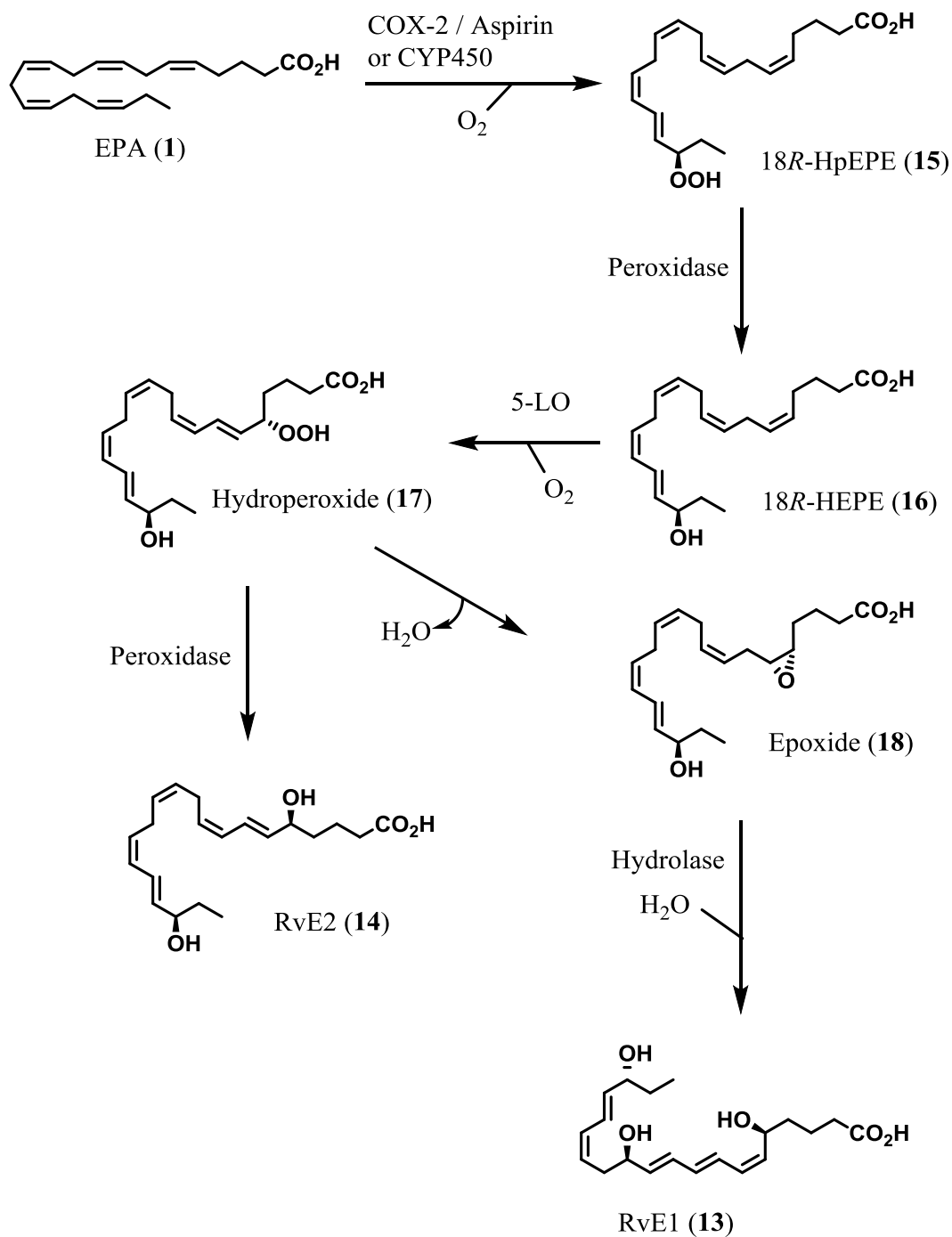
Figure 7. Biosynthetic pathways for RvE1 (**13**) and RvE2 (**14**).

Two major *in vivo* studies have been performed in order to evaluate the pro-resolving actions of RvE1. Mice with zymosan-induced periodontitis were injected with 100 ng of either RvE1 or the clinically used COX-2 inhibitor indometacin, and the results showed that RvE1 was twice as effective in inhibiting leukocyte recruitment in this disease model.[33] The other

disease model studied was a cytokine-induced dorsal air pouch, where injection of 100 ng RvE1 gave equivalent reduction of PMN infiltration as 1.0 mg of aspirin, clearly demonstrating the superior potency of the former substance.[15] Other pro-resolving actions demonstrated by RvE1 include prevention of periodontitis and bone-destruction, reducing pain caused by inflammation, and stimulating macrophage-mediated efferocytosis.[15]

The metabolome of RvE1 has been characterized by utilizing LC-MS/MS experiments, revealing that at least four different metabolic pathways exist in mammalian tissue (Figure 8).[34] These pathways seem to be specific for different types of species, organs and cell types. ω- and ω-1 oxidations are two important pathways, leading to 19- and 20-hydroxylated metabolites. Furthermore, a pathway involving eicosanoid oxidoreductases has been identified. The oxidoreductase enzymes catalyze oxidation of alcohol groups into the corresponding ketones, which may then be followed by reduction of an adjacent conjugated double bond. This ketone may then be reduced back into an alcohol. Not all of these pathways lead to inactive metabolites, but the ω-1 hydroxylated metabolite (**19**) as well as 10,11-dihydro-RvE1 (**24**) have shown to be practically without biological effects.[34]
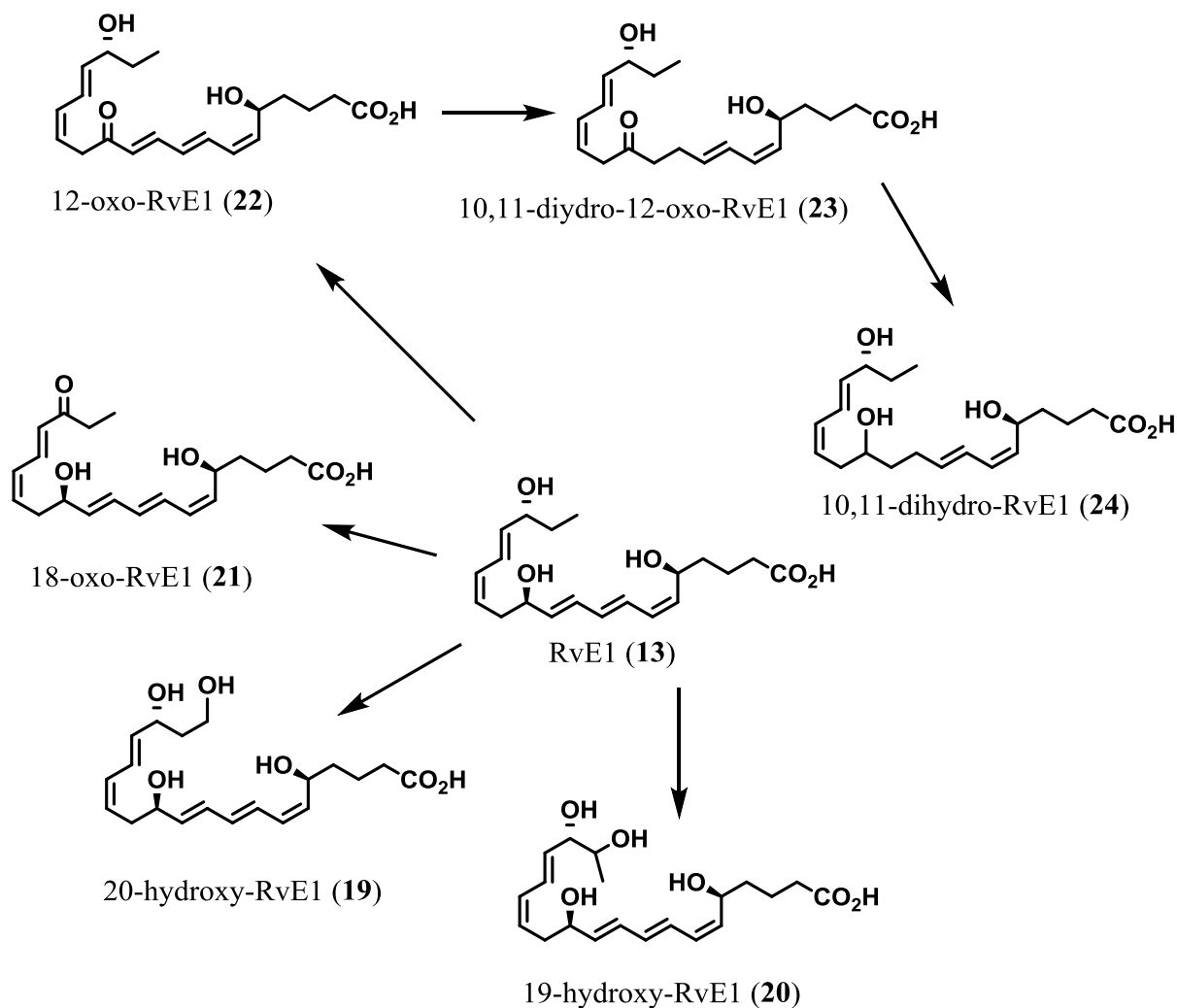
Figure 8. Metabolic pathways for RvE1 (**13**).

D-series resolvins

Currently, six RvDs have been identified (RvD1-6).[15] The biosynthetic pathways for resolvin D1 (**25**, RvD1) and resolvin D2 (**26**, RvD2) involve a transformation of DHA (**2**) into the hydroperoxide 17*S*-HpDHA (**27**) by 15-LO, followed by formation of 17*S*-HpDHA (**28**). This is followed by another lipoxygenation by 5-LO, generating the hydroperoxide (**29**). The hydroperoxide is further converted into an epoxide intermediate (**30**), and the trihydroxylated resolvins RvD1 (**25**) and RvD2 (**26**) are then formed by enzymatic hydrolysis of said epoxide.[14,15]
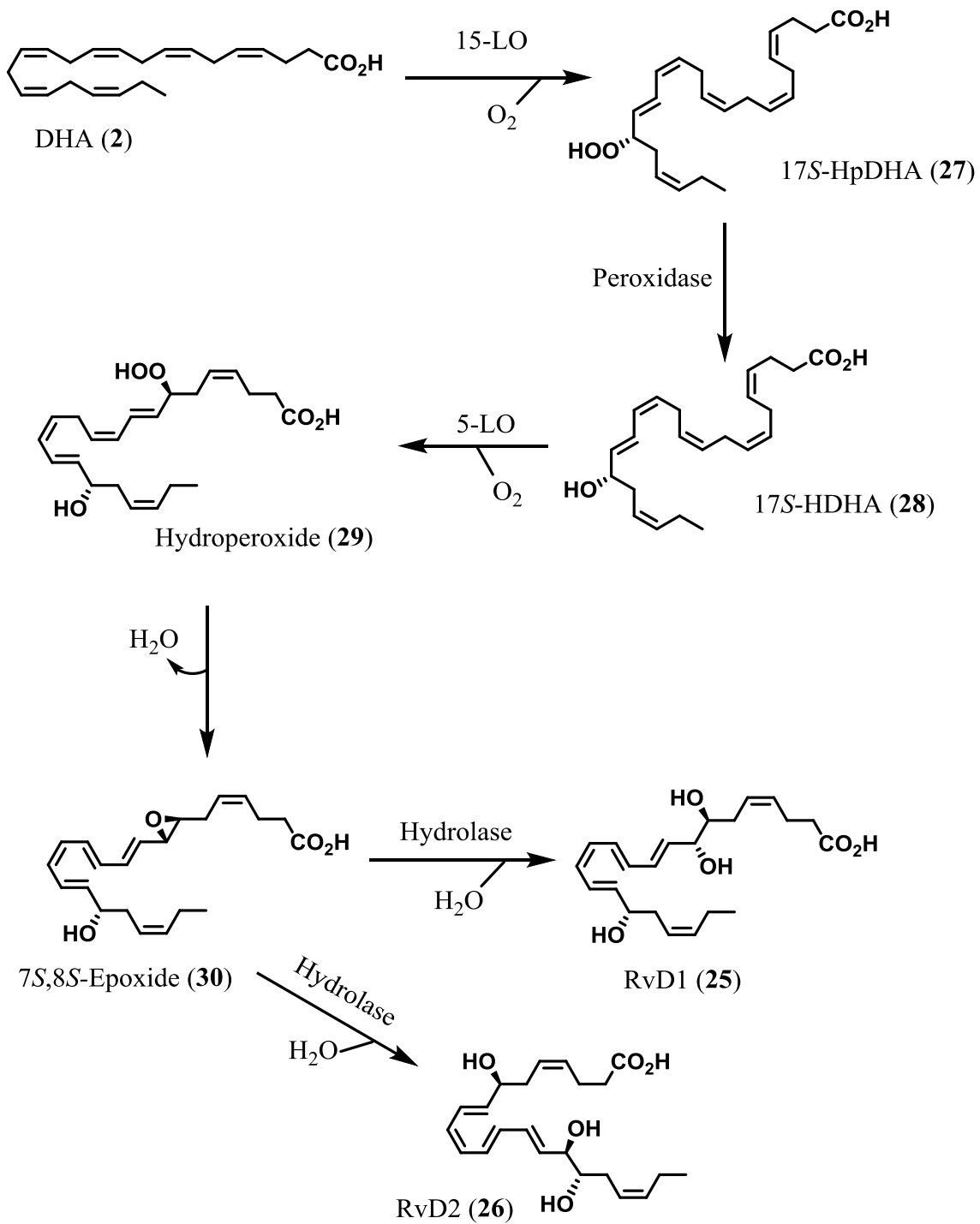
Figure 9. Resolvins of the D-series: RvD1 (**25**) and RvD2 (**26**).

RvD1 and RvD2 have displayed potent pro-resolving actions in several *in vivo* mouse disease models involving peritonitis (inflammation of the inner wall of the abdomen) and zymosan-induced inflammation among others. Interestingly, increased survival of mice with bacterial infections has been demonstrated for RvD2. Several *in vitro* studies have also been conducted on the two RvDs, in which these SPMs decreased the number of pro-inflammatory cytokines and interleukins in inflammatory models.[15]

The metabolome for the resolvins of the D-series are analogous to those for the E-series, with oxidation of alcohol groups to the corresponding ketones appearing to be the most important metabolic fates for these compounds.[15]
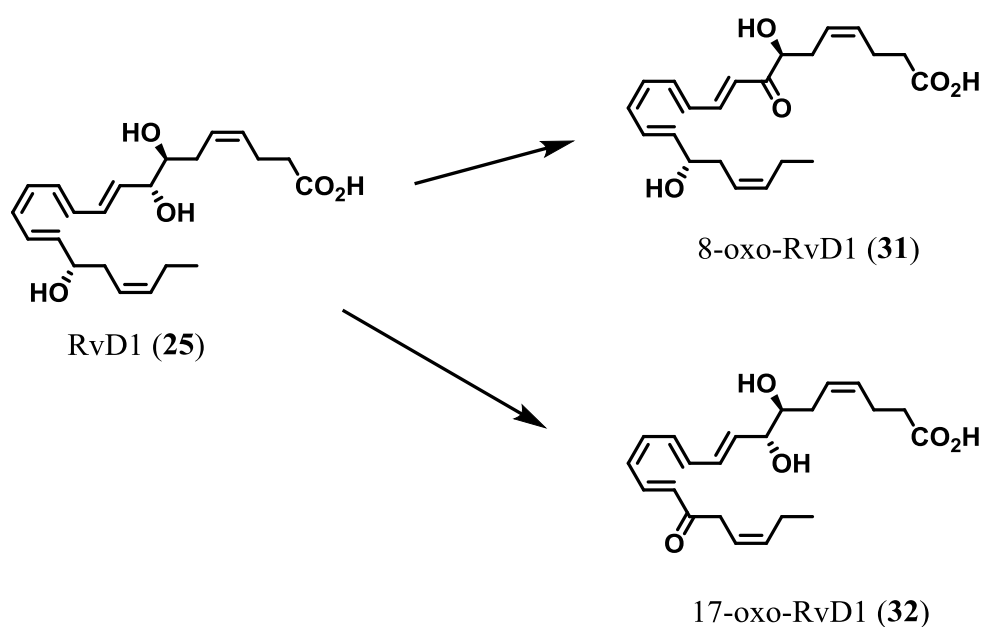
Figure 10. Metabolism of RvD1 (**25**).

Maresins

DHA is also a precursor for another group of SPMs which are called the maresins. The proposed biosynthesis of maresin 1 (**33**, MaR1) involves lipoxygenation of DHA (**2**) by 12-LO. The resulting 14S-hydroperoxide (**34**) is then transformed to an 13S,14S-epoxide intermediate (**35**),[35] which is further enzymatically converted to MaR1 (**33**).[35-37]
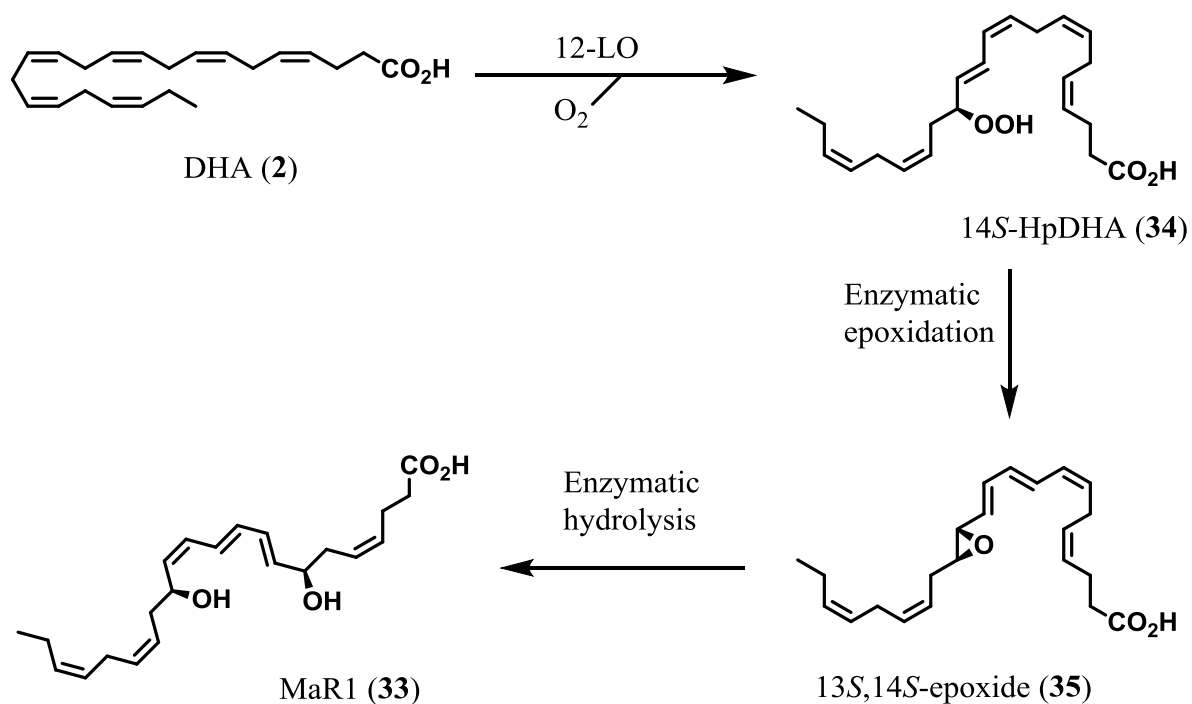
Figure 11. Biosynthesis of Mar1 (**32**).

The pro-resolving actions of the maresins have been evaluated through *in vitro* studies of bacterial periodontitis, with the results showing decreased leukocyte infiltration, increased phagocytosis and increased destruction of bacterial pathogens. MaR1 was even more effective than RvD1 in increasing efferocytosis of human apoptotic PMNs by human macrophages. *In vivo* studies on mice with induced peritonitis have also been performed, with MaR1 being injected on a ng scale. In this study, MaR1 (**33**) showed great efficacy in inhibiting PMN infiltration. Moreover, MaR1 (**33**) reduces inflammation-mediated pain in mice, and has also been shown to stimulate tissue regeneration in surgically injured planarians.[36,37]

Pathways of metabolic inactivation of maresins have yet to be investigated. Likely mechanisms such as ω-oxidation and oxidation of alcohol groups may be anticipated from knowledge of the metabolisms of other SPMs.[15]

Lipoxins

The lipoxins LXA$_4$ (**36**) and LXB$_4$ (**37**) are as previously mentioned biosynthesised from AA (**3**), and can be generated through pathways involving either 15-LO or 5-LO (Figure 12).[30,38] When 15-LO acts upon AA (**3**), 15S-HpETE and subsequently 15S-HETE are produced. 5-LO mediated lipoxygenation followed by enzymatic dehydration generates an epoxide, which is acted upon by a hydrolase to produce LXA$_4$ or LXB$_4$. The other route starts with 5-LO acting on AA, forming the leukotriene intermediate LTA$_4$. Then either 12-LO or 15-LO converts this intermediate to the epoxide intermediate, which again is further transformed into LXs such as lipoxin A$_4$ (**36**, LXA$_4$) and lipoxin B$_4$ (**37**, LXB$_4$). A last pathway involves COX-2 acetylated by aspirin. When AA is subjected to the actions of this altered enzyme, the intermediate product 15R-HETE is formed. This is in turn is transformed to LX epimers such as **38**, which have been entitled aspirin-triggered lipoxins.[30,38,39]
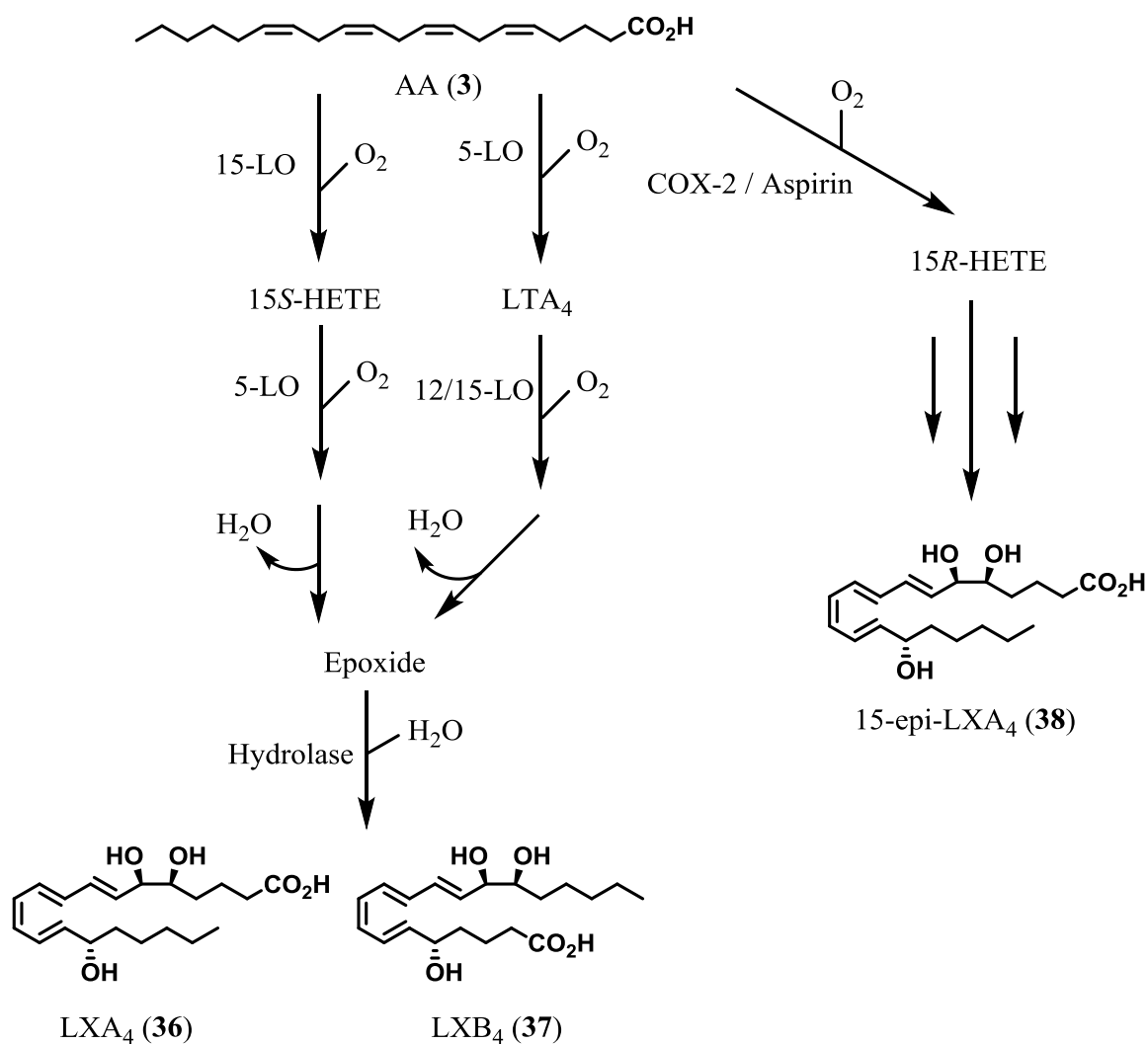
Figure 12. Biosynthetic pathways from AA (**3**) to lipoxins and aspirin-triggered lipoxins.

The biological actions of lipoxins have been evaluated through *in vitro* studies, and chemical and metabolic stable analogs retaining LX-activity (Figure 13) have been synthesized and utilized in *in vivo* studies.[30,38] These studies reveal that lipoxins have potent pro-resolving qualities, inhibiting PMN recruitment and activation, preventing secretion of chemokines and cytokines, and stimulating macrophage efferocytosis. A number of animal studies on different disease models demonstrate that the stable LX analogs show potent actions against inflammatory diseases like colitis, skin inflammation, asthma, periodontitis, cystic fibrosis and several autoimmune diseases. One analog even inhibited angiogenesis, which indicates that LXs may have some cancer-protecting potential. The synthetic analog **39** is orally active, and is currently approaching clinical trials against inflammatory diseases.[38]
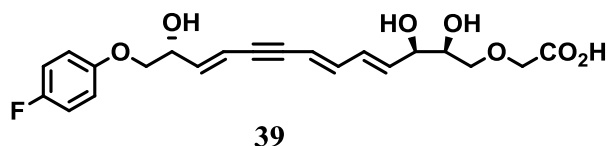
Figure 13. The chemically and metabolically stable LX analog **39**.

In much the same manner as the other SPMs, lipoxins are metabolised primarily through oxido-reductases, and in some degree through ω oxidation. The enzyme 15-prostaglandin dehydrogenase (15-PGDH) catalyzes oxidation of the alcohol in the 15 position. Then another enzyme named 15-oxo-prostaglandin 13-reductase (PGR) reduces the adjacent double bond. 15-PGDH may then reduce the ketone back to an alcohol.[38] Some metabolic pathways of LXA$_4$ (**35**) are portrayed in Figure 14.
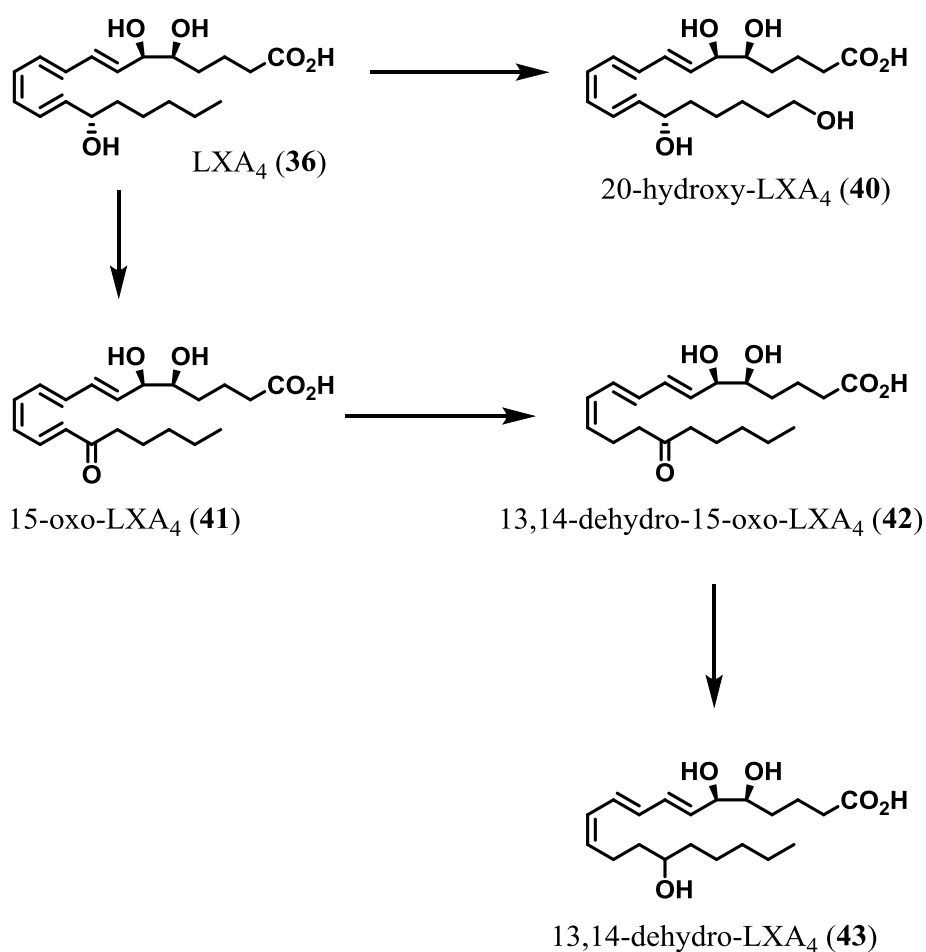
Figure 14. Metabolism of lipoxin A$_4$ (**36**).

1.1.5 Protectins

The final group of SPMs derived from DHA are the protectins. The most prominent of these is protectin D1 (**44**, PD1), also called neuroprotectin D1 (NPD1) when formed in neural tissue.[40] Biosynthesis of this compound commences with the enzymation actions of 15-LO on DHA (**2**), producing 17*S*-HpDHA (**45**), which is further enzymatically converted to PD1 (Figure 15).[15] Evidence that the 16*S*,17*S* epoxide (**46**) is in fact an intermediate in the biosynthesis was provided by Serhan, Hansen and co-workers[41] in 2015. This was achieved by organic synthesis of epoxide (**46**), followed by successful conversion of the compound into PD1 by human macrophages.

16
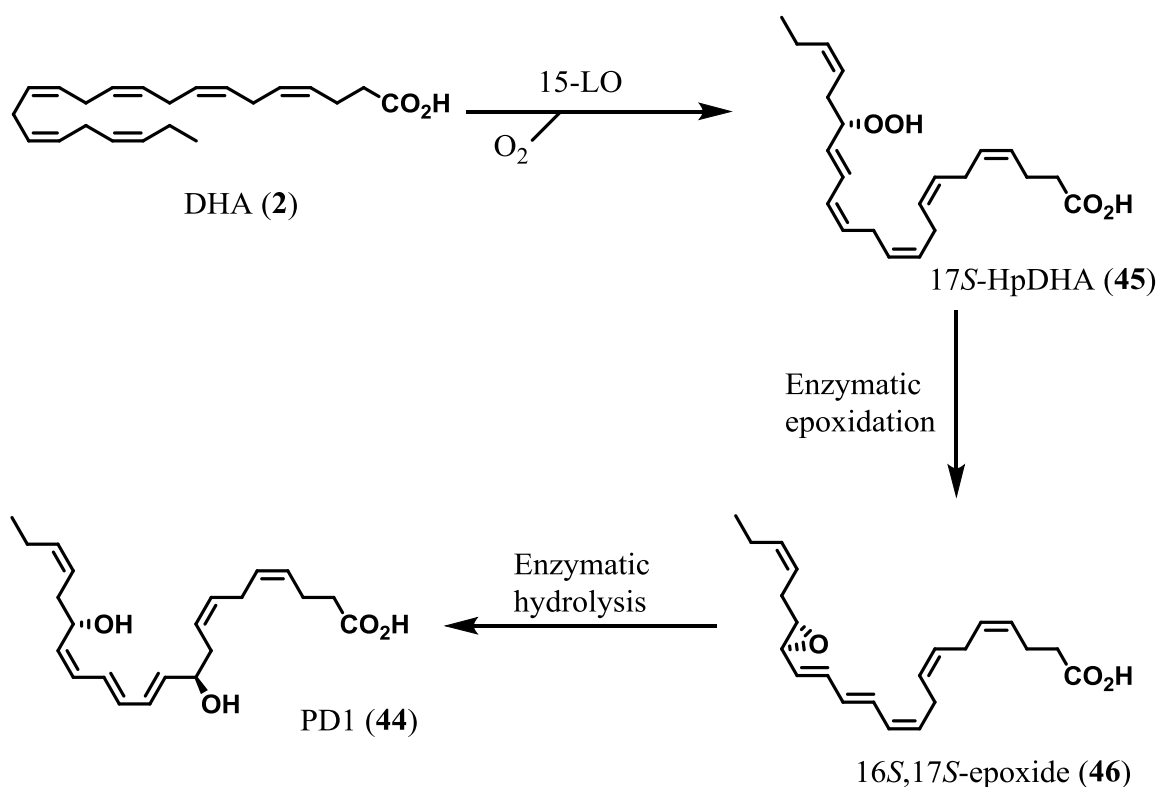
Figure 15. Biosynthesis of PD1 (**44**).

The biological activities of PD1 (**44**) have been thoroughly investigated. The substance showed remarkably potent pro-resolving actions in mice with peritonitis, with 1 ng causing reduction of PMN infiltration by approximately 40%.[42] PD1 has been found to be biosynthesized *in vivo* during ischemia-reperfusion of renal tissue, where it combats the harmful effects this process may have on kidneys.[43] Biosynthesis of PD1 in mice infected with the Lyme disease has been observed, where it possibly stimulates resolution of this infection.[44] NPD1 inhibits cell death of retinal cells and stimulates photoreceptor cell renewal by protecting these cells from oxidative metabolic stress.[45-47] In obese mice, PD1 has been found to affect levels of adiponectin, a protein involved in fatty-acid metabolism and regulation of insulin, and thus prevent development of insulin-resistance.[48] Beta-amyloid induced inflammation is an important part in the development of Alzheimer's disease, and *in vitro* studies show that NPD1 protects human neurons from such inflammation and subsequent neuronal cell death by mechanisms involving secretase enzymes and PPARγ.[49,50] A PD1 isomer called PDX has also been found to exhibit pro-resolving actions in peritonitis, and interestingly also inhibits platelet aggregation.[51]

Comprehensive data on the metabolism of PD1 has not been reported, but one study has reported a metabolite, namely 22-hydroxy-PD1 (22-OH-PD1, **47**, Figure 16) caused by ω-oxidation.[52] This metabolite was prepared by organic synthesis by the LIPCHEM group at UiO, and was found to have potent pro-resolving activities.[53] It is likely that additional metabolic pathways of PD1 are mediated through oxido-reductases in the same way as for the other SPMs, although further studies are needed for confirmation and elucidation of this.

22-hydroxy-PD1 (**47**)
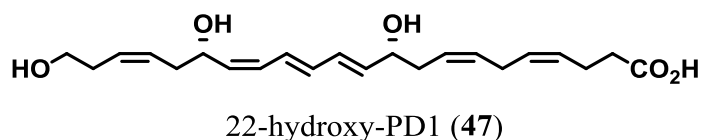
Figure 16. The 22-hydroxylated metabolite **47** of PD1.

1.1.6 Isolation and structure confirmation of protectin D1$_{\text{n-3 DPA}}$

As well as AA, DHA and EPA, several SPMs have been discovered to be derived from the polyunsaturated fatty acid n-3 docosapentaenoic acid (**48**, n-3 DPA, see Figure 17). This was reported in 2013 by Dalli *et al.*, by observing leukocytes from human and murine plasma during induced inflammation. n-3 DPA was found to be converted to a series of oxygenated compounds with structural similarities to the resolvins, maresins and protectins. The formation of products was monitored by LC-MS/MS, and fragmentation patterns were used in order to assign postulates of the structures of these compounds. One such product was assigned the structure (7*Z*,11*E*,13*E*,15*Z*,17*S*,19*Z*)-10,17-dihydroxydocosa-7,11,13,15,19-pentaenoic acid, and was because of its similarity to PD1, given the name protectin D1$_{\text{n-3 DPA}}$ (**49**, PD1$_{\text{n-3 DPA}}$).[32]
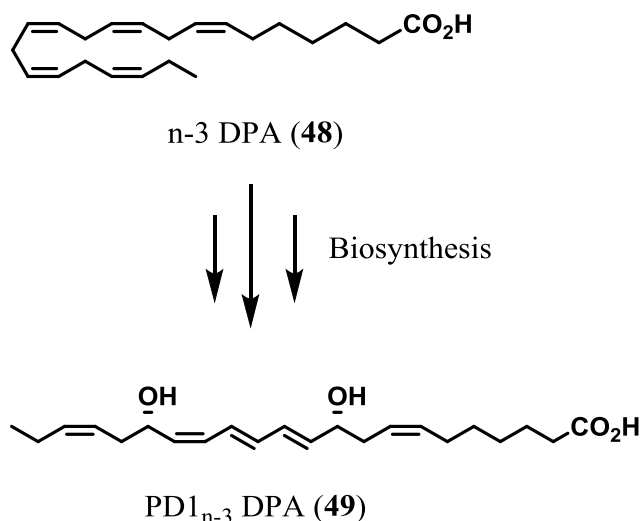
Figure 17. Structure of n-3 DPA (**48**) and confirmed structure of PD1 $_{\text{n-3 DPA}}$ (**49**).

There were several issues with the initial structural assignment of PD1$_{\text{n-3 DPA}}$. The assignment was solely based on LC-MS/MS fragmentation experiments, where PD1$_{\text{n-3 DPA}}$ actually was indistinguishable from another novel SPM that was generated during the same experiment (RvD5$_{\text{n-3 DPA}}$). Complete assignment of the double-bond geometry in the conjugated triene system was thus needed. Furthermore, the stereochemistry of the C-10 alcohol remained unidentified, and the *S*-configuration of the C-17 alcohol was based on biosynthetic considerations. As a result of this, total organic synthesis was needed in order to unequivocally confirm the structure of of PD1$_{\text{n-3 DPA}}$ with complete configurational assignments.[32]

With multimiligram quantities of synthetic PD1$_{\text{n-3 DPA}}$ provided by Serhan, Hansen and co-workers, the *Z/E* geometry of the double bonds were assigned by two-dimensional NMR, and the remaining structural assignments were deduced by a combination of ^{1}H, ^{13}C, COSY and HMBC spectra. The synthesized compound was then matched with natural material collected from exudates, in order to confirm that PD1$_{\text{n-3 DPA}}$ was indeed the same as the synthesized compound. The synthetic compound was compared with endogenous PD1$_{\text{n-3 DPA}}$ from human macrophages and exudates from mice with zymosan-induced peritonitis. Employing a tandem LC-MS/MS method, synthetic PD1$_{\text{n-3 DPA}}$ gave the same retention time as the endogenous substance. Furthermore, the recorded MS/MS spectra for both synthetic and natural PD1$_{\text{n-3}}$ $_{\text{DPA}}$ spectra were identical. All together, these data confirm the structure of PD1$_{\text{n-3 DPA}}$ to be

the (7*Z*,10*R*,11*E*,13*E*,15*Z*,17*S*,19*Z*)-10,17-dihydroxydocosa-7,11,13,15,19-pentaenoic acid (**49**), see Figure 17.[54]

1.1.7 Biosynthesis and metabolism of protectin D1$_{n-3\ DPA}$

A proposed biosynthetic pathway for PD1$_{n-3\ DPA}$ was suggested by Dalli *et al.*, (Figure 18) commencing with transformation of n-3 DPA (**48**) into 17*S*-HpDPA (**50**) by lipoxygenation. This hydroperoxide is then converted enzymatically to an 16*S*,17*S*-epoxide (**51**), which is acted upon by a hydrolase, producing PD1$_{n-3\ DPA}$ (**49**). This pathway involving an epoxide intermediate is in agreement with previous reports of the enzymatic conversions of the other groups of SPMs[15,38], pathways discovered by Corey in 1986[55], as well as the work of Serhan, Hansen and co-workers in 2015, establishing the existence of a 16*S*,17*S* epoxide intermediate in the biosynthesis of PD1.[41]
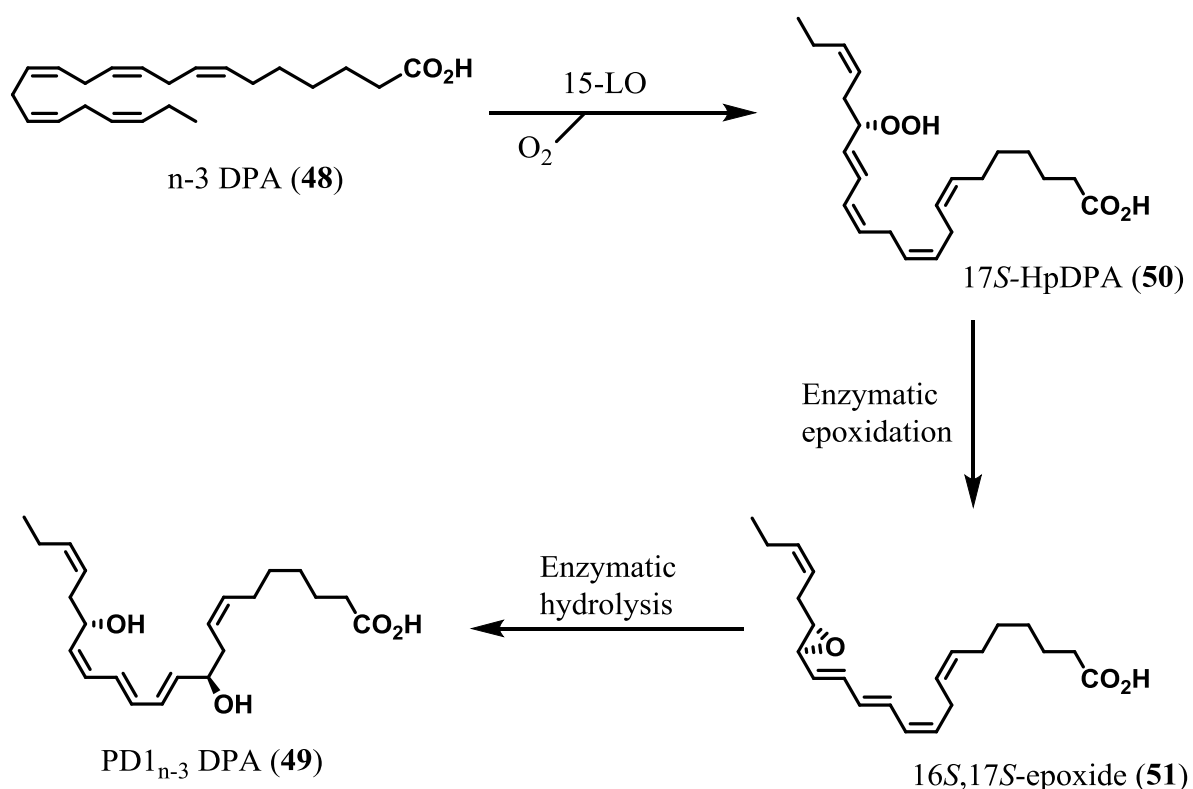
Figure 18. Proposed biosynthetic pathway for PD1n-3 $_{DPA}$ (**49**).

Additional experiments were then performed to support the notion that this biosynthetic pathway existed for $PD1_{n-3\ DPA}$. This was achieved by incubating n-3 DPA with 15-lipoxygenase, and then opening the epoxide with a solution of acidic MeOH. The products were then analyzed by LC-MS/MS experiments, and fragmentation patterns were used in order to assign their structures. Results from this experiment were in accordance with the previously proposed biosynthetic pathway involving acid- or enzyme catalyzed opening of an 16,17-epoxide.[54]

The metabolism of $PD1_{n-3\ DPA}$ has not been explicitly investigated. Probable metabolic pathways can nevertheless be deduced from the structural and chemical similarities to PD1, the other groups of SPM and the available knowledge of the metabolism of these substances.[15,38,53] As such, the most likely pathways involve β- and ω-oxidation, as well as actions of oxidoreductases on the two alcohol groups (Figure 19).

17-oxo-PD1$_{n-3\ DPA}$ (**53**)

15,16-dehydro-17-oxo-PD1$_{n-3\ DPA}$ (**54**)

PD1$_{n-3\ DPA}$ (**49**)

15,16-dehydro-PD1$_{n-3\ DPA}$ (**55**)

22-hydroxy-PD1$_{n-3\ DPA}$ (**52**)
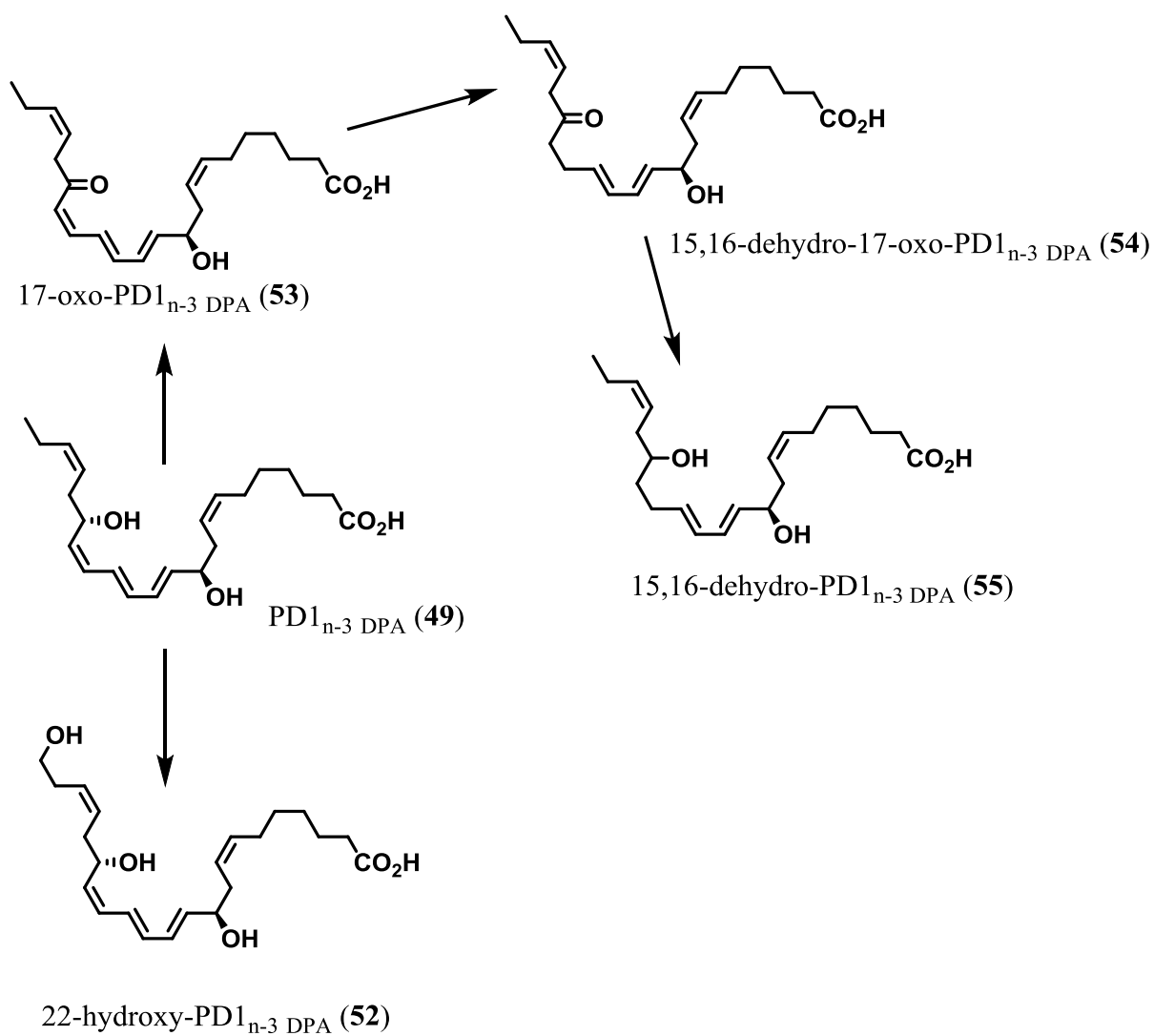
Figure 19. Possible metabolic pathways for PD1 n-3 $_{DPA}$ (**49**).

1.1.8 Biological activities of protectin D1$_{n-3\ DPA}$

Confirmation of the pro-resolving actions of PD1$_{n-3\ DPA}$ (**49**) was acquired by one *in vivo* and two *in vitro* experiments, see Figure 20.[54] First, mice with zymosan-induced peritonitis were administered 10 ng PD1$_{n-3\ DPA}$ (**49**), which gave a significant decrease in number of neutrophils, similar to that of PD1 (**44**). Then stimulation of human macrophage phagocytosis was investigated. PD1$_{n-3\ DPA}$ (**49**) was incubated with these macrophages, and the results showed an increase in zymosan-induced phagocytosis of apoptopic neutrophils. These actions were also comparable to those of PD1. The final experiment examined efferocytosis against apoptopic human neutrophils. PD1$_{n-3\ DPA}$ was found to be a potent stimulator of this process at picomolar concentrations, in a manner similar to PD1. The results from this study confirm that PD1$_{n-3\ DPA}$ is in fact a true SPM which exhibits potent pro-resolving properties.
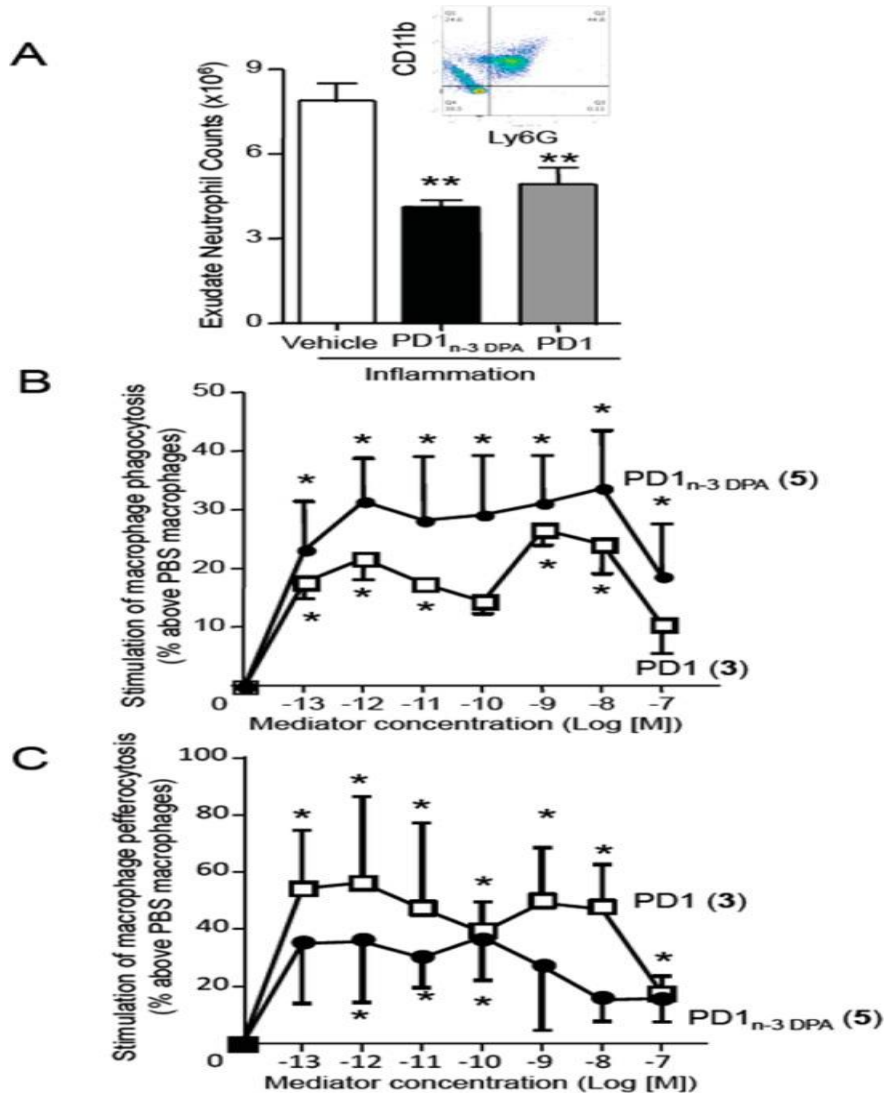
Figure 20. PD1$_{n-3DPA}$ (**49**) exhibits potent pro-resolving actions comparable to PD1 (**44**). A: Mice were intravenously administered 10 ng of either PD1 n-3 DPA (**49**) or PD1 (**44**), or vehicle consisting of saline with 0.01% EtOH. After 5 min, 1 mg zymosan was administered intraperitoneally. Exudates were collected after 4 hours, and the number of infiltrated neutrophils was counted. B and C: Human macrophages were incubated with either vehicle, **44** or **49** (both in concentrations between 10 pM to 100 nM). Then either zymosan (B) or apoptopic human neutrophils (C) were added. Incubation was stopped after 1 hour, and phagocytosis was assessed.

1.1.9 Total synthesis of protectin D1$_{n-3 \text{ DPA}}$

A stereoselelective total synthesis of PD1$_{n-3 \text{ DPA}}$ (**49**) was reported in 2014 by Aursnes *et al.*[54] from the LIPCHEM group at the University of Oslo.

Retrosynthetic analysis of this SPM revealed three fragments **56**, **57** and **58** (Scheme 1). Middle fragment **57** had already been prepared by the group for the synthesis of other SPMs, where the key step was an Evans-Nagao stereoselective aldol reaction. Fragment **56** had also been previously prepared in the synthesis of the related compound protectin D1.[56] Synthesis of the α-fragment was based on a previously reported procedure by Mioskowsky *et al.*,[57] affording an iodide which was easily transformed into the desired Wittig salt **58**.
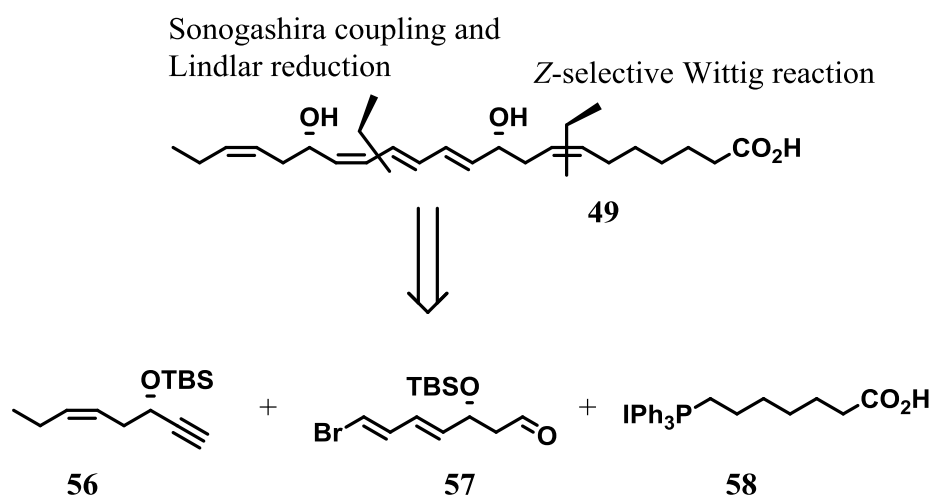
Scheme 1. Retrosynthetic analysis of PD1$_{n-3 \text{ DPA}}$ (**49**).

A *Z*-selective Wittig reaction was performed to connect the α-fragment **58** and middle fragment **57**, affording the vinyl bromide ester **59**. A Sonogashira coupling between this vinylic bromide **59** and alkyne **56** yielded the product **60** with all the carbon atoms of protectin D1$_{n-3 \text{ DPA}}$. Removal of the protective silyl ethers with TBAF afforded the diol **61**. Then reduction of the internal alkyne to *Z*-alkene **62** was accomplished by hydrogenation with Lindlar's catalyst. Finally, hydrolysis of the methyl ester with LiOH yielded the desired protectin D1$_{n-3 \text{ DPA}}$ **49** (Scheme 2).
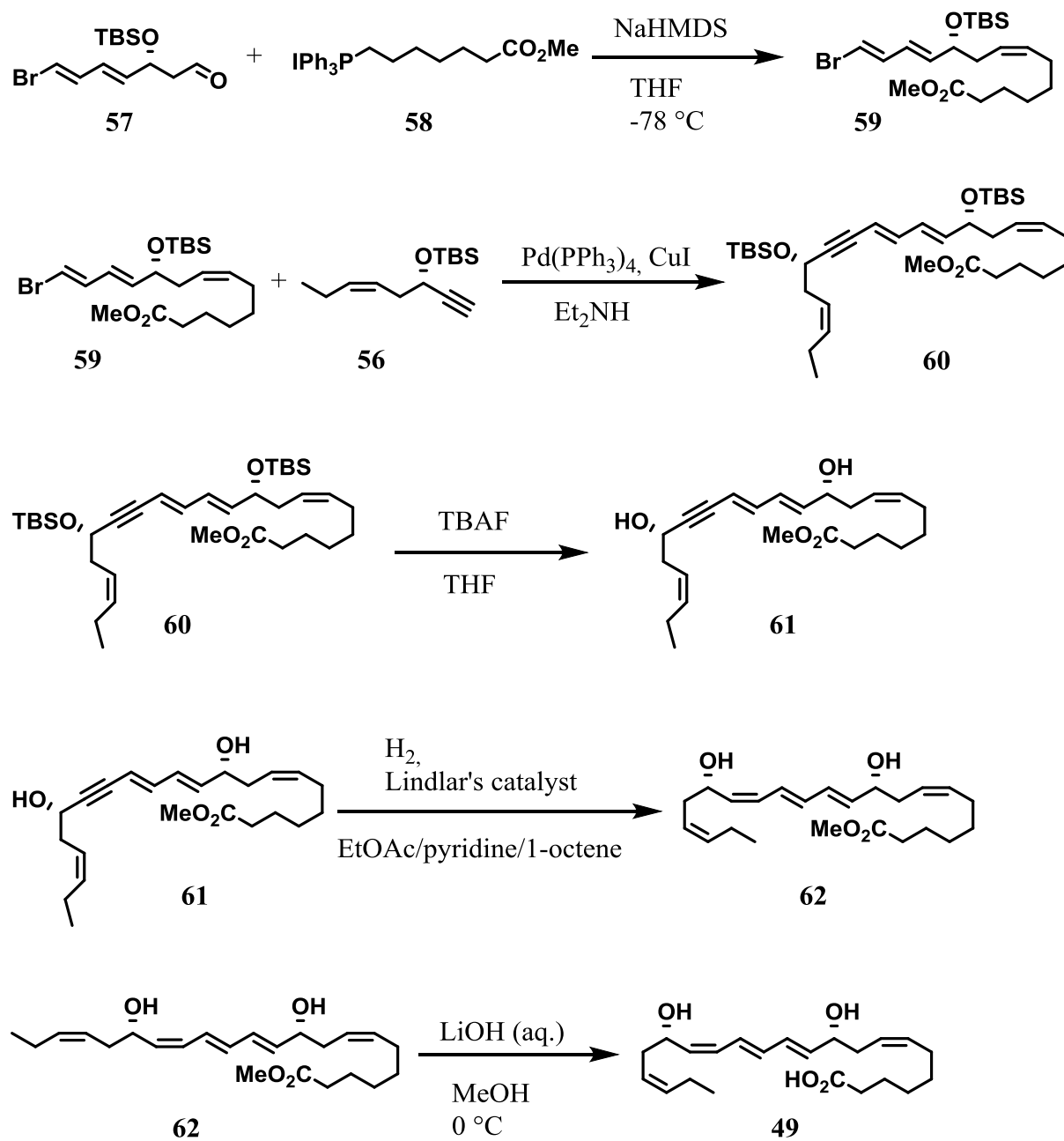
Scheme 2. Synthesis of PD1$_{n-3\text{ DPA}}$ (**49**).

The synthesis of PD1$_{n-3\text{ DPA}}$ was done in a convergent manner, in 10 steps and in an overall yield of 9%.

1.2 Synthetic methods

1.2.1 Wittig and *Z*-selective Wittig reactions

The Wittig reaction is a useful method for the preparation of an alkene from ketones or aldehydes. This reaction was first reported in 1953 by the German chemist Georg Wittig, who received the Nobel Prize in Chemistry in 1979 for his work in developing this reaction.[58] The Wittig reaction is particularly useful as there is no uncertainty in the position of the double bond, and *Z/E* stereoselectivity is often predictable based on the nature of reagents and reaction conditions.[58,59]

The Wittig reaction commences with the preparation of a phosphonium salt **63**, which is achieved by reacting an alkyl halide **64** with triphenylphosphine **65**. A phosphonium salt carries a positive charge on its phosphorus atom, which in turn makes the neighboring proton atom acidic. A base is then able to deprotonate the phosphonium salt to form a resonance-stabilized phosphorus ylide **66**. A phosphorus ylide carries a negative charge on a carbon atom directly bonded to a phosphorus atom with a positive charge. This nucleophilic ylide very easily reacts with the electrophilic carbonyl carbon atom in a ketone **67** or aldehyde via an oxaphosphetane intermediate **68**, which rearranges to form an alkene **69**. One proposed mechanism for the Wittig reaction is shown in Scheme 3.[58,59] The main byproduct in this reaction is triphenylphosphine **70**, which can be removed by precipitation in cold hexane or Et_2O, and/or flash chromatography.
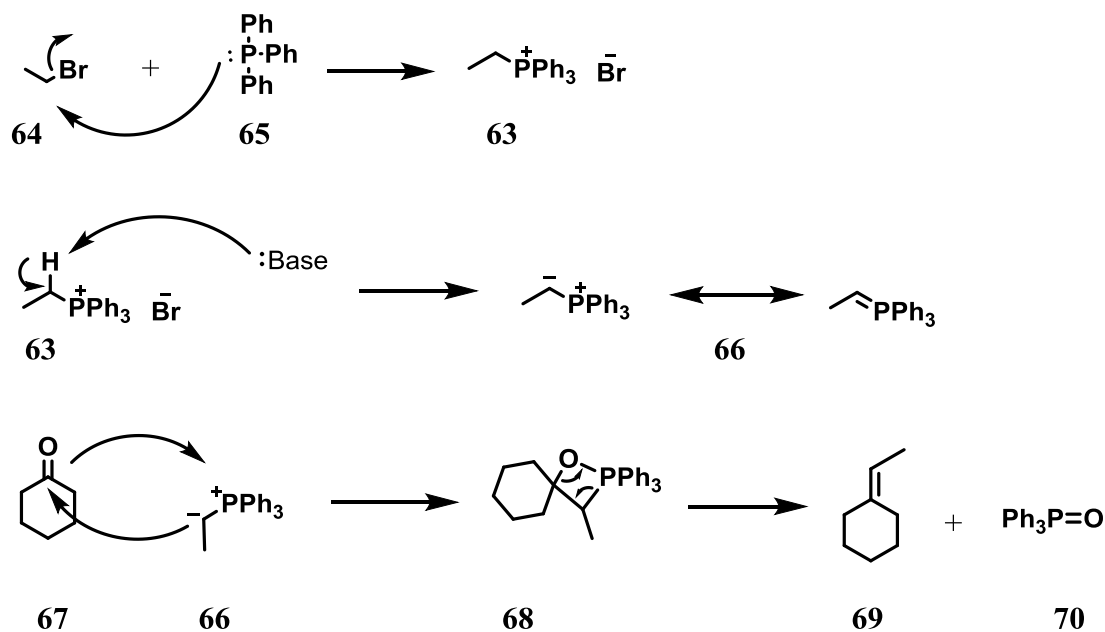
Scheme 3. Mechanism of the Wittig reaction.

As mentioned above, the Wittig reaction can be either *Z*- or *E*-selective. Selectivity depends greatly of the substituents on the ylide. If the ylide has an anion-stabilizing group adjacent to the negative charge, it is characterized as a stabilized ylide, and most often give *E* selective Wittig reactions.[58,59]

When the substituent is a regular alkyl group, the ylide is characterized as non-stabilized, and usually react in a *Z*-selective manner in the Wittig reaction. In order to prepare non-stabilized ylides, a base is added to the phosphonium salt shortly before the ketone or aldehyde is added to the reaction mixture. *Z*-selectivity can also be achieved by using lithium-free conditions, where NaHMDS or KHMDS is used as the base instead of bases like LiHMDS or *n*-BuLi. Further *Z*-selectivity is possible by performing the reaction at low temperatures, often at -78 °C (Scheme 4).[58,59]
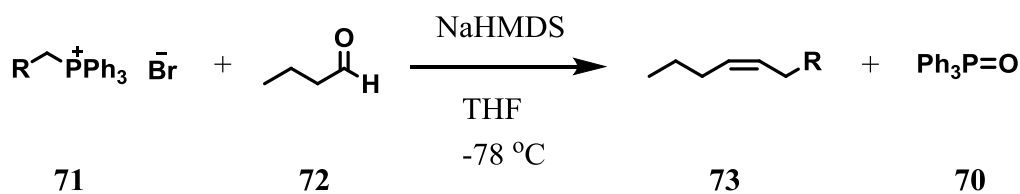
Scheme 4. *Z*-selective Wittig reaction.

1.2.2 Evans-Nagao stereoselective aldol reaction

The aldol reaction was discovered independently by Wurtz and Borodin in 1872 and is an important and valuable method of forming carbon-carbon bonds.[60] In the typical aldol addition an enol or enolate is reacted with a ketone or aldehyde, affording a β-hydroxy carbonyl compound. The product can then eventually undergo elimination of H_2O and generate an α,β-unsaturated carbonyl. (Scheme 5).[61] The mechanism commences with a nucleophilic addition of an enolate to the carbonyl of an aldehyde or ketone.[62] One important aspect of aldol reactions is that up to two new stereocenters can be generated, and consequently as many as four stereoisomers can be formed. In contemporary organic synthesis though, enantiomerically pure compounds are often desired, and hence a demand for diastereoselective aldol reactions was created.
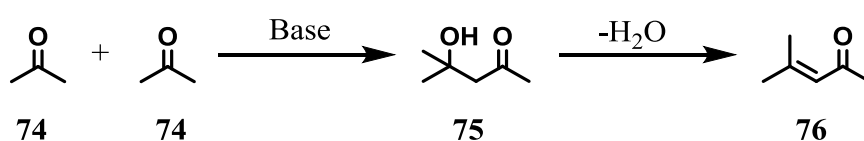
Scheme 5. An aldol reaction followed by dehydration.

The first use of chiral auxiliaries for aldol additions was reported by Evans and co-workers in 1981.[63,64] Evans utilized chiral acyl oxazolidinones (Figure 21) in order to produce chiral boron enolates used in aldol reactions. After completion of the aldol reaction, removal of the auxiliary affords the desired aldol product often with excellent diastereoselectivity. This variation of the aldol addition has been named the Evans aldol reaction. There are many factors which affect the diastereoselectivity of this reaction. Choice of solvent, Lewis acid and

amine base can dramatically change selectivity, as can the stoichiometric amounts of these reagents and solvents.[63]
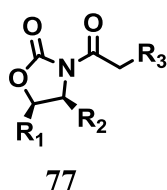
Figure 21. Evan's acyl oxazolidinone (**77**).

In 1989 Nagao *et al.* reported the synthesis and application of thiazolidinethiones as chiral auxiliaries in Evans aldol reactions, in excellent yields and diastereomeric excesses.[65] An Evans type aldol addition using Nagao's chiral auxiliary is entitled an Evans-Nagao stereoselective aldol reaction. The mechanism of this reaction involves a closed transition state, as outlined in Scheme 6.[56]
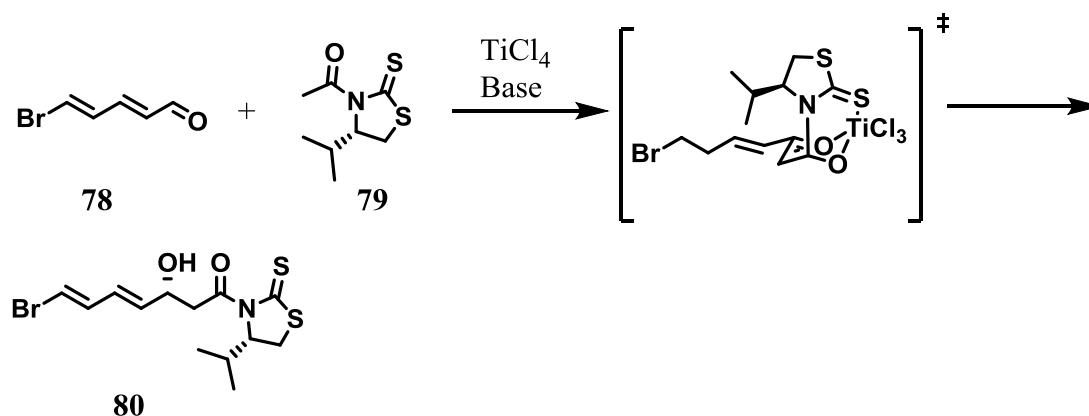
Scheme 6. Example of an Evans-Nagao stereoselective aldol reaction.

The Evans-Nagao reaction is highly applicable in the synthesis of natural products, and has been utilized in the total synthesis of various natural products and SPMs such as maresins, protectins and leukotrienes.[53,54,56,66,67]

1.2.3 The Sonogashira coupling reaction

The Sonogashira cross-coupling reaction (Scheme 7) allows cross-coupling between a terminal alkyne and either a vinylic or arylic halide, in the presence of a palladium catalyst and a copper co-catalyst.[68] The reaction requires an amine base, which may also be used as the reaction solvent. The Sonogashira coupling was first reported by Kenkichi Sonogashira and Nobue Hagihara in 1975. They added a copper co-catalyst to the coupling reactions of Heck[69] and Cassar,[70] and observed that the reaction rate increased significantly.[71] This allowed the coupling to be performed at room temperature, which was a major improvement over the harsh conditions required for the Heck and Cassar coupling reactions. Sonogashira reactions generally require oxygen-free conditions, as the active Pd(0) and Cu(I) catalysts are air-sensitive, and the presence of oxygen promotes homocoupling of acetylenes.
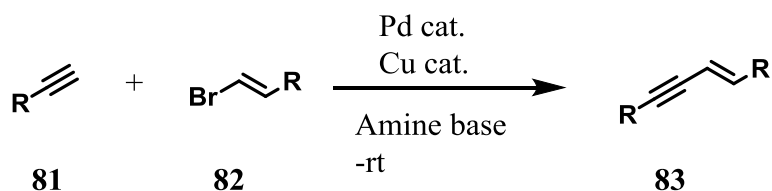
Scheme 7. The Sonogashira coupling

The exact reaction mechanism of the Sonogashira coupling has not been fully established since it is challenging to isolate and characterize the organometallic intermediates from the reaction mixture. One of the generally accepted proposed mechanisms involves a palladium cycle and a copper cycle. (Scheme 8).[68]
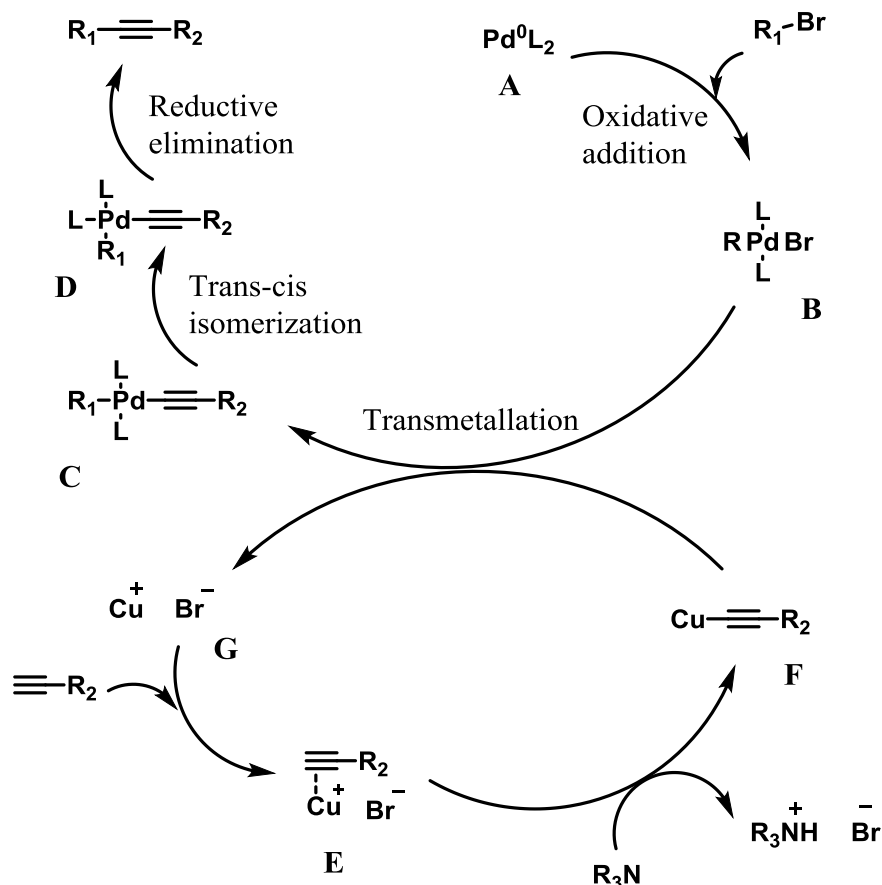
Scheme 8. Catalytic cycles for the Sonogashira reaction.

Palladium cycle

The active Pd(0) catalyst A reacts with the vinyl or aryl halide in an oxidative addition, creating a Pd(II) organometallic intermediate B. This palladium-complex reacts in a transmetallation with the copper acetylide created from the copper cycle, producing the intermediate C, while regenerating the copper halide. The ligands in intermediate C are *trans* oriented, and these are transformed to *cis* by a *trans/cis* isomerization. The final step in the palladium cycle is a reductive elimination. This generates the alkyne cross-coupling product, and regenerates the Pd^0 catalyst.

Copper cycle

The terminal alkyne reacts with a copper halide, and the intermediate complex E makes the terminal acetylenic proton more acidic. An amine base can therefore deprotonate this, which creates the copper acetylide F. This reacts with intermediate B from the palladium cycle in a transmetallation, regenerating copper halide G.

Sonogashira couplings are versatile and generally easy to perform, and have been utilized in the synthesis of a number of natural products, including several SPMs.[53,54,56,66,67,72]

1.2.4 Aim of thesis and retrosynthetic analysis

Aim of thesis

The aim of this master thesis is to synthesize the analog **84** of $PD1_{n-3\ DPA}$ (Figure 22). It is expected that long-term resolution of inflammation is desirable in the treatment of diseases characterized by chronic inflammation. There is thus a demand for analogs of $PD1_{n-3\ DPA}$ with high metabolic stability and extended biological half-lives for future biological studies. Part of the metabolism of $PD1_{n-3\ DPA}$ is most likely mediated through oxido-reductases acting on the alcohol group on C-17. By making this alcohol tertiary, these enzymes will be unable to oxidize the alcohol to a ketone, thus blocking this metabolic pathway. It is hypothesized that this will increase the half-life of the protectin analog, providing knowledge of SAR and possibly making way for synthesis of more drug-like analogs of $PD1_{n-3\ DPA}$,
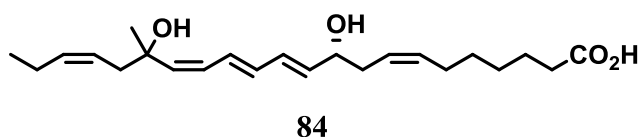
Figure 22. The $PD1_{n-3\ DPA}$ analog **84**.

If prepared, this analog will be submitted to biological evaluations in order to investigate its pro-resolving activities.

Retrosynthetic analysis
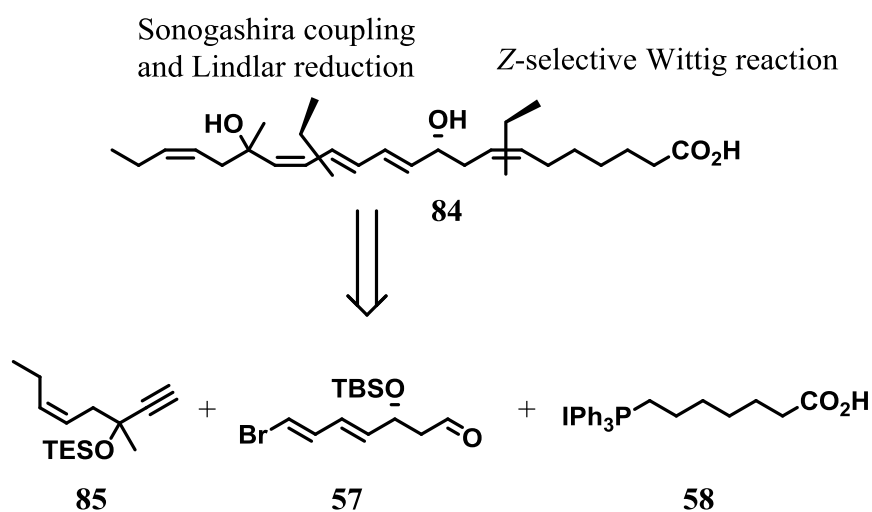
Scheme 9. Retrosynthetic analysis of **84**.

A retrosynthetic analysis of **84** (Scheme 9) revealed the three fragments **85**, **57** and **58**, which allows the use of a convergent synthesis. The synthetic strategy will be based on an approach similar to that used for the published synthesis of PD1$_{n-3 DPA}$.[54] Aldehyde **57** can be connected to **58** in a Z-selective Wittig reaction, and the resulting vinyl bromide ester can be coupled with alkyne **85** in a Sonogashira reaction. **85** will be synthesized as a racemate, and the resulting analog **84** will thus be prepared as two diastereomers.

2 Results and Discussion

2.1 Overview of the synthetic strategy

The Z-alkene **85** was prepared from commercially available 4-hydroxybutanone, **86**, as shown in Scheme 10. This was done according to an unpublished procedure[73] as shown in Scheme 10, developed by Dr. Jens M. J. Nolsøe from the LIPCHEM group at the University of Oslo. This synthesis commenced with the addition of at least two equivalents ethynylmagnesium bromide to the commercially available ketone **86**, which afforded the diol **87**. Reacting this diol with at least two equivalents of TES triflate produced the *bis*-protected alcohol **88**. A Swern oxidation of **88** with oxalyl chloride and DMSO gave aldehyde **89**, which was used immediately in a Z-selective Wittig reaction with propyltriphenylphosphonium bromide to afford the desired Z-alkene **85**. These syntheses are discussed in more detail in section 2.2.1-2.2.7.
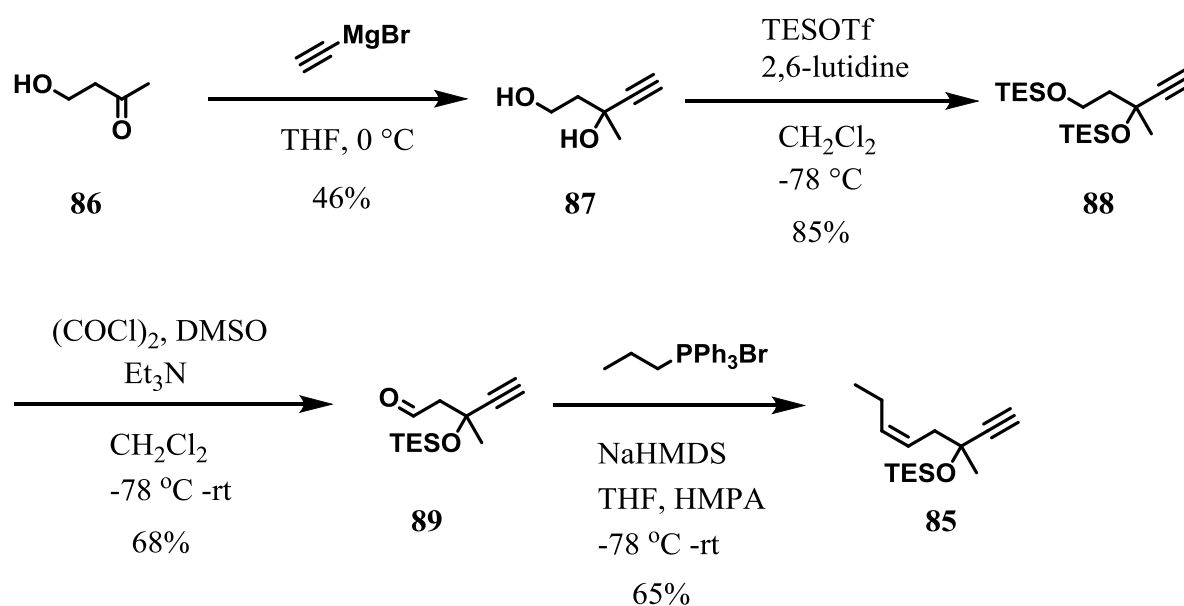
Scheme 10. Synthesis of ω-fragment **85**.

Wittig salt **58** was prepared as shown in Scheme 11, using a procedure published by the LIPCHEM group for the synthesis of PD1$_{n-3\ DPA}$.[54] Commercially available cycloheptanone **90** was treated with *m*CPBA , transforming it to lactone **91**. This lactone was subjected to a Fisher esterification with catalytic H_2SO_4 in methanol, affording methyl ester **92**. Then the alcohol functional group was converted to the corresponding iodide **93** by an Appel reaction. The resulting iodide was reacted with triphenylphosphine in MeCN, affording the desired Wittig salt **58**. The synthetic steps to the prepared Wittig salt **58** are discussed in more detail in section 2.2.9-2.2.13.
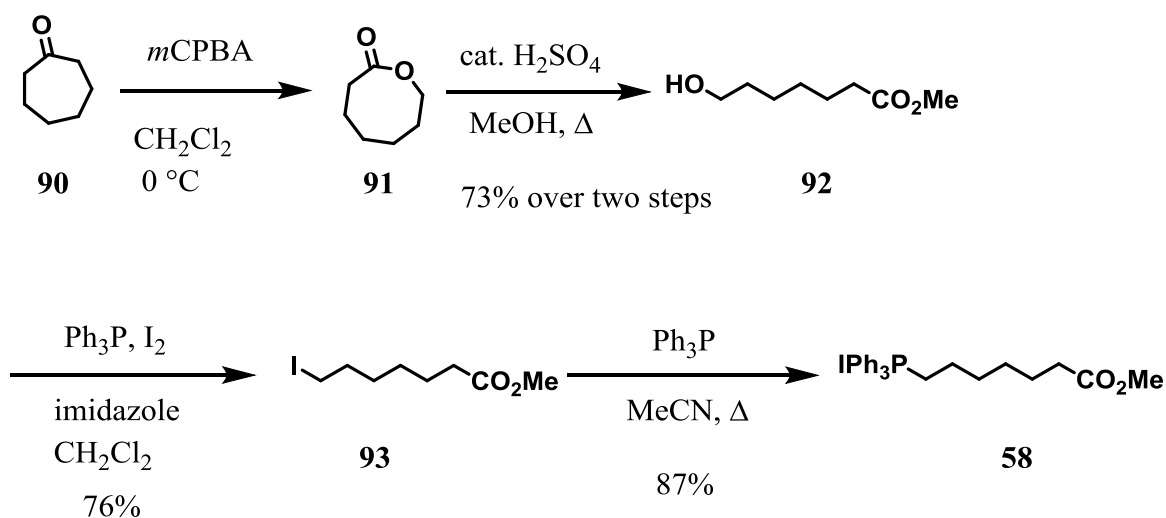
Scheme 11. Synthesis of α-fragment **58**.

For the synthesis of the middle fragment **57**, the LIPCHEM group had already prepared and stored the precursor **94**; a thiazolidinethione-protected aldehyde. The key step in the preparation of this compound was an Evans-Nagao stereoselective aldol reaction, using conditions established by Olivio *et al.*[63] Compound **94** was reduced to aldehyde **57** by a reaction with DIBAL-H, in accordance with the published procedure, see Scheme 12.[54]
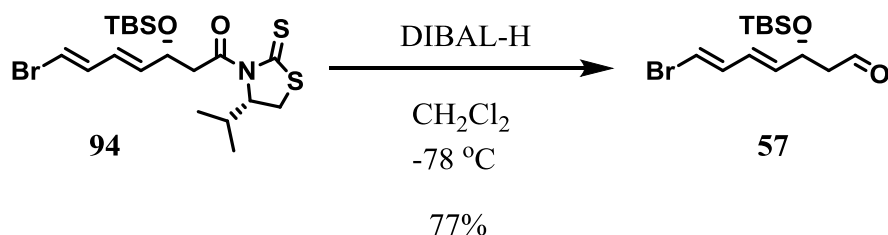
Scheme 12. Synthesis of middle fragment **58**.

For the assembly of the three fragments, a *Z*-selective Wittig reaction between the ylide of Wittig salt **58** and aldehyde **57** was first performed to prepare the vinyl bromide **95**. Reacting vinyl bromide **95** with alkyne **85** in a Sonogashira cross-coupling reaction provided compound **96**, containing all the carbon atoms of the desired analog **84**. Removal of the two silyl groups with TBAF afforded the diol **97**. The free carboxylic acid of **97** is also a potential analog of PD1$_{n\text{-}3\ DPA}$ (**48**), as SAR studies of lipoxins revealed that acetylenic derivatives both retained biological activities and improved chemical stability.[38] A Lindlar reduction was then attempted to reduce the internal alkyne of **97** to the desired *Z*-alkene **98**. This reaction proved to be over-active, and could not be stopped at the alkene. A Boland reduction was then performed, which sadly also gave an over-reduced and dehydrated product. There are thus two remaining steps in the synthesis; reduction of alkyne to *Z*-alkene **98**, and saponification of the methyl ester of this compound with LiOH in order to produce the desired analog **84**.
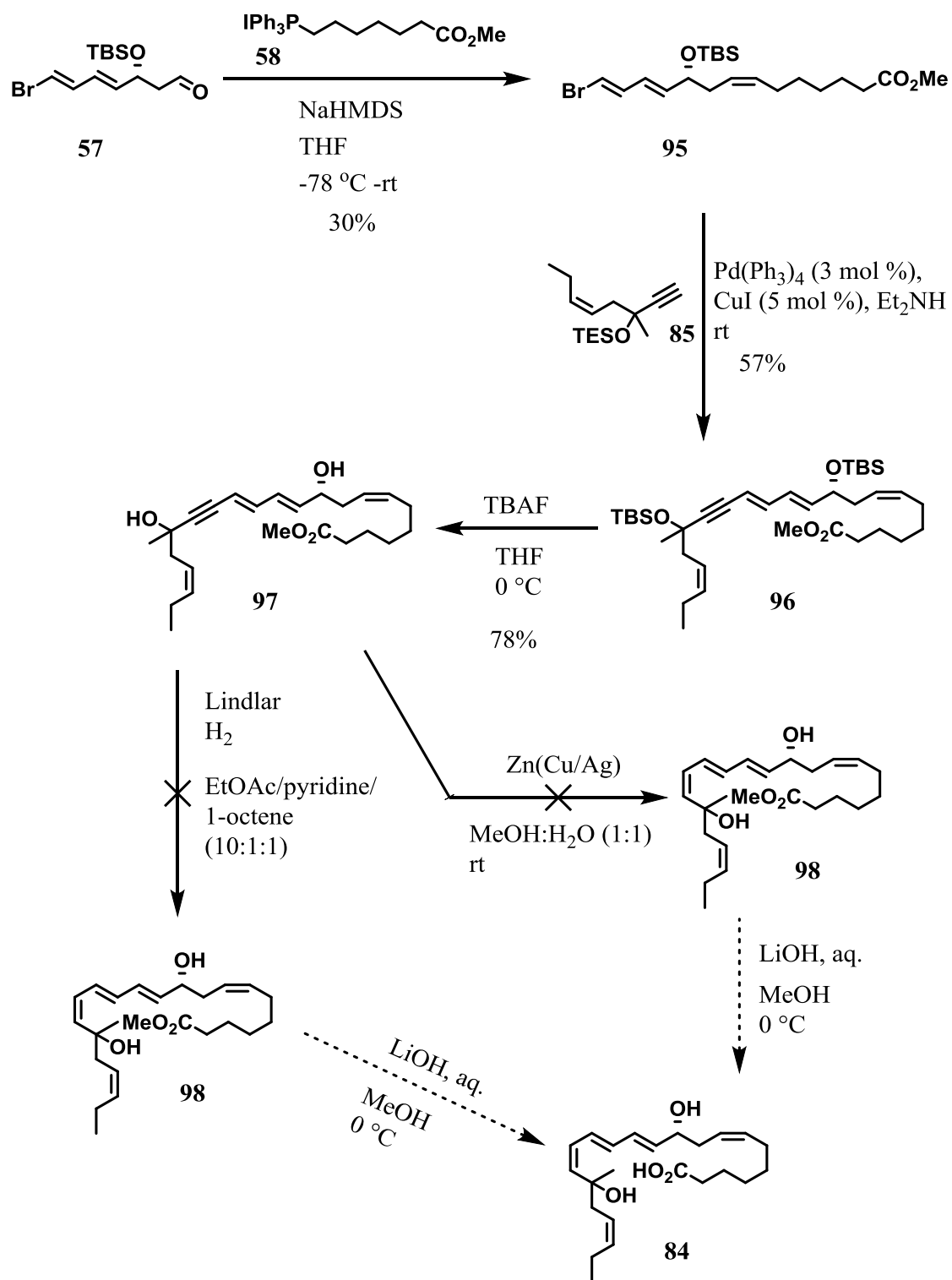
Scheme 13. Final steps in the synthesis of the PD1$_{n-3 \, DPA}$ analog **84**.

2.2 Synthesis of compound 98

2.2.1 Synthesis of 3-methylpent-4-yne-1,3-diol

The first step in the synthesis of the ω-fragment was a Grignard reaction on 4-hydroxybutanone **86**.[73] 4-Hydroxybutanone **86** was reacted with 2.5 equivalents of ethynylmagnesium bromide in THF at 0 °C, under anhydrous conditions under an argon atmosphere (Scheme 14). The reaction mixture was stirred overnight. After acidic work-up, the crude was purified by column chromatography on silica gel to afford the diol **87** in 46% yield as a yellow oil.
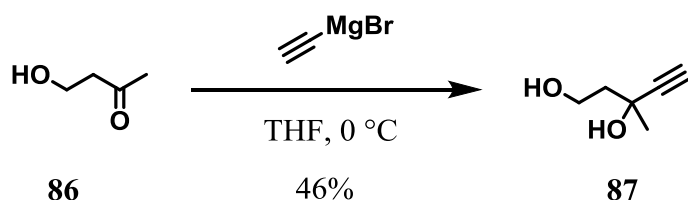
Scheme 14. Synthesis of 3-methylpent-4-yne-1,3-diol (**87**).

2.2.2 Characterization of 3-methylpent-4-yne-1,3-diol

NMR characterization of 3-methylpent-4-yne-1,3-diol

The recorded ^{1}H NMR spectrum shows the methyl group as the most upfield signal at 1.48 ppm, as a singlet integrating for three protons. The acetylenic proton shows up as a singlet integrating for one proton at 2.48 ppm, in the characteristic region for acetylenic protons. The spectra shows two multiplets integrating for two protons each. The two protons from the methylene group vicinal to the primary alcohol give the most downfield multiplet at 3.87 ppm. The two protons from the methylene group vicinal to the tertiary carbon give the most upfield multiplet at 1.90 ppm. The two protons from the alcohol groups do not show up in the spectra. Except for these two protons, the number of protons in the spectra is in accordance with the compound's total of 10 protons.

The ^{13}C NMR spectrum shows six signals, which are in agreement with the molecular formula ($C_6H_{10}O_2$) of the compound and its lack of symmetry. The most downfield signal at

87.0 ppm comes from the internal acetylenic carbon atom, and the signal at 72.1 ppm from the terminal acetylenic carbon. The two signals at 68.5 and 60.3 ppm come from the carbons attached to hydroxyl groups. The signal at 43.4 ppm comes from the methylene carbon vicinal to the tertiary carbon, while the more shielded methyl-carbon gives rise to the signal at 30.5 ppm. This accounts for all 6 carbon atoms in the compound.

The obtained NMR spectra for **87** are in accordance with the previously reported data.[73]

Figure 23. Assignment of ^{1}H and ^{13}C NMR signals for 3-methylpent-4-yne-1,3-diol (**87**).

2.2.3 Synthesis of 3,3,9,9-tetraethyl-5-ethynyl-5-methyl-4,8-dioxa-3,9-disilaundecane

The next step was to protect both alcohol groups of the compound with TES groups.[73] The diol **87** was protected using four equivalents of triethylsilyl trifluoromethanesulfonate (TESOTf), 2,6-lutidine as base, and stirred in in dry CH_2Cl_2 at -78 °C (Scheme 15). The reaction was allowed to slowly heat to room temperature overnight, followed by acidic work-up. After flash chromatography the desired *bis*-protected silyl ether **88** was obtained in 86% yield as a clear oil.
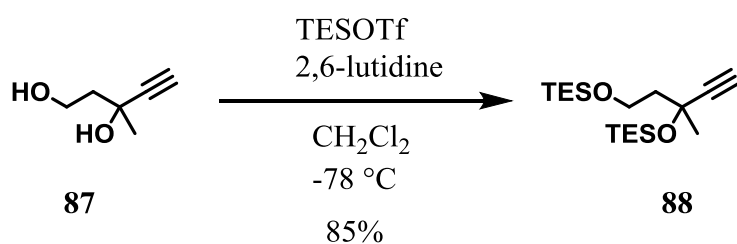
Scheme 15. Synthesis of 3,3,9,9-tetraethyl-5-ethynyl-5-methyl-4,8-dioxa-3,9-disilaundecane (**88**).

2.2.4 Characterization of 3,3,9,9-tetraethyl-5-ethynyl-5-methyl-4,8-dioxa-3,9-disilaundecane

NMR characterization of 3,3,9,9-tetraethyl-5-ethynyl-5-methyl-4,8-dioxa-3,9-disilaundecane

The two most upfield signals in the ^{1}H NMR are due to the two TES-groups in the molecule. The most upfield signal is a multiplet at 0.63 ppm, integrating for 12 protons. These come from the six methylene moieties in the TES groups. The second most upfield signal is a multiplet at 0.97 ppm, which integrates for 18 protons. These come from the six methyl groups in the TES-groups. A singlet integrating for three protons is found at 1.48 ppm, which is caused by the three protons in the methyl group attached to the tertiary carbon atom. The acetylenic proton gives a singlet at 2.41 ppm, which integrates for one proton. The two protons on the methylene that is adjacent to the tertiary carbon show up as a multiplet integrating for two protons at 1.94 ppm. The remaining two protons are those from the carbon bound to the oxygen in the silyl ether. These are more deshielded than the two previous protons, and therefore give a more downfield signal. They appear as the triplet at 3.84 ppm, integrating for two protons. This accounts for all the 38 protons in the compound.

The ^{13}C NMR spectrum shows 10 signals, and this is in agreement with the molecular formula ($C_{18}H_{38}O_2Si_2$) of the compound, and that there are four groups with each containing three equivalent carbon atoms. There should thus be four more signals in the spectra than for the previous compound, due to the TES groups. The internal acetylenic carbon gives the signal at 88.0 ppm, and the terminal acetylenic carbon shows as the signal at 72.1 ppm. The two carbons bound to oxygen show up as the signals at 67.6 and 59.7 ppm. The carbon adjacent to the tertiary carbon atom gives the signal at 47.8 ppm, and the more shielded methyl-carbon appears a signal at 31.6 ppm. The last 12 carbon atoms from the TES groups show up as the four signals at 7.1, 6.9, 6.2 and 4.6 ppm, thus accounting for all 18 carbons in the compound.

The obtained NMR spectra for **88** are in accordance with the previously reported data.[73]
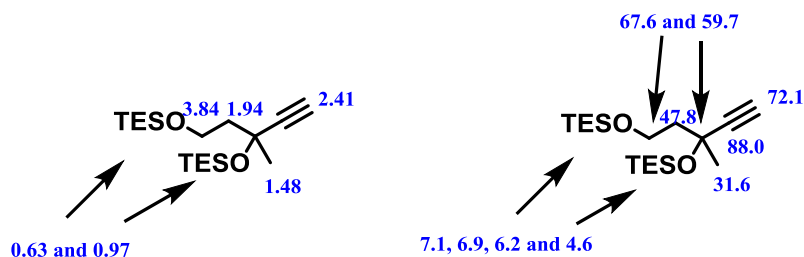
Figure 24. Assignment of ^{1}H and ^{13}C NMR signals for 3,3,9,9-tetraethyl-5-ethynyl-5-methyl-4,8-dioxa-3,9-disilaundecane (**88**).

2.2.5 Synthesis of 3-methyl-3-((triethylsilyl)oxy)pent-4-ynal

The next step in the synthesis was an oxidation of the TES-protected primary alcohol to an aldehyde. This aldehyde was prepared by a Swern oxidation of **88**, see Scheme 16.[73] DMSO was reacted with oxalyl chloride in dry CH_2Cl_2 at -78 °C, forming the reactive chlorodimethylsulfonium chloride intermediate. The *bis*-protected alcohol **88** was added dropwise and the mixture was stirred for 1 hour. Then the reaction mixture was heated to -20 °C by changing the acetone/dry ice cooling bath to a brine/ice cooling bath, and the reaction was stirred at this temperature for another 45 min. The mixture was then re-cooled to -78 °C, and the base Et_3N was added in order to complete the reaction. After aqueous work-up the crude product was purified by flash chromatography, yielding aldehyde **89** in 68 % yield as a yellow oil.
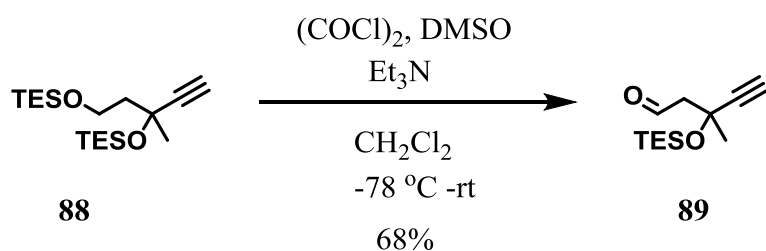
Scheme 16. Synthesis of 3-methyl-3-((triethylsilyl)oxy)pent-4-ynal (**89**).

2.2.6 Characterization of 3-methyl-3-((triethylsilyl)oxy)pent-4-ynal

NMR characterization of 3-methyl-3-((triethylsilyl)oxy)pent-4-ynal

In the recorded ^{1}H NMR spectrum the aldehyde proton is found in its characteristic region as a triplet at 9.89 ppm, integrating for one proton. The two protons of the methylene group adjacent to the aldehyde show up as a doublet at 2.62 ppm, integrating for two protons. Since this signal has the same coupling constant as the aldehyde signal ($J = 2.8$ Hz), this is a further indication that this signal comes from these protons. The acetylenic proton gives the expected singlet at 2.57 which integrates for one proton. At 1.58 the spectra shows a singlet integrating for three protons, and this signal comes from the three protons in the methyl group. The nine protons from the three methyl groups in the TES give the triplet at 0.96 which integrates for nine protons. The remaining six protons from the three methylene moieties in the TES group are found as a quartet of doublets integrating for six protons at 0.70 ppm. Thus, the number of protons in the spectra is in accordance with the total of 22 protons in the compound.

The ^{13}C NMR spectrum shows eight signals, which is as expected since one TES group has been removed. With the removal of one TES group, there are six fewer carbons, amounting to two fewer equivalent carbon atoms in the compound. The signal from the aldehyde is found as the signal most downfield at 201.7 ppm, in the characteristic region for aldehydes. Two signals are observed at 86.6 and 73.9 ppm, which come from respectively the internal and terminal acetylenic carbons, respectively. At 66.4 ppm one finds the signal from the carbon atom attached to the oxygen in the silyl ether. The methylene carbon adjacent to the tertiary carbon atom gives the signal at 57.3 ppm, and the methyl carbon appears as the signal at 31.6 ppm. Most upfield in the spectra two signals show up at 7.0 and 6.1 ppm, which accounts for the six remaining carbon atoms in the TES group. All 12 carbon atoms in the compound are thus accounted for.

The obtained NMR spectra for **89** are in accordance with the previously reported data.[73]
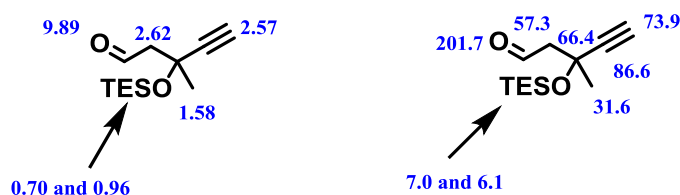
Figure 25. Assignment of ^{1}H and ^{13}C NMR signals for 3-methyl-3-((triethylsilyl)oxy)pent-4-ynal (**89**).

2.2.7 Synthesis of triethyl(((5*Z*)-3-methyloct-5-en-1-yn-3-yl)oxy)silane

This final step in the synthesis of the ω-fragment was a *Z*-selective Wittig reaction on the aldehyde **89** with propyltriphenylphosphonium bromide, as performed previously in our group. (Scheme 17).[73] First the Wittig salt was suspended in dry THF, and HPMA was added as a co-solvent. After cooling the suspension to -78 °C, NaHMDS was added dropwise in order to deprotonate the Wittig salt and thus generate the phosphonium ylide. Then the mixture was briefly taken out of the cooling bath, and stirred at ambient temperature for five minutes to ensure that the mixture was homogenous. Subsequently the mixture was re-cooled to -78 °C, aldehyde **89** was added, and the reaction was allowed to slowly heat to room temperature overnight. After aqueous work-up and purification on column chromatography, the *Z*-alkene **85** was afforded in 65% yield as a colorless oil.
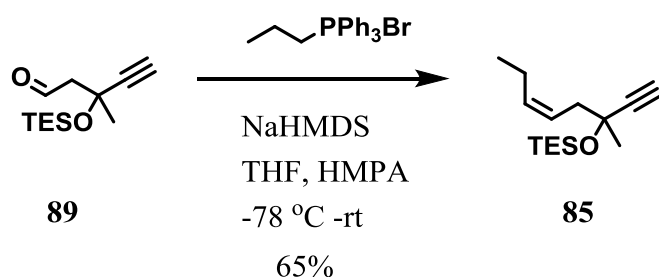
Scheme 17. Synthesis of triethyl(((5*Z*)-3-methyloct-5-en-1-yn-3-yl)oxy)silane (**85**).

2.2.8 Characterization of triethyl(((5*Z*)-3-methyloct-5-en-1-yn-3-yl)oxy)silane

NMR characterization of triethyl(((5*Z*)-3-methyloct-5-en-1-yn-3-yl)oxy)silane

The ^{1}H NMR shows a multiplet at 5.51 ppm, integrating for two protons. This signal is caused by the two *Z*-alkenyl protons, which are expected to give a signal in this region because of the deshielding effects of the π-bond. *Z*-alkenyl protons have smaller coupling constants than *E*-alkenyl protons. The coupling constant for this signal is small ($J = 11.9$ Hz), which is a strong indication that the product is the correct *Z*-isomer. The two protons in the methylene adjacent to the tertiary carbon overlap with the acetylenic proton and give a multiplet at 2.42 which integrates for three protons. The protons from the other methylene moiety appear as a multiplet at 2.05, integrating for two protons. At 0.97 ppm the spectra shows a triplet integrating for 12 protons. This signal comes from the six methyl protons in the TES group, and the three protons from the primary methyl group. The three protons of the methyl group attached to the tertiary carbon atom give the singlet at 1.44 ppm, integrating for three protons. A multiplet is found at 0.69 ppm, integrating for six protons. These are the six protons from the methylene moieties in the TES group. As such, the number of protons in the spectra is in accordance with the compounds total of 28 protons.

In the recorded ^{13}C NMR spectrum there are 11 signals, which is in agreement with the molecular formula of the compound ($C_{15}H_{28}OSi$), and the number of equivalent carbon atoms in the TES group. The aldehyde carbon observed for the previous compound is no longer present in the current ^{13}C spectrum, and this is a good indication that the starting material was consumed in the Wittig reaction. The two most upfield signals at 6.3 and 7.1 ppm come from the six carbons in the TES group. As observed previously, the internal acetylenic carbon gives the signal at 88.5 ppm, and the terminal acetylenic carbon atom causes the signal at 72.0 ppm. The tertiary carbon atom shows as the signal at 69.0 ppm, and the adjacent methylene carbon gives the signal at 42.9 ppm. The peak at 30.6 ppm is caused by the methyl carbon attached to the tertiary carbon. One finds the most downfield signals at 134.3 and 124.1 ppm, and these signals come from the two deshielded alkene carbon atoms. The last two signals in the spectra are found at 21.0 and 14.3 ppm, and come from respectively the ω-2 and ω-1 carbon atoms. As such, all 15 carbon atoms in the compound are accounted for.

The obtained NMR spectra for **85** are in accordance with the previously reported data.[73]
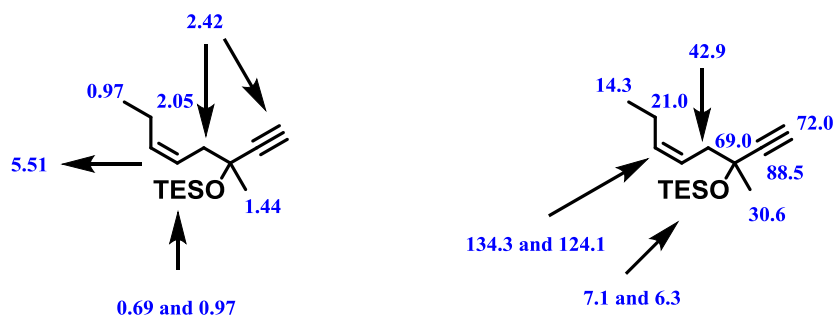
Figure 26. Assignment of ^1H and ^{13}C NMR signals for triethyl(((5Z)-3-methyloct-5-en-1-yn-3-yl)oxy)silane (**85**).

MS characterization of triethyl(((5*Z*)-3-methyloct-5-en-1-yn-3-yl)oxy)silane

In the recorded MS spectrum, the molecular ion peak is the base peak. This peak shows a mass/charge of 275.2, corresponding with the calculated molecular mass of the sodium adduct of **85** (275.2).

The recorded HRMS (HRESTOFMS) spectrum shows a peak with the measured *m/z* of 275.1801. This is very close to the calculated exact mass of 275.1802 for the sodium adduct of compound **85**. More importantly, the error is 0.3 ppm, clearly within the normal 10 ppm error criteria for HRMS spectra.

The obtained MS spectra for **85** are in accordance with the previously reported data.[73]

GC analysis of triethyl(((5*Z*)-3-methyloct-5-en-1-yn-3-yl)oxy)silane

The obtained chromatogram for gas chromatography analysis of **85** shows two peaks with retention times r_t = 7.58 and 8.08 min. Using a non-polar HP-5 column, polar compounds will show lower retention times than non-polar substances. There is a minor peak at 7.58 min, which may be some unreacted aldehyde starting material, while the large peak at 8.08 min is the desired product **85**. Integration of the peaks gives an estimated chemical purity of 98.2%, which is satisfactory for an intermediate compound.

2.2.9 Synthesis of methyl 7-hydroxyheptanoate

The first two steps in the synthesis of the α-fragment **58** was a Baeyer-Villiger oxidation of cycloheptanone **90** with *m*CPBA, followed by a Fisher esterification of the lactone product **91** with MeOH (Scheme 18). This was done as previously reported by Aursnes *et al.*[54] The preparation commenced with dissolving 1.5 equivalents of *m*CPBA in CH_2Cl_2, and cooling the solution to 0 °C. Cycloheptanone **90** was then added, and the reaction mixture was stirred for five days at room temperature. The mixture was filtrated, washed with an aqueous solution of $NaHCO_3$, and concentrated *in vacuo*. This crude lactone product **91** was then dissolved in dry MeOH and stirred at reflux for 24 hours. After the mixture had cooled to ambient temperature, aqueous $NaHCO_3$ was added, and MeOH was evaporated *in vacuo*. The crude product was subjected to basic aqueous work-up and purified by flash column chromatography on silica gel. This yielded the methyl ester **92** as a clear brown oil in 73% yield over two steps from **90**.
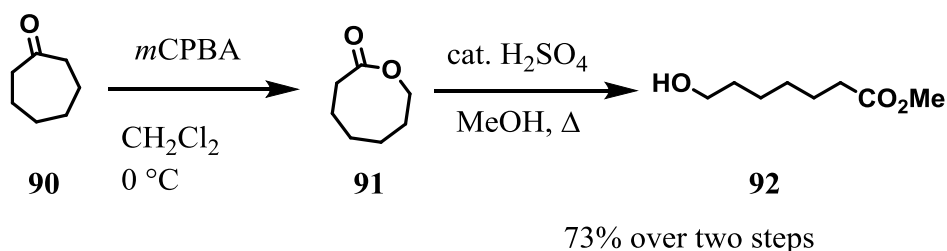
Scheme 18. Synthesis of 7-hydroxyheptanoate (**92**).

2.2.10   Characterization of methyl 7-hydroxyheptanoate

NMR characterization of methyl 7-hydroxyheptanoate

A singlet integrating for three protons are found at 3.66 ppm in the recorded ^{1}H NMR spectrum. This singlet comes from the three protons in the methyl group of the ester. The signal from the two protons on the carbon adjacent the alcohol is located at 3.63 ppm. Since these protons have two neighbor protons, this signal is split into a triplet integrating for two protons. The two α-carbonyl protons show up as a triplet at 2.31 ppm, integrating for two protons. There is a broad singlet at 1.99 ppm, which integrates for one proton. Broad singlets are characteristic for alcohols, so this signal comes from the proton in the primary alcohol.

The remaining eight protons in compound **92** show up as the multiplets in the aliphatic region at 1.60 and 1.47 ppm, integrating for four protons each. This accounts for all the 16 protons in the compound.

There are eight peaks in the ^{13}C NMR, which corresponds with the compound's molecular formula ($C_8H_{16}O_3$) and the lack of symmetry in the molecule. As expected, there is a peak in the carbonyl region at 174.4 ppm. This signal is caused by the carbonyl carbon in the ester. The carbon atom attached the alcohol gives the signal at 63.0 ppm. Because the α-carbonyl carbon is slightly more shielded, this gives the signal at 51.6. The five remaining signals at 34.1, 32.7, 29.0, 25.5 and 25.0 ppm are in the typical aliphatic region of the spectra. These come from the carbon in the methyl group of the ester, and the four remaining carbons in the aliphatic chain. As such, all 8 carbon atoms in the compound have been accounted for.

The obtained NMR spectra for **92** are in accordance with the previously reported data.[54]

Figure 27. Assignment of ^1H and ^{13}C NMR signals for methyl 7-hydroxyheptanoate (**92**).

2.2.11   Synthesis of methyl 7-iodoheptanoate

After preparing the hydroxy-ester **92**, the next step was to utilize a variation of the Appel reaction to convert the alcohol to the corresponding iodide **93**. This was according to the procedure reported by Aursnes *et al.*,[54] see Scheme 19. First the hydroxy-ester **92** was dissolved in dry CH_2Cl_2, followed by addition of triphenylphosphine and imidazole. After cooling the mixture down to -20 °C on an ice/salt/H_2O bath, nearly two equivalents of iodine was added. The reaction was stirred at this temperature for 15 minutes, taken off the bath and stirred an additional 35 minutes at ambient temperature. The mixture was quenched using a saturated aqueous solution of sodium sulfite. This was done in order to convert the remaining elemental iodine into hydroiodic acid, which in turn was neutralized by the imidazole in the reaction mixture. The crude product was purified using column chromatography on silica gel, affording the iodide **93** in 76% yield as a colorless oil.
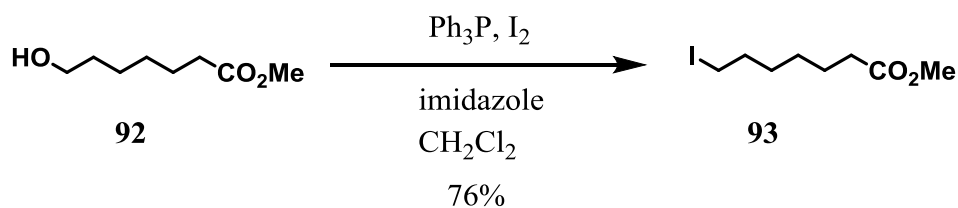
Scheme 19. Synthesis of 7-iodoheptanoate (**93**).

2.2.12 Characterization of methyl 7-iodoheptanoate

NMR characterization of methyl 7-iodoheptanoate

In the recorded ^{1}H NMR the alcohol signal has disappeared, indicating consumption of the starting material. The three protons from the methyl ester group show up as a singlet at 3.66 ppm, which integrates for three protons. The two protons on the α-carbonyl carbon give a triplet at 2.30 ppm, integrating for two protons. This signal shows the same coupling constant ($J = 7.5$ and 7.6 Hz) as the pentet at 1.63 ppm, which also integrates for two protons. The pentet is therefore caused by the two protons on C-3. There is then one remaining triplet integrating for two protons at 3.17 ppm, which must then come from the only other protons which couple with two protons. These are the two protons on the carbon bonded to iodine (C-7). These protons couple with the adjacent two protons on C-6, which appear as the pentet integrating for two protons at 1.81 ppm ($J = 7.0$ Hz). Finally, the multiplet at 1.37 ppm integrates for four protons, and comes from the remaining four protons on carbon number 4 and 5. This accounts for all 15 protons in the compound. There are some additional signals around 7.3-7.9 ppm, characteristic for aromatic protons. It is possible that these signals come from remaining triphenylphosphine oxide, which is a major byproduct in the Appel reaction.

The recorded ^{13}C NMR spectrum shows eight signals, in accordance with the molecular formula of the compound ($C_8H_{15}O_3I$). As previously, the carbonyl carbon in the ester gives a signal at 174.1 ppm. The α-carbonyl carbon atom also shows as the expected signal at 51.6 ppm. There are then six signals left at 34.0, 33.4, 30.2, 28.1, 24.8 and 7.0. ppm. These signals arise from the remaining five carbons in the aliphatic chain, as well as the methyl carbon in the ester group. In addition there seems to be some weak signals in the aromatic region between 125-135 ppm. These may come from some remaining triphenylphosphine oxide. All eight carbon atoms in the compound have thus been accounted for.

The obtained NMR spectra for **93** are in accordance with the previously reported data.[54]

Figure 28. Assignment of ^{1}H and ^{13}C NMR signals for methyl 7-iodoheptanoate (**93**).

2.2.13 Synthesis of (7-methoxy-7-oxoheptyl)triphenylphosphonium iodide

The final step in the synthesis of the α-fragment was the preparation of the Wittig salt **58** from iodide **93**, as previously reported by Aursnes *et al.*[54] Iodide **93** was refluxed with an excess of triphenylphosphine in dry acetonitrile for 12 hours (Scheme 20). The crude product was purified using column chromatography, affording the Wittig salt **58** in 87% yield as a sticky oil.
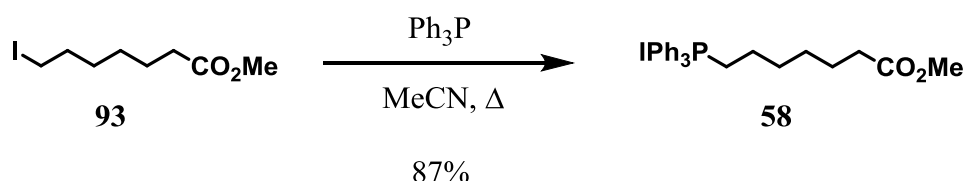
Scheme 20. Synthesis of (7-methoxy-7-oxoheptyl)triphenylphosphonium iodide (**58**).

2.2.14 Characterization of (7-methoxy-7-oxoheptyl)triphenylphosphonium iodide

NMR characterization of (7-methoxy-7-oxoheptyl)triphenylphosphonium iodide

The fifteen aromatic protons in **58** shown in the ^{1}H NMR spectrum as a multiplet integrating for 15 protons. This signal shows at 7.75 ppm, in the aromatic region. The singlet at 3.60 ppm integrating for three protons corresponds with the protons from the methyl group of the ester. The two protons in α position to the carbonyl show up as the triplet at 2.24 ppm, integrating for two protons. The electronegativity of phosphorus makes the two adjacent methylene

protons deshielded as well, and these give the multiplet integrating for two protons at 3.66 ppm. The last eight protons in the compound give the two multiplets at 1.60 and 1.30 ppm, which integrate for respectively six and two protons. All of the 30 protons in the compound are thus accounted for.

There are 13 signals in the recorded ^{13}C NMR spectrum, which is in agreement with the molecular formula ($C_{26}H_{30}IO_2P$) and the number of equivalent carbon atoms of the compound. The most downfield signal at 174.2 ppm comes from the carbonyl carbon in the ester. There are four non-equivalent carbon atoms in the triphenylphosphine group, which corresponds with the four doublets at 135.2, 133.8, 130.7 and 118.2 ppm in the aromatic region of the spectra. This accounts for the 18 aromatic carbon atoms in the compound. The carbon which is adjacent the carbonyl is more deshielded than regular alkyl carbons, and thus gives the signal at 51.5 ppm. The carbon in position 7 is directly attached to a phosphorous atom, and is therefore expected to give a doublet in ^{13}C NMR spectra. As such, this carbon most probably gives the doublet at 30.1 ppm. There are five remaining carbon atoms in the compound; the four alkane carbons number 3, 4, 5, and the methyl carbon in the ester. These show up as the five signals in the alkyl region at 33.9, 28.6, 24.4, 23.2, and 22.5 ppm. Thus all 26 carbon atoms in the compound are accounted for.

The obtained NMR spectra for **58** are in accordance with the previously reported data.[54]

Figure 29. Assignment of ^{1}H and ^{13}C NMR signals for (7-methoxy-7-oxoheptyl)triphenylphosphonium iodide (**58**).

2.2.15 Synthesis of (3*R*,4*E*,6*E*)-7-bromo-3-((*tert*-butyldimethylsilyl)oxy)hepta-4,6-dienal

The middle fragment aldehyde **57** was prepared by a DIBAL-H reduction of the protected thiazolidinethione **94**, which provided by Aursnes *et al.*[54] The reduction was performed as previously reported,[54] see Scheme 21. Thiazolidinethione **94** was dissolved in dry CH_2Cl_2, cooled to -78 °C, and stirred under argon. Then 1.3 equivalents of DIBAL-H were slowly added to the solution in a dropwise manner. The mixture was stirred at the above-mentioned temperature for 2.5 hours. TLC analysis of the mixture, revealed incomplete conversion of the thiazolidinethione to the aldehyde. Additional 0.65 equivalents of DIBAL-H was therefore added and the mixture was allowed to stir for two more hours. The reaction was quenched with aqueous $NaHCO_3$, and Rochelle Salt® (Na-K tartrate) was added to break the emulsion caused by the formation of aluminum hydroxide. After work-up and evaporation, the crude product was purified by column chromatography to afford aldehyde **57** in 77% yield as a yellow oil.
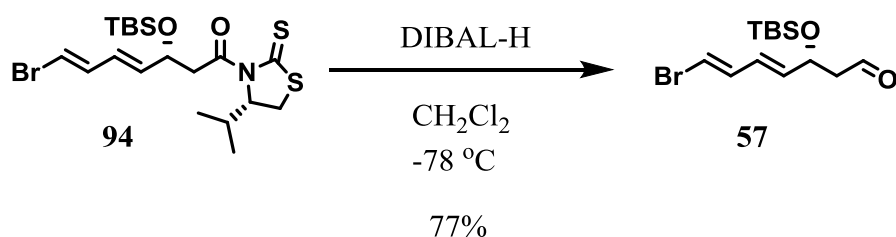
Scheme 21. Synthesis of (3*R*,4*E*,6*E*)-7-bromo-3-((*tert*-butyldimethylsilyl)oxy)hepta-4,6-dienal (**57**).

2.2.16 Characterization of (3*R*,4*E*,6*E*)-7-bromo-3-((*tert*-butyldimethylsilyl)oxy)hepta-4,6-dienal

NMR characterization of (3*R*,4*E*,6*E*)-7-bromo-3-((*tert*-butyldimethylsilyl)oxy)hepta-4,6-dienal

In the recorded ^{1}H NMR spectrum the aldehyde proton is found as expected as a triplet at 9.76 ppm, integrating for one proton. There are 15 protons in the TBS protecting group. Nine of these are in the *tert*-butyl group and give the singlet at 0.88 ppm, integrating for nine protons. The remaining six protons come from the two methyl groups, and these give the two singlets

at 0.07 and 0.04 ppm, integrating for two protons each. There are four protons in the conjugated *E,E* alkene system in this compound. There is a doublet at 6.34 ppm with a coupling constant of $J = 13.5$ Hz, integrating for one proton. This is indicative of an *E*-alkene. The only alkene proton that only couples with one other proton is that in the 7 position, on the carbon atom attached to the bromine. Therefore, the signal at 6.34 is from this proton. The most downfield signal is the doublet of doublets at 6.70 ppm, which integrates for one proton. Since this signal has the same coupling constant ($J = 13.5$ Hz) as the proton in the 7 position, this signal must come from the alkenyl proton in the 6 position. This signal also has a coupling constant of $J = 10.9$ Hz, which is the same as the signal at 6.17 ppm ($J = 10.7$ Hz). Because of this, and since the signal at 6.17 ppm integrates for one proton, this signal is caused by the alkenyl proton in the 5 position. Both the signal at 6.17 and 5.76 has the same coupling constant ($J = 15.0$ and $J = 15.2$ Hz), and the signal at 5.76 integrates for one proton. So this signal is caused by the alkenyl proton in the 4 position. The proton attached to the tertiary carbon atom gives the doublet of doublets at 4.67 ppm, integrating for one proton. The last two protons in the compound are those on the methylene carbon, and these give rise to the multiplet at 2.59 ppm, which integrates for two protons. This accounts for all the 23 protons in this compound. There is an additional singlet at 5.30 ppm, which corresponds to the characteristic signals caused by trace amounts of the solvent CH_2Cl_2.[74]

There are 11 signals in the recorded ^{13}C NMR, which corresponds with the molecular formula of the compound ($C_{13}H_{23}BrO_2Si$), and the symmetry of the TBS protecting group. The characteristic signal for aldehydes is found at 201.0 ppm. There are four alkenyl carbons in this compound, and they are expected to give signals approx. in the 100-170 ppm region. In this spectra, these alkenyl carbons give the signals at 136.6, 136.2, 127.6 and 109.6 ppm. From the α-carbonyl carbon one finds the signal at 51.5 ppm, and the slightly more deshielded carbon atom attached to the oxygen shows as the signal at 68.6 ppm. There are then four remaining signals, which come from the TBS group. The three equivalent methyl carbons in the *tert*-butyl moiety show up as the signal at 18.3 ppm, and the signal from the quaternary carbon appears as the slightly more downfield signal at 25.9. Then the two last carbon atoms are those in the two methyl groups directly attached to the silicone. Because of the shielding effect of silicone, these diastereotopic carbons give the two signals at -4.2 and -4.8 ppm. All 13 carbon atoms are thus accounted for.

The obtained NMR spectra for **57** are in accordance with the previously reported data.[54]
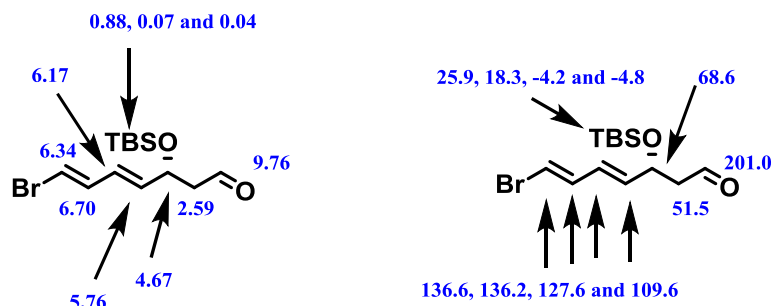
Figure 30. Assignment of ^{1}H and ^{13}C NMR signals for (3R,4E,6E)-7-bromo-3-((*tert*-butyldimethylsilyl)oxy)hepta-4,6-dienal (**57**).

2.2.17   Synthesis of methyl (10R,7Z,11E,13E)-14-bromo-10-(*tert*-butyldimethylsilyl)oxy)tetradeca-7,11,13-trienoate

The α- and the middle fragments were connected by a *Z*-selective Wittig reaction between aldehyde **57** and the ylide from phosphonium salt **58**, performed according to the procedure of Aursnes *et al.*[54] (Scheme 22). The phosphonium salt **58** was first dissolved in dry THF and cooled to -78 °C. NaHMDS was then added to deprotonate the phosphonium salt, and the mixture was stirred for one hour. Aldehyde **57** was dissolved in dry THF, and slowly added to the solution containing the ylide. The reaction was stirred for 24 hours, allowing the solution to slowly warm to ambient temperature. After aqueous work-up and flash chromatography the product **95** was obtained as a pale yellow oil in 30% yield.
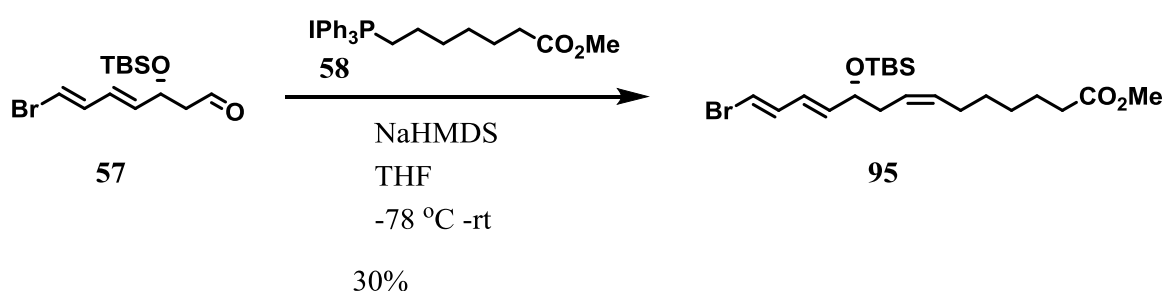
Scheme 22. Synthesis of methyl (10R,7Z,11E,13E)-14-bromo-10-(*tert*-butyldimethylsilyl)oxy)tetradeca-7,11,13-trienoate (**95**).

2.2.18 Characterization of methyl (10*R*,7*Z*,11*E*,13*E*)-14-bromo-10-(*tert*-butyldimethylsilyl)oxy)tetradeca-7,11,13-trienoate

NMR characterization of methyl (10*R*,7*Z*,11*E*,13*E*)-14-bromo-10-(*tert*-butyldimethylsilyl)oxy)tetradeca-7,11,13-trienoate

In the recorded ^{1}H NMR spectrum there are a total of 37 protons, which corresponds with the molecular formula for this compound ($C_{21}H_{37}BrO_3Si$). The product of this Wittig reaction is a *Z*-alkene between carbon 7 and 8. There are two protons in this carbon-carbon double bond, and they show up as the multiplet at 5.39, which integrates for two protons. Evidence that the double bond is *Z* and not *E* comes from the coupling constant of this signal. The idealized first order signal for these two protons should be a doublet of triplets, but the recorded spectra shows a more complex multiplet. After careful consideration of the peaks however, it was possible to calculate the coupling constant $J = 12.3$ Hz, which indicates a *Z*-alkene. The TBS group contains 15 protons, and nine of these are in the *tert*-butyl group. These give the singlet at 0.89 ppm, integrating for nine protons. The other six protons come from the two methyl groups attached to the silicone, and these give the two singlets at 0.05 and 0.02 ppm, integrating for three protons each. As for the aldehyde starting material, there are four *E*-alkene protons in this compound, and they give similar signals for this compound as well. The doublet at 6.27 ppm integrating for one proton is caused by the proton in the 14 position. This proton couples with the proton in the 13 position, which shows as the doublet of doublets integrating for one proton at 6.68 ppm. Evidence for this is that their signals have the same coupling constant ($J = 13.6$ and 13.5 Hz). The proton in the 13 position also couples with the doublet of doublets at 6.08 ppm ($J = 10.8$ ppm). This signal integrates for one proton, and is therefore expected to come from the alkenyl proton in the 12 position. The signal at 6.08 ppm also couples with the signal at 5.72 ppm ($J = 15.2$ Hz). The signal at 5.72 ppm integrates for one proton, and is thus caused by the proton in the 11 position. The proton on the tertiary carbon shows as the doublet of doublets at 4.14 ppm, which integrates for one proton. There are two protons on the methylene carbon between the *Z*-alkene and the silyl ether, (in the 9 position), and these appear as the multiplet at 2.48 ppm, integrating for two protons. The two protons in the α-position to the carbonyl couple with the two adjacent protons to give the triplet integrating for two protons at 2.30 ppm. The three protons in the methyl ester moiety give the singlet integrating for three protons at 3.67 ppm. The two protons in the 6 position have three neighboring protons, and thus show up as the quartet integrating for two protons at

2.01 ppm. The last protons in the compound are from position 3, 4 and 5. They appear as the quintet at 1.62 ppm and the multiplet at 1.36 ppm, integrating for respectively two and four protons. This accounts for all 37 of the protons in this compound.

There are 19 signals in the recorded ^{13}C NMR spectrum, in agreement with the compounds molecular formula ($C_{21}H_{37}BrO_3Si$) and the symmetry in the TBS protecting group. The most downfield peak at 174.3 ppm comes from the carbonyl carbon in the ester. There are six alkenyl carbon atoms in this compound, and these show up as the six signals at 138.1, 137.2, 131.9, 126.6, 125.2 and 108.2 ppm. The signal at 72.7 ppm comes from the carbinol in the silyl ether, and the more shielded α-carbonyl carbon gives the signal at 51.6 ppm. In the *tert*-butyl moiety in the TBS group there are three equivalent methyl carbons, showing as the signal at 18.4 ppm. The two diastereotopic carbons in the methyl groups directly bonded to silicone show up as the signals at -4.4 and -4.6 ppm. Then there are remaining seven signals at 36.3, 34.2, 29.4, 29.0, 27.4, 26.0 and 25.0 ppm, which come from carbon number 3, 4, 5, 6, 8, the tertiary carbon in the TBS group and the methyl carbon in the ester. This accounts for all 21 carbon atoms in this compound.

The obtained NMR spectra for **95** are in accordance with the previously reported data.[54]
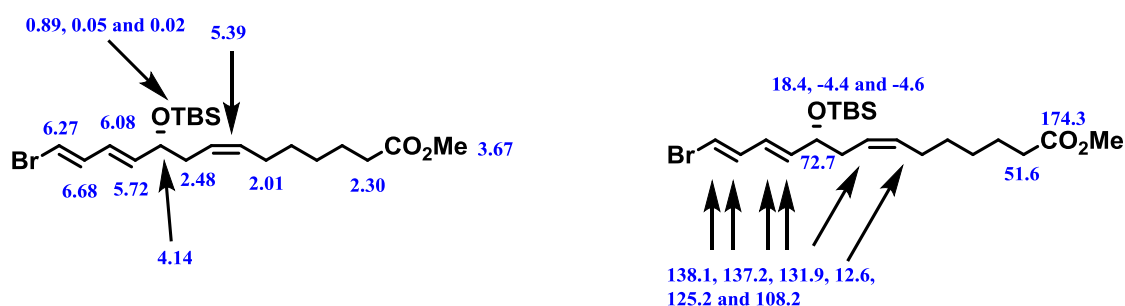
Figure 31. Assignment of ^{1}H and ^{13}C NMR signals for methyl (10*R*,7*Z*,11*E*,13*E*)-14-bromo-10-(*tert*-butyldimethylsilyl)oxy)tetradeca-7,11,13-trienoate (**95**).

Specific optical rotation of methyl (10*R*,7*Z*,11*E*,13*E*)-14-bromo-10-(*tert*-butyldimethylsilyl)oxy)tetradeca-7,11,13-trienoate

The specific optical rotation of compound **95** was calculated to be $[\alpha]^{20}_D$ −11 (*c* = 0.1, MeOH). This is somewhat lower than the previously reported value of $[\alpha]^{20}_D$ −18 (*c* = 0.09, MeOH)[54], though the sign of the value is the same, and the values are in the same order of magnitude. There are several experimental uncertainties that can explain this difference. Calculation of the specific rotation is very sensitive to concentration of the compound. Therefore even small errors in weighing out the compound or measuring the volume of solvent can have a significant effect on the calculated specific rotation. Furthermore, calculation of specific rotation is temperature-specific. The older polarimeter used for the previously reported value did not have temperature control, so it is not certain that the temperature actually was 20 °C. However, the values were not obtained on the same instrument. The polarimeter used for this thesis did have temperature control, so it is possible that -11° is a more accurate value for this compound.

2.2.19 Synthesis of methyl (7*Z*,10*R*,11*E*,13*E*,19*Z*)-10-((*tert*-butyldimethylsilyl)oxy)-17-methyl-17-((triethylsilyl)oxy)docosa-7,11,13,19-tetraen-15-ynoate

The ω-fragment **85** was connected to the vinyl bromide **95** by a Sonogashira coupling as shown in Scheme 23. First the vinyl bromide **95** was dissolved in Et_2NH and benzene. The solution was then added 3 mol % of the catalyst $Pd(PPh_3)_4$, and the mixture was stirred for 45 minutes while protected from light. CuI was added in 5 mol %, before dropwise addition of a solution of alkyne **85** in a small amount of Et_2NH. This mixture was stirred for 20 hours at room temperature, before acidic work-up. The crude product was purified on column chromatography, affording the desired product **96** in 57% yield as a yellow oil.
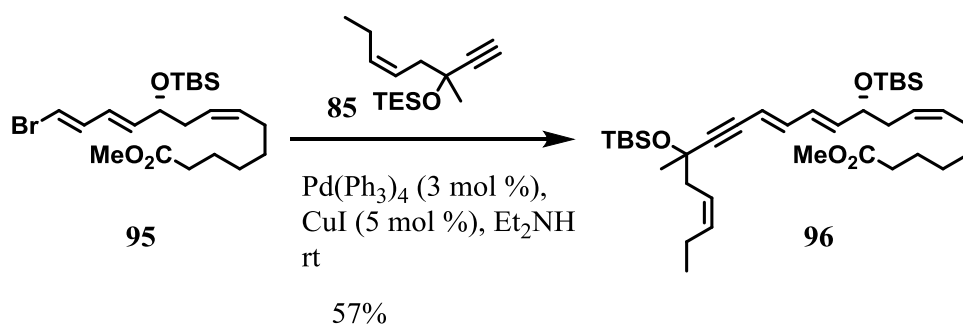
Scheme 23. Synthesis of methyl (7*Z*,10*R*,11*E*,13*E*,19*Z*)-10-((*tert*-butyldimethylsilyl)oxy)-17-methyl-17-((triethylsilyl)oxy)docosa-7,11,13,19-tetraen-15-ynoate (**96**).

2.2.20 Characterization of methyl (7*Z*,10*R*,11*E*,13*E*,19*Z*)-10-((*tert*-butyldimethylsilyl)oxy)-17-methyl-17-((triethylsilyl)oxy)docosa-7,11,13,19-tetraen-15-ynoate

NMR characterization of methyl (7*Z*,10*R*,11*E*,13*E*,19*Z*)-10-((*tert*-butyldimethylsilyl)oxy)-17-methyl-17-((triethylsilyl)oxy)docosa-7,11,13,19-tetraen-15-ynoate

The ^{1}H spectrum shows signals integrating for a total of 64 protons, corresponding with the molecular formula of the expected coupling product ($C_{36}H_{64}O_4Si_2$). The spectrum shows a doublet at 0.04 ppm, integrating for six protons. This comes from the six protons from the two methyl groups directly bonded to silicone in the TBS group. The nine protons in the *tert*-butyl group in TBS give the singlet at 0.89, integrating for nine protons. The signal at 0.67 ppm integrates for six protons, and is caused by the three methylene moieties in the TES group. These protons couple with those on the neighboring methyl groups, splitting the signal to a quartet. The nine methyl protons in the TES group should show up as a triplet integrating for nine protons. In this spectra though, their signal overlap with the signal from the three protons in the ω-methyl moiety, giving a multiplet integrating for 12 protons at 0.98 ppm. The three protons from the methyl ester give the singlet at 3.67 ppm, integrating for three protons. There are three protons from the 17-methyl, which show as a singlet at 1.43 ppm, integrating for three protons. The proton attached to carbon number 10 shows up as the multiplet at 4.19 ppm, integrating for one proton. The two protons in α-position to the carbonyl give the triplet integrating for two protons at 2.30 ppm. The doublet of doublets at 6.19 integrating for one

proton comes from the alkenyl proton on carbon number 13. This proton couples with the neighboring proton on carbon number 14, which shows as the signal at 6.49 ppm, integrating for one proton. These signals show the same coupling constants (J = 15.5, 10.9 Hz and J = 15.2, 11.4 Hz). The alkenyl proton on carbon number 12 also couples with the proton on carbon number 13 (, J = 15.0, 5.8 Hz), and therefore give the signal at 5.76 ppm, integrating for one proton. There is a multiplet at 5.42 ppm, which integrates for five protons. This signal comes from the four protons in the two Z-alkenyl groups, as well as the last E-alkenyl proton in position number 11. The signals from the four protons on carbon number 6 and 18 overlap and show as a multiplet at 2.42 ppm, integrating for four protons. On C-21, the two protons give a multiplet at 2.24 ppm, which integrates for two protons. The two protons on carbon number 9 give the triplet at 2.42 ppm, integrating for two protons. The remaining signals are a quintet at 1.62 ppm, integrating for two protons, and a multiplet at 1.31 integrating for four protons. These two signals come from the six protons on carbon number 3, 4, and 5. Thus all protons in the compound have been accounted for.

The recorded ^{13}C NMR shows 30 signals, which corresponds with the molecular formula of the compound ($C_{36}H_{64}O_4Si_2$) and the equivalent carbon atoms from the TBS and TES groups. ^{13}C NMR spectra from the starting materials vinyl bromide and alkyne gave respectively 19 and 11 signals, so the coupling product was expected to give 30 signals. As previously, the carbonyl peak is found downfield at 174.3 ppm. There are eight alkenyl carbons in this compound, giving the signals at 140.9, 139.3, 134.2, 131.9, 128.7, 125.4, 124.4 and 110.7 ppm. The two acetylenic carbon atoms appear as the two peaks at 96.4 and 83.2 ppm. At 72.9 ppm the signal from the alkoxy carbon in position 10 is located, while the tertiary alkoxy carbon in the 17 position shows up as the peak at 69.6 ppm. The signal at 51.6 ppm comes from the carbon in α-position to the carbonyl. The most upfield signals are found at -4.3 and -4.6 ppm, and come from the two diastereotopic methyl carbon atoms attached to silicone in the TBS protecting group. Signals from the two non-equivalent carbons in the TES group are found at 6.3 and 7.2 ppm. The remaining 12 signals at 43.0, 36.4, 34.2, 30.6, 29.4, 29.0, 27.4, 26.0, 25.0, 21.0, 18.4 and 14.4 ppm are in the typical alkane region of the spectra. These signals come from the carbons in position 3, 4, 5, 6, 9, 18, 21, 22, the 17-methyl carbon, the methyl ester carbon, the quaternary carbon in the TBS, and the three equivalent methyl carbons from the *tert*-butyl moiety in the same group. As such, all 36 carbon atoms in the compound have been accounted for.

MS characterization of methyl (7*Z*,10*R*,11*E*,13*E*,19*Z*)-10-((*tert*-butyldimethylsilyl)oxy)-17-methyl-17-((triethylsilyl)oxy)docosa-7,11,13,19-tetraen-15-ynoate

In the recorded MS spectrum, the molecular ion peak is the base peak, which shows a *m/z* of 639.4. This corresponds with the calculated molecular mass of the sodium adduct of compound **96** (also 639.4).

The HRMS (HRESTOFMS) spectrum shows a peak at *m/z* 639.4232, close to the calculated exact mass of 639.4235 for the sodium adduct of compound **96**. The error is 0.5 ppm; satisfactorily within the 10 ppm error criteria for HRMS spectrums.

2.2.21 Synthesis of methyl (7*Z*,10*R*,11*E*,13*E*,19*Z*)-10,17-dihydroxy-17-methyldocosa-7,11,13,19-tetraen-15-ynoate

The two protecting groups were removed by a reaction of the *bis*-protected silyl ether **96** with TBAF, performed according to the procedure of Aursnes *et al.*[54] (Scheme 24). The TES/TBS-protected alcohol **96** was dissolved in dry THF, cooled to 0 °C and the solution was added 5 equivalents of TBAF. When the mixture had stirred for seven hours, phosphate buffer (pH = 7.2) was added to quench the reaction. After work-up and purification by column chromatography, the diol **97** was afforded in 78% yield as a pale yellow oil.
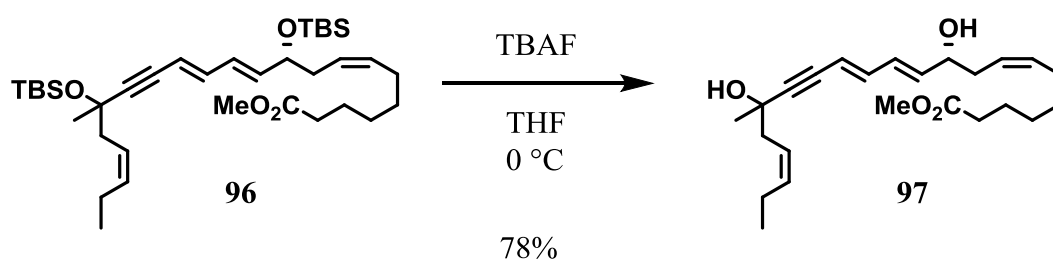
Scheme 24. Synthesis of methyl (7*Z*,10*R*,11*E*,13*E*,19*Z*)-10,17-dihydroxy-17-methyldocosa-7,11,13,19-tetraen-15-ynoate (**97**).

2.2.22 Characterization of methyl (7*Z*,10*R*,11*E*,13*E*,19*Z*)-10,17-dihydroxy-17-methyldocosa-7,11,13,19-tetraen-15-ynoate

NMR characterization of methyl (7*Z*,10*R*,11*E*,13*E*,19*Z*)-10,17-dihydroxy-17-methyldocosa-7,11,13,19-tetraen-15-ynoate

The signals in the ^{1}H NMR spectrum integrate for a total of 36 protons, consistent with the molecular formula of the compound ($C_{24}H_{36}O_4$). A singlet is observed at 3.66 ppm, integrating for three protons. This signal is caused by the three protons from the methyl ester. Another singlet is found at 1.43 ppm, also integrating for three protons. This singlet comes from the three protons on the tertiary methyl group in position 17. The doublet of doublets at 6.28 ppm integrates for one proton, and comes from the alkenyl proton on carbon number 13. Coupling constants (15.8, 10.0 Hz) reveal that this proton couples with the doublet of doublets integrating for one proton at 6.53 ppm (15.5, 10.8 Hz), which must be caused by the alkenyl proton on carbon number 14. The proton on alkenyl carbon number 12 also couple with the one on carbon 13, and is found as the doublet of doublets at 5.81 ppm, integrating for one proton. The last *E*-alkenyl proton on carbon number 11 is found as a doublet at 5.66 ppm, which integrates for one proton. There are four *Z*-alkenyl protons in this compound, on carbon 7, 8, 19 and 20. The signals from these protons overlap, giving a multiplet at 5.48 ppm, integrating for four protons. A multiplet integrating for one proton is found at 4.13 ppm, which comes from the proton on carbon number 10. Three multiplets are found at 2.44, 2.28 and 2.10 ppm, integrating for a total of nine protons. These signals are caused by the eight protons on carbon number 6, 9, 18 and 21, in addition to one proton from one of the alcohols in the compound. The other alcohol gives a broad singlet at 1.70 ppm, which integrates for one proton. Most upfield in the spectra at 0.99 ppm, there is a triplet integrating for three protons. This signal is caused by the three methyl protons on the terminal carbon number 22. The pentet at 1.62 ppm integrates for two protons, and is caused by the two protons on carbon number 3, which couple with those on the α-carbonyl ($J = 7.4$ Hz), which show up as the triplet at 2.33 ppm, integrating for two protons. There are then four remaining protons from carbon number 4 and 5, which give the multiplet at 1.35 ppm, integrating for four protons. As such, all 36 protons in the compound have been accounted for.

There are 24 signals in the recorded ^{13}C NMR, in agreement with the compounds molecular formula ($C_{24}H_{36}O_4$) and the lack of symmetry in the molecule. The carbonyl signal from the ester is found downfield in the spectra at 176.0 ppm. There are eight alkenyl carbons in the

compound, which appear as the eight signals at 142.3, 139.7, 135.4, 132.9, 130.3, 126.1, 124.9 and 111.8 ppm. As before, the two acetylenic carbons give signals at 96.3 and 83.0 ppm. The carbon in position 10, in the secondary alcohol gives the signal at 72.8 ppm, while the tertiary alcohol carbon in position 17 shows as the peak at 68.9 ppm. The signal at 52.0 ppm is caused by the α-carbonyl carbon. Then there are 10 signals remaining in the alkane region of the spectra, at 42.3, 36.3, 34.8, 30.3, 29.4, 28.2, 25.9, 24.8, 21.8 and 13.9 ppm. These signals come from the last 10 carbon atoms in position 3, 4, 5, 6, 9, 18, 21, 22, the tertiary carbon in position 17 and the carbon in the methyl ester. Thus, all 24 carbon atoms in the compound have been accounted for.

MS characterization of methyl (7*Z*,10*R*,11*E*,13*E*,19*Z*)-10,17-dihydroxy-17-methyldocosa-7,11,13,19-tetraen-15-ynoate

In the recorded MS spectrum, the base peak does not correspond to the mass of the molecular ion or its sodium adduct. The peak from the sodium adduct is found in a very low intensity of 1.5% at *m/z* 411.3. The base peak shows an m/z of 242.3, which must be a highly stable fragment of diol **97**.

The recorded HRMS spectrum shows a peak at *m/z* 411.2508, which approximates the calculated exact mass of 411.2506 of the sodium adduct of diol **97**, within the normal 10 ppm error criteria.

2.3 Attempted synthesis of compound 99

2.3.1 Synthesis of methyl (7*Z*,10*R*,11*E*,13*E*,15*Z*,19*Z*)-10,17-dihydroxy-17-methyldocosa-7,11,13,15,19-pentaenoate

A *Z*-selective Lindlar reduction was attempted in order to prepare the *Z*-alkene **98** from internal alkyne **97**.The reaction was done according to the procedure of Aursnes *et al.,*[54] shown in Scheme 25. A mixture of EtOAc:pyridine:1-octene (10:1:1) was used to dissolve alkyne **97**. Lindlar's catalyst was added to the solution, which was evacuated using a rotary evaporator, and then refilled with argon. Placing the flask under a balloon filled with hydrogen gas, the mixture was stirred for seven hours. The reaction mixture was then concentrated *in vacuo* and directly purified by chromatography, yielding 7 mg of a pale yellow oil.
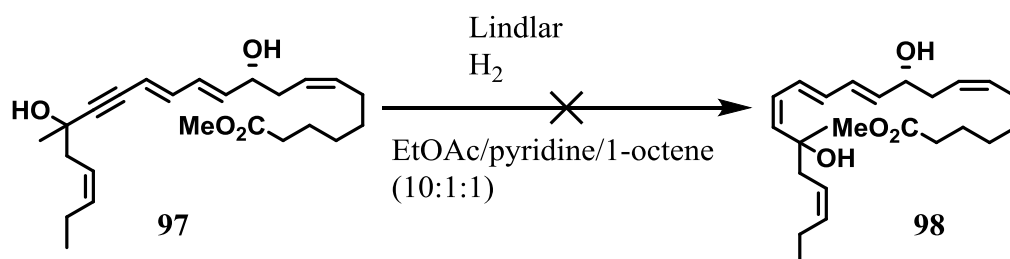
Scheme 25. Attempted synthesis of methyl (7Z,10R,11E,13E,15Z,19Z)-10,17-dihydroxy-17-methyldocosa-7,11,13,15,19-pentaenoate (**98**).

2.3.2 NMR characterization of methyl (7*Z*,10*R*,11*E*,13*E*,15*Z*,19*Z*)-10,17-dihydroxy-17-methyldocosa-7,11,13,15,19-pentaenoate

The recorded ^{1}H spectrum shows signals with high intensity in the typical alkane region. There are some very weak signals in the region where alkenes typically resonate.

The ^{13}C NMR also shows peaks in the alkane region, and no visible signals from any alkenyl carbons.

A typical problem with semi-hydrogenation of alkynes is that it often is difficult to stop the reaction at the alkene, even with poisoned catalysts like the Lindlar variant. This results in over-reduction of one or more alkene groups to alkanes.

Another problem lies in the chemical instability of **97**. It has a secondary alcohol in C-10, and a tertiary alcohol in C-17. Both of these, and particularly the tertiary alcohol are prone to dehydration by E1 mechanism. Dehydration is even further favored because the reaction leads to a conjugated product.

From the recorded NMR data, it seems to be very likely that over-reduction and possibly dehydration occurred during the Lindlar reduction of **97**, which failed to afford the desired compound **98**.

The reaction was monitored by TLC analysis, and additionally utilizing $AgNO_3$-impregnated TLC plates since this has been experienced by members of the LIPCHEM group to give better separation of alkynes and alkenes. No change in R_f was observed during the reaction, so it was difficult to ascertain when the reaction was complete. Only after purification by flash chromatography on silica, an increased R_f was observed. This problem could probably have been improved by monitoring the reaction by GC or LC, which unfortunately was not available at the time.

2.3.3 Synthesis of methyl (7*Z*,10*R*,11*E*,13*E*,15*Z*,19*Z*)-10,17-dihydroxy-17-methyldocosa-7,11,13,15,19-pentaenoate

A Boland reduction[75] was then attempted to reduce alkyne **97** to *Z*-alkene **98** (Scheme 26). As previously reported, zinc dust was activated with $Cu(OAc)_2$ and $AgNO_3$, filtered and then washed sequentially with H_2O, MeOH, acetone and Et_2O. The activated zinc was added to a solution of alkyne **97** in MeOH and H_2O (1:1) which was allowed to stir under argon at room temperature and protected from light. TLC analysis gave no indication of the progression of the reaction after 2.5 hours, so the reaction mixture was filtered through a small pad of Celite to remove the activated zinc, subjected to aqueous work-up and purified by column chromatography on silica gel to yield 3 mg of a pale yellow oil.
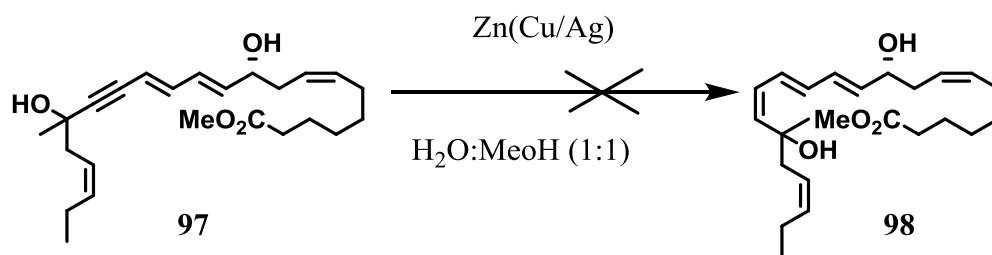
. **Scheme 26.** Attempted synthesis of methyl (7*Z*,10*R*,11*E*,13*E*,15*Z*,19*Z*)-10,17-dihydroxy-17-methyldocosa-7,11,13,15,19-pentaenoate (**98**).

2.3.4 NMR characterization of (7Z,10R,11E,13E,15Z,19Z)-10,17-dihydroxy-17-methyldocosa-7,11,13,15,19-pentaenoic acid (17-methyl PD1$_{n-3\ DPA}$)

The ^{1}H NMR spectrum does not show any signals in the alkene-region, which indicates that the Boland reduction also reduced the carbon double bonds of compound **97**. Since the signal at 4.12 ppm is still present, this indicates that at least the alcohol group at C-10 did not dehydrate.

Similarly, the ^{13}C NMR spectrum only shows peaks in the typical region for alkanes.

The recorded NMR spectra indicate that over-reduction occurred during the Boland reduction of **97**, which failed to afford the desired compound **98**.

As for the Lindlar reduction, this reaction was also monitored by TLC and AgNO$_3$-impregnated TLC. No change in R$_f$ was observed during the reaction. Monitoring the reduction by GC or LC could prove beneficial in order to determine when to stop the reaction.

3 Summary, Conclusions and Future Studies

The synthetic efforts reported herein resulted in the successful synthesis of compound **97**, with only two steps remaining for completion of the total synthesis of the 17-methylated analog of PD1$_{n-3 \ DPA}$ **84**. All 22 carbon atoms in the target molecule have been assembled. This was done in 7 steps and in 6% yield from the known cycloheptanone **90**. The synthesis was done in a convergent manner and provided multimilligram quantities of the intermediate **97**.

As mentioned in the synthesis strategy, the free carboxylic acid of **97** is also of interest as a potential analog of PD1$_{n-3 \ DPA}$. A milligram of this was thus saved for biological testing. The methyl ester was not hydrolyzed into free carboxylic acid because of known chemical stability problems of SPMs such as PD1$_{n-3 \ DPA}$. If they are not stored at -70 °C under an inert atmosphere, these compounds are prone to elimination of the two alcohol groups, leading to a comprehensively conjugated system. The risk of elimination reactions occurring in analog **97** is even higher since the alcohol group on C-17 is tertiary. The two remaining steps in order to produce analog **84** are reduction of the alkyne to a *Z*-alkene, and hydrolysis of the methyl ester. Lindlar and a Boland reductions of **97** were attempted, but unfortunately these reactions failed to produce the desired *Z*-alkene, probably due to over-reduction and dehydration. If more time and quantities of **97** were available, optimization of either the Lindlar or Boland reduction would be attempted, considering reaction time, temperature, quantities of catalysts and by monitoring the reactions by either GC or LC.

The prepared analog **97** will be submitted to biological studies at the Serhan group at Harvard Medical School in Boston. The methyl ester will be hydrolyzed in order to perform *in vitro* experiments to investigate the pro-resolving activities of the free carboxylic acid. Results from these studies will be reported elsewhere.

Future studies based on this thesis could include more comprehensive SAR studies, evaluating the effects that different substituents in the 17-position have on potency, chemical stability and metabolic half-life. Because the alcohol in the 10-position is of similar metabolic importance, similar SAR studies could also be done on this position. Structural changes which

may prevent β- and ω-oxidation should also be investigated. Possible candidates are compound **99** and **100**, depicted in Figure 32.

In **99**, the C-2 of $PD1_{n-3\ DPA}$ is exchanged with oxygen in order to prevent β-oxidation and increase bioavailability, the 15,16-*cis* double bond is replaced with an alkyne to give greater chemical stability, both alcohol groups are made tertiary so as to avoid metabolism by oxido-reductases, and the ω-end is replaced by a para-fluorophenoxy-moiety to prevent ω-oxidation. Compound **100** is similarly designed, with the difference being a bioisosteric substitution of the carboxylic acid with 1H-tetrazole.
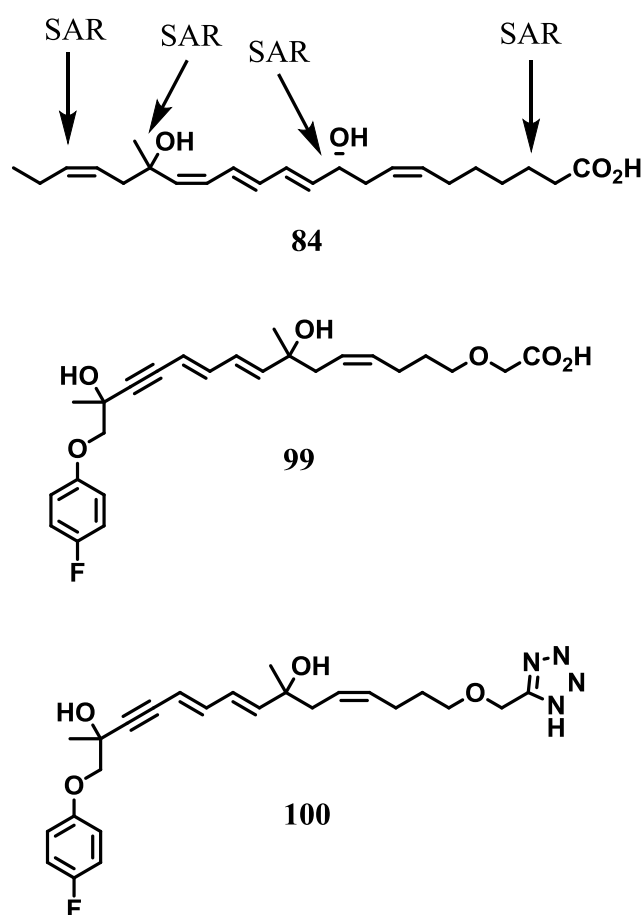
Figure 32. Synthetic candidates for future SAR studies of protectins.

The knowledge obtained from such studies could be utilized in order to make chemically and metabolically stable, crystalline analogs, some of which could be forerunners to potential lead compounds to be used in the effort of making new pro-resolving drugs.

Serhan and collaborators recently discovered a new class of SPMs which are peptide-conjugated.[76] These mediators show significant pro-resolving and tissue regenerative effects and belong to the protectin, maresin and resolvin classes of SPMs.[76,77] The class belonging to the protectins has been named protectin conjugates in tissue regeneration (PCTR).[77] So far, three different PCTRs have been reported to be synthesized, and these are entitled PCTR 1, 2 and 3.[78] PCTR 1 (**101**, Figure 33) has already been prepared by organic synthesis and subjected to biological testing. *In vivo* and *in vitro* studies revealed its potent pro-resolving and anti-inflammatory actions in bacterial infection.[79] Future studies on this front could be evaluations of how different peptides or even other biological polymers in conjugation will affect the pro-resolving actions of the PCTRs.

101
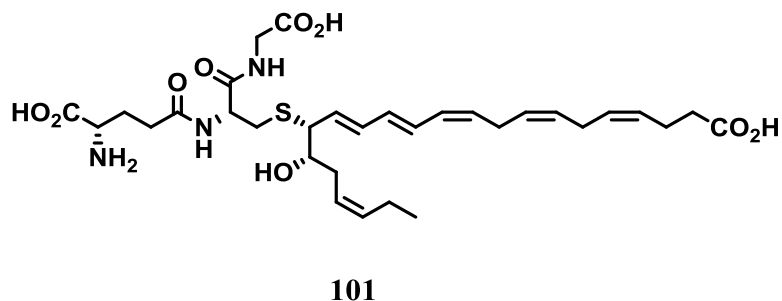
Figure 33. The protectin-peptide conjugate PCTR1 (**101**).

4 Experimental

4.1 Materials and apparatus

All commercially available reagents and solvents were purchased and used without further purification unless stated otherwise. All reactions were performed under an argon atmosphere using Schlenk techniques. The stated yields are based on isolated material. Analytical thin layer chromatography (TLC) was performed on Merck 250 μm silica gel 60 F_{254} aluminum-backed plates. Silica gel 60 (40-63 μm) produced by Merck was used to perform flash column chromatography. NMR spectra were recorded on a Bruker AVII400 or a Bruker AVII600 spectrometer at 400 or 600 MHz, respectively, for ^{1}H NMR and 101 or 151 MHz, respectively, for ^{13}C NMR. Coupling constants (J) are reported in hertz and chemical shifts are reported in parts per million (δ) relative to the central residual protium solvent resonance in ^{1}H NMR (CDCl$_3$ = δ 7.27 and MeOH-d_4 = δ 3.31) and the central carbon solvent resonance in ^{13}C NMR (CDCl$_3$ = δ 77.00 and MeOH-d_4 = δ 49.00). Mass spectra were recorded at 70 eV on a Waters Prospec Q, with EI, ES or CI as methods of ionization. High resolution mass spectra were recorded at the Department of Chemistry at UiO on Waters Prospec Q, using ES or EI as methods of ionization. GC analyses were performed on an Agilent 7820A with a FID detector, HP-5 capillary column, with helium as the carrier gas and by applying the conditions stated. Optical rotations were measured on an Anton Paar MCP 100 polarimeter using a 0.7 mL or a 2.0 mL cell with 1.0 dm path lengths.

4.2 Experimental procedures

4.2.1 Synthesis of 3-methylpent-4-yne-1,3-diol

86   46%   **87**
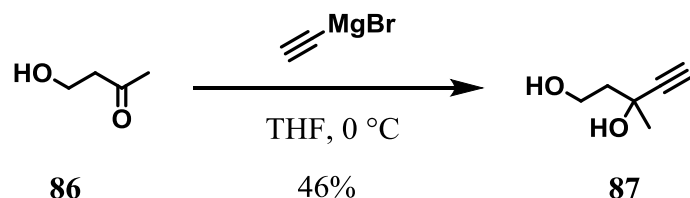
Diol **87** was prepared by a Grignard reaction from 4-hydroxybutanone **86** according to the procedure of Dr. Jens M. J. Nolsøe.[73] 4-Hydroxubutanone **86** (2.00 g, 1.96 mL, 22,7 mmol) was dissolved in dry THF (100 mL), and cooled to 0 °C while stirring under argon. Ethynylmagnesium bromide (100 mL, 0.50 M in THF, 57.5 mmol) was then added dropwise. As this was added, the mixture changed to a white cloudy suspension, and then to a dark yellow solution. The mixture was allowed to slowly warm to room temperature overnight, and was then cooled to 0 °C and quenched with sat. aq. NaH_2PO_4 (30 mL). The phases were separated and the aq. phase was extracted with Et_2O (3 x 50 mL). Combined organic layers were dried ($MgSO_4$) and filtered, before concentrated *in vacuo*. The crude product was purified by column chromatography on silica (heptane:EtOAc 1:1) to afford the title compound **87** as clear, yellow oil. All spectroscopic and physical data were in agreement with those who were reported in literature.[73] Yield: 1.2 g (46%); ^{1}H NMR (400 MHz, $CDCl_3$) δ 4.12 − 3.82 (m, 2H), 2.48 (s, 1H), 2.02 − 1.67 (m, 2H), 1.48 (s, 3H); ^{13}C NMR (101 MHz, $CDCl_3$) δ 87.0, 72.1, 68.5, 60.3, 43.4, 30.5. TLC (heptane:EtOAc 1:1, $KMnO_4$ stain): R_f = 0.18.

4.2.2 Synthesis of 3,3,9,9-tetraethyl-5-ethynyl-5-methyl-4,8-dioxa-3,9-disilaundecane
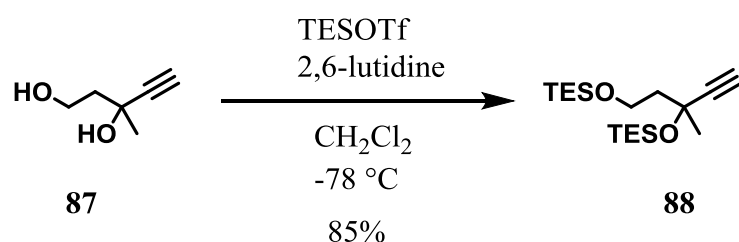
According to the procedure of Dr. Jens M. J. Nolsøe[73], both alcohol groups in the diol **87** were protected with a TES-group. Diol **87** (0.8 g, 7.0 mmol) was dissolved in dry CH_2Cl_2 (80 mL) and cooled to -78 °C. After the solution had stirred for 10 minutes, 2,6-lutidine (5.0 mL, 4.6 g, 42.9 mmol) was added. Then TESOTf (6.5 mL, 7.6 g, 28.8 mmol) was added. The solution was slowly heated to room temperature overnight, before being quenched with sat. aq. NH_4Cl (80 mL) and diluted with CH_2Cl_2 (80 mL). The phases were separated and the aq. phase was extracted with CH_2Cl_2 (3 x 65 mL). Organic phases were combined, dried (Na_2SO_4), filtered and concentrated *in vacuo*. The crude product was purified by column chromatography on silica (heptane:Et_2O 95:5) to afford the title compound **88** as a clear oil. All spectroscopic and physical data were in agreement with those who were reported in literature.[73] Yield: 2.04 g (85%); ^1H NMR (400 MHz, $CDCl_3$) δ 3.84 (t, 2H), 2.41 (s, 1H), 2.02 – 1.85 (m, 2H), 1.48 (s, 3H), 1.01 – 0.91 (m, 18H), 0.72 – 0.55 (m, 12H); ^{13}C NMR (101 MHz, $CDCl_3$) δ 88.0, 72.1, 67.6, 59.7, 47.8, 31.6, 7.1, 6.9, 6.2, 4.6. TLC (heptane:Et_2O 95:5, CAM stain): $R_f = 0.57$.

## 4.2.3 Synthesis of 3-methyl-3-((triethylsilyl)oxy)pent-4-ynal
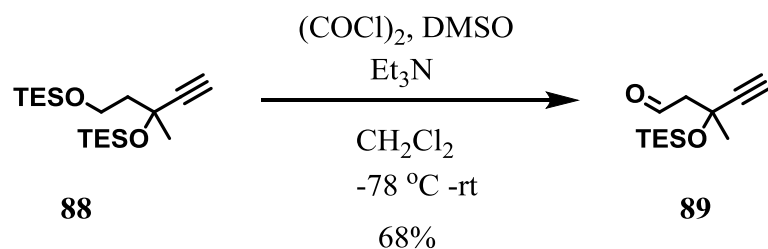
Aldehyde **89** was prepared by a Swern oxidation of the *bis*-TES-protected diol **88**, according to the procedure of Dr. Jens M. J. Nolsøe.[73] DMSO (3.0 mL, 3.3 g, 42 mmol) was dissolved in

dry CH_2Cl_2 (13 mL) and the solution was cooled to -78 °C. Then oxalyl chloride (1.8 mL, 2.7 g, 21 mmol) was added dropwise, and the solution stirred for 15 minutes. A solution of the TES-protected diol **88** (1.38 g, 4.03 mmol) in CH_2Cl_2 (7 mL) was added dropwise. After 1 h the reaction mixture was heated to -20 °C and stirred at this temperature for 45 min. Then the mixture was re-cooled to -78 °C, and $E_{t3}N$ (9.0 mL) was added. The reaction mixture was warmed to room temperature, quenched with water (35 mL) and diluted with CH_2Cl_2 (40 mL). The phases were separated and the aq. phase was extracted with CH_2Cl_2 (4 x 30 mL). Organic phases were combined, dried (Na_2SO_4), filtered and concentrated *in vacuo*. The crude product was purified by column chromatography on silica (heptane:Et_2O 95:5) to afford the title compound **89** as a yellow oil. All spectroscopic and physical data were in agreement with those reported in literature.[73] Aldehyde **89** was directly used in synthesis 4.2.4. Yield: 0.62 g (68%); ^{1}H NMR (400 MHz, $CDCl_3$) δ 9.89 (t, *J* = 2.8 Hz, 1H), 2.62 (d, *J* = 2.8 Hz, 2H), 2.57 (s, 1H), 1.58 (s, 3H), 0.96 (t, *J* = 7.9 Hz, 9H), 0.70 (qd, *J* = 7.8, 2.2 Hz, 6H); ^{13}C NMR (101 MHz, $CDCl_3$) δ 201.7, 86.6, 73.9, 66.4, 57.3, 31.6, 7.0, 6.1. TLC (heptane:EtOAc 1:1, CAM stain): R_f = 0.77.

4.2.4 Synthesis of triethyl(((5*Z*)-3-methyloct-5-en-1-yn-3-yl)oxy)silane
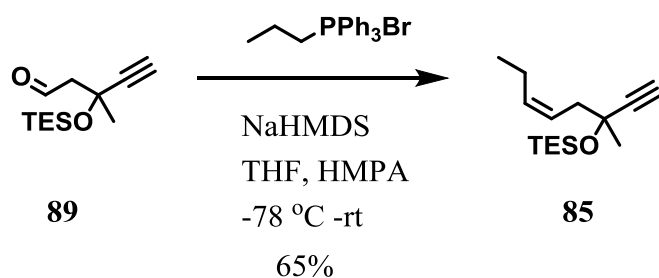
Utilizing a *Z*-selective Wittig reaction, the alkene **85** was prepared from aldehyde **89**, consistent the procedure of Dr. Jens M. J. Nolsøe.[73] Propyltriphenylphosphonium bromide (1.0 g, 2.6 mmol) was suspended in dry THF (25 mL) and HMPA (4.2 mL). This suspension was cooled to -78 °C, before NaHMDS (0.6 M in toluene, 4.4 mL, 2.6 mmol) was added dropwise. The reaction mixture was brought to room temperature and stirred for 5 min to ensure dissolution of the Wittig salt. The solution was then re-cooled to -78 °C and a solution of aldehyde **89** (0.57 g, 2.5 mmol) in THF (7.0 mL) was added in a dropwise manner. The

reaction mixture was allowed to slowly attain room temperature overnight, before being quenched with phosphate buffer (9.0 mL, pH = 7.2) and diluted with water (35 mL). The phases were separated and the aq. phase was extracted with Et_2O (3 x 45 mL). Organic phases were combined, dried (Na_2SO_4), filtered and concentrated *in vacuo*. The crude product was purified by column chromatography on silica (heptane:Et_2O 95:5) to afford the title compound **85** as a clear, colorless oil. All spectroscopic and physical data were in agreement with those reported in literature.[73] Yield: 0.41 g (65%); ^{1}H NMR (400 MHz, $CDCl_3$) δ 5.62 – 5.40 (m, J = 12.1, 11.9 Hz, 2H), 2.51 – 2.33 (m, 3H), 2.15 – 1.97 (m, 2H), 1.44 (s, 3H), 0.97 (t, J = 7.9 Hz, 12H), 0.74 – 0.64 (m, 6H); ^{13}C NMR (101 MHz, $CDCl_3$) δ 134.3, 124.1, 88.5, 72.0, 69.0, 42.9, 30.6, 21.0, 14.3, 7.1, 6.3; HRESTOFMS m/z 275.1801 [M + Na]$^+$ (calcd for $C_{15}H_{28}NaOSi$, 275.1802); TLC (heptane:Et_2O 95:5, CAM stain) R_f = 0.78. The chemical purity (98.2%) was determined by GC analysis: Initial temperature 100 °C, rate 2 °C/min to 150 °C, then 6 °C/min to 300 °C, t_r(major) = 8.08 min and t_r(minor) = 7.58 min.

4.2.5 Synthesis of methyl 7-hydroxyheptanoate

90   0 °C   91   92

73% over two steps
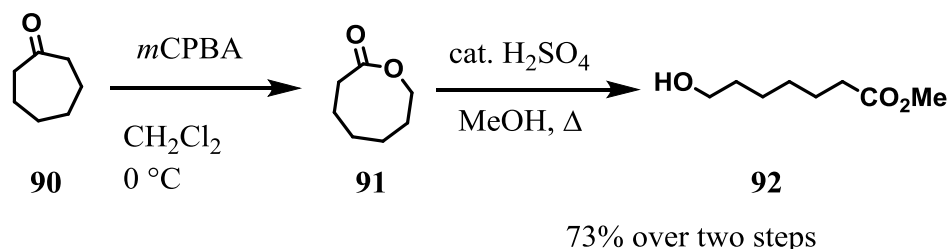
The alcohol ester **92** was prepared from cycloheptanone **90** by a Baeyer-Villiger reaction followed by a Fisher esterification, according to the procedure of Aursnes *et al.*[54] *m*CPBA (14.5 g, 84.2 mmol) was dissolved in CH_2Cl_2 and cooled to 0 °C. Then cycloheptanone **90** (6.3 g, 56.2 mmol) was added, and the solution was allowed to stir at room temperature for 5 days. The mixture was cooled to 0 °C, filtered, washed with sat. aq. $NaHCO_3$ (40 mL), dried (Na_2SO_4) and concentrated *in vacuo*. The crude lactone product **91** was dissolved in dry MeOH (120 mL), and a few drops of conc. H_2SO_4 were added. The reaction mixture was heated to reflux for 24 h, and was then cooled to room temperature and added sat. aq. $NaHCO_3$ (12 mL). The mixture was concentrated *in vacuo*, and diluted with additional $NaHCO_3$ (40 mL). The phases were separated and the aq. phase was extracted with Et_2O (4 x 80 mL). Organic phases were combined, dried (Na_2SO_4), filtered and concentrated *in vacuo*.

The crude product was purified by column chromatography on silica (heptane:EtOAc 4:1) to afford the title compound **92** as a clear brown oil. All spectroscopic and physical data were in agreement with those who were reported in literature.[54] Yield: 6.54 g (73% over two steps); ^{1}H NMR (400 MHz, Chloroform-*d*) δ 3.66 (s, 3H), 3.63 (t, *J* = 6.5 Hz, 2H), 2.31 (t, *J* = 7.5 Hz, 2H), 1.99 (bs, 1H), 1.68 – 1.52 (m, 4H), 1.43 – 1.30 (m, 4H); ^{13}C NMR (101 MHz, CDCl$_3$) δ 174.4, 63.0, 51.6, 34.1, 32.7, 29.0, 25.5, 25.0. TLC (heptane:EtOAc 4:1, KMnO$_4$ stain): R_f = 0.11.

4.2.6 Synthesis of methyl 7-iodoheptanoate
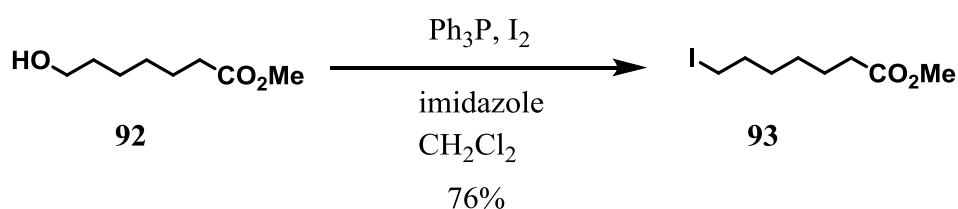
The alcohol ester **92** was converted into the corresponding iodide **93** by an Appel reaction according to the procedure of Aursnes *et al.*[54] Alcohol ester **92** (6.0 g, 37 mmol) was dissolved in dry CH$_2$Cl$_2$ and added triphenylphosphine (16 g, 59 mmol) and imidazole (4.1 g, 60 mmol). The mixture was cooled to -20 °C and then iodide (15 g, 60 mmol) was added in one portion. The mixture was stirred at -20 °C for 15 min and then at room temperature for additional 35 min. Then aq. sat. Na$_2$SO$_3$ (50 mL) was added, the phases separated and the aq. phase was extracted with CH$_2$Cl$_2$ (2 x 200 mL). The combined organic layers were dried (Na$_2$SO$_4$) and filtered, before concentrated *in vacuo*. The crude product was purified by column chromatography on silica (heptane:EtOAc 92:8) to afford the title compound **93** as a clear oil. All spectroscopic and physical data were in agreement with those reported in literature.[54] Yield: 7.65 g (76%); ^{1}H NMR (400 MHz, Chloroform-*d*) δ 3.66 (s, 3H), 3.17 (t, *J* = 7.0 Hz, 2H), 2.30 (t, *J* = 7.5 Hz, 2H), 1.81 (p, *J* = 7.0 Hz, 2H), 1.63 (p, *J* = 7.6 Hz, 2H), 1.47 – 1.26 (m, 4H). ^{13}C NMR (101 MHz, CDCl$_3$) δ 174.1, 51.6, 34.0, 33.4, 30.2, 28.1, 24.8, 7.0. TLC (heptane:EtOAc 92:8, KMnO$_4$ stain): R_f = 0.28.

4.2.7 Synthesis of (7-methoxy-7-oxoheptyl)triphenylphosphonium iodide
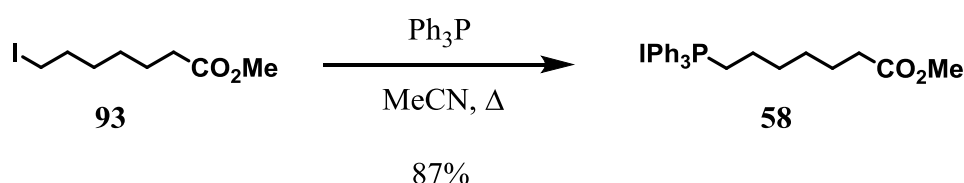
The Wittig salt **58** was prepared from iodide **93** by a reaction with triphenylphosphine according to the procedure of Aursnes et al.[54] Iodide **93** (1.5 g, 5.6 mmol) was dissolved in dry MeCN (50 mL) and triphenylphosphine (3.7g, 14 mmol) was added. The reaction mixture was then refluxed for 12 h. Then the mixture was cooled to room temperature, concentrated *in vacuo*, and the crude product was directly purified by chromatography on silica (CH_2Cl_2:MeOH 95:5) to afford the title compound **58** as a clear oil. All spectroscopic and physical data were in agreement with those who were reported in literature.[54] Yield: 2.56 g (87%); ^{1}H NMR (400 MHz, CDCl$_3$) δ 7.91 – 7.58 (m, 15H), 3.69 – 3.62 (m, 2H), 3.60 (s, 3H), 2.24 (t, J = 7.3 Hz, 2H), 1.72 – 1.47 (m, 6H), 1.37 – 1.22 (m, 2H); ^{13}C NMR (101 MHz, Chloroform-*d*) δ 174.2, 135.2 (d, J = 3.1 Hz), 133.8 (d, J = 10.0 Hz), 130.7 (d, J = 12.5 Hz), 118.2 (d, J = 86.0 Hz), 51.5, 33.9, 30.1 (d, J = 15.8 Hz), 28.6, 24.4, 23.2 (d, J = 50.1 Hz), 22.5 (d, J = 4.5 Hz). TLC (CH_2Cl_2/MeOH 95:5, KMnO$_4$ stain): R_f = 0.30.

4.2.8 Synthesis of (3*R*,4*E*,6*E*)-7-bromo-3-((*tert*-butyldimethylsilyl)oxy)hepta-4,6-dienal
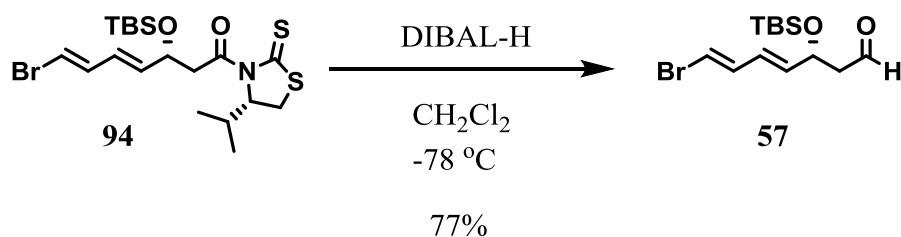
The aldehyde **57** was prepared by reducing the protected thiazolidinethione **94** with DIBAL-H according to the procedure of Aursnes et al.[54] Thiazolidinethione **94** (300 mg, 0.62 mmol, 1.0 equiv.) was dissolved in dry CH_2Cl_2 and cooled to -78 °C. DIBAL-H (0.81 mL, 1.0 M in hexanes, 1.3 equiv.) was added to the solution, which was allowed to stir for 2.5 h. As full conversion of the starting material was not realized, more DIBAL-H (0.4 mL, 1.0 M in

hexanes, 0.65 equiv.) was added, and the solution was stirred for another 2 h. The mixture was quenched with sat.aq. NaHCO$_3$ (9.0 mL), before the flask was removed from the cooling bath. The mixture was added solid Na-K tartrate (0.6 g) and stirred for 40 min at room temperature. Then the reaction mixture was diluted with Et$_2$O (3 x 20 mL). The layers were separated and the aq. phase was extracted with Et$_2$O (3 x 20 mL). Combined organic layers were dried (Na$_2$SO$_4$), filtered and concentrated *in vacuo*. The crude product was purified by column chromatography on silica (heptane:EtOAc 95:5) to afford the title compound **57** as an yellow oil. All spectroscopic and physical data were in agreement with those reported in literature.[54] The product was immediately used in synthesis 4.2.9 Yield: 153 mg (77%); ^{1}H NMR (400 MHz, Chloroform-*d*) δ 9.76 (t, *J* = 2.3 Hz, 1H), 6.70 (dd, *J* = 13.5, 10.9 Hz, 1H), 6.34 (d, *J* = 13.5 Hz, 1H), 6.17 (ddd, *J* = 15.0, 10.7, 1.5 Hz, 1H), 5.76 (ddd, *J* = 15.2, 6.0, 0.9 Hz, 1H), 4.67 (dd, *J* = 6.5, 5.7 Hz, 1H), 2.76 − 2.42 (m, 2H), 0.88 (s, 9H), 0.07 (s, 3H), 0.04 (s, 3H); ^{13}C NMR (101 MHz, CDCl$_3$) δ 201.0, 136.6, 136.2, 127.6, 109.6, 68.6, 51.5, 25.9, 18.3, -4.2, -4.8. TLC (heptane:EtOAc 9:1, CAM stain): R_f = 0.24.

4.2.9 Synthesis of methyl (10*R*,7*Z*,11*E*,13*E*)-14-bromo-10-(*tert*-butyldimethylsilyl)oxy)tetradeca-7,11,13-trienoate
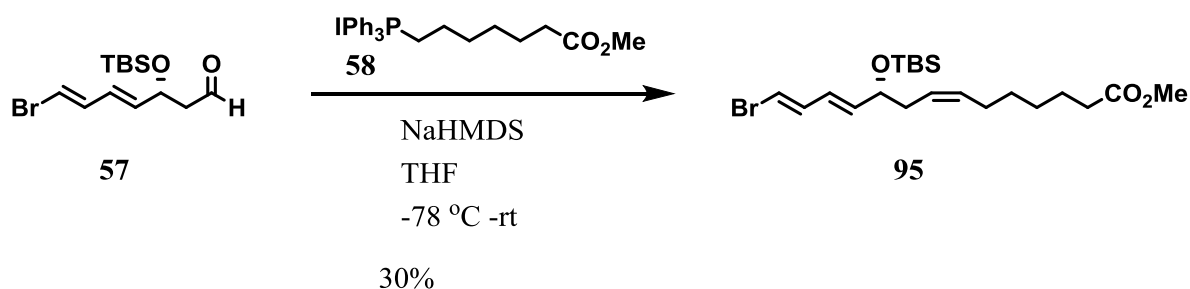
A *Z*-selective Wittig reaction was used to prepare the vinyl bromide **95** from Wittig salt **58** and aldehyde **57**, according to the procedure of Aursnes *et al*.[54] The Wittig salt **58** (0.27 g, 0.51 mmol, 1.1 equiv.) was dissolved in dry THF (9.0 mL) and cooled to -78 °C. NaHMDS (0.85 mL, 0.60 M in toluene, 1.1 equiv.) was added in a dropwise manner, and the solution was stirred for 1 h. A solution of aldehyde **57** (152 mg, 0.48 mmol, 1.0 equiv.) in dry THF (3.0 mL) was added to the solution. The reaction mixture was stirred and allowed to slowly attain room temperature over 24 h. Then the mixture was quenched with phosphate buffer (7.0 mL, pH = 7.2) and diluted with Et$_2$O (12 mL). The phases were separated, and the aq. phase

was extracted with Et$_2$O (3 x 15 mL). Combined organic layers were dried (Na$_2$SO$_4$), filtered and concentrated *in vacuo*. The crude product was purified by column chromatography on silica (heptane:EtOAc 98:2) to afford the title compound **95** as clear, colorless oil. All spectroscopic and physical data were in full agreement with those reported in the literature.[54] Yield: 64 mg (30%); $[\alpha]^{20}_D$ −11 (c = 0.1, MeOH); ^{1}H NMR (400 MHz, Chloroform-*d*) δ 6.68 (dd, J = 13.5, 10.8 Hz, 1H), 6.27 (d, J = 13.6 Hz, 1H), 6.08 (dd, J = 15.2, 10.8 Hz, 1H), 5.72 (dd, J = 15.2, 9.3 Hz, 1H), 5.50 − 5.28 (m, J = 12.3 Hz, 2H), 4.14 (dd, J = 6.1, 1.6 Hz, 1H), 3.67 (s, 3H), 2.30 (t, J = 7.6 Hz, 2H), 2.37 − 2.15 (m, 2H), 2.01 (q, J = 7.0 Hz, 2H), 1.62 (p, J = 7.4 Hz, 2H), 1.42 − 1.30 (m, 4H), 0.89 (s, 9H), 0.05 (s, 3H), 0.02 (s, 3H); ^{13}C NMR (101 MHz, CDCl$_3$) δ 174.3, 138.1, 137.2, 131.9, 126.6, 125.2, 108.2, 72.7, 51.6, 36.3, 34.2, 29.4, 29.0, 27.4, 26.0, 25.0, 18.4, -4.4, -4.6. TLC (heptane:EtOAc 95:5, CAM stain) R_f = 0.23.

4.2.10 Synthesis of methyl (7*Z*,10*R*,11*E*,13*E*,19*Z*)-10-((*tert*-butyldimethylsilyl)oxy)-17-methyl-17-((triethylsilyl)oxy)docosa-7,11,13,19-tetraen-15-ynoate
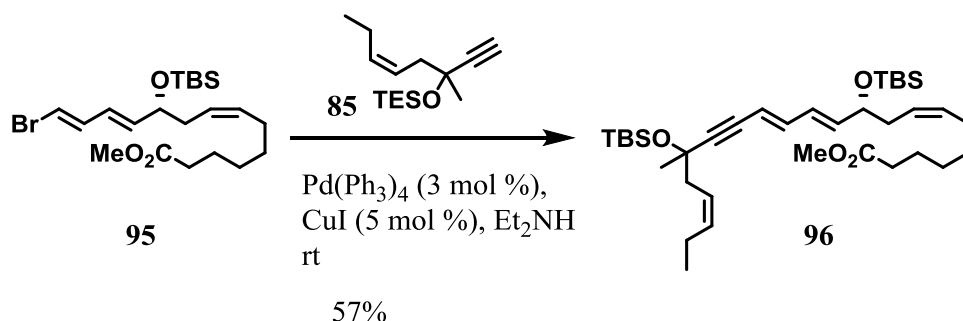
Compound **96** was prepared by a Sonogashira coupling between vinyl bromide **95** and alkyne **85**. Vinyl bromide **95** (53 mg, 0.12 mmol, 1.0 equiv) was dissolved in Et$_2$NH (0.35 mL) and benzene (0.20 mL). This solution was added Pd(PPh$_3$)$_4$ (4.1 mg, 0.0035 mmol, 3 mol %), and was stirred for 45 min while protected from light using Al-foil. This mixture was added CuI (1.2 mg, 0.0063 mmol, 5 mol %) in a small amount of Et$_2$NH. A solution of alkyne **85** (31 mg, 0.13 mmol, 1,1 equiv) in Et$_2$NH was added dropwise to the reaction. The reaction mixture was stirred at room temperature for 20 h. It was then quenched with sat. aq. NH$_4$Cl (4 mL), and diluted with Et$_2$O (4 mL). The phases were separated and the aq. phase was extracted with Et$_2$O (3 x 5 mL). Combined organic layers were dried (Na$_2$SO$_4$), filtered and concentrated *in vacuo*. The crude product was purified by column chromatography on silica

(heptane:EtOAc 95:5) to afford the title compound **96** as a yellow oil. Yield: 42 mg (57%); ^{1}H NMR (400 MHz, Chloroform-*d*) δ 6.49 (dd, *J* = 15.5, 10.9 Hz, 1H), 6.19 (dd, *J* = 15.2, 11.4 Hz, 1H), 5.76 (dd, *J* = 15.0, 5.8 Hz, 1H), 5.64 − 5.28 (m, 5H), 4.25 − 4.12 (m, 1H), 3.67 (s, 3H), 2.42 (t, *J* = 5.7 Hz, 2H), 2.30 (t, *J* = 7.4 Hz, 2H), 2.31 − 2.15 (m, 2H), 2.13 − 1.96 (m, 4H), 1.62 (p, *J* = 6.7, 6.2 Hz, 2H), 1.43 (s, 3H), 1.38 − 1.23 (m, 4H), 1.03 − 0.92 (m, 12H), 0.89 (s, 9H), 0.67 (q, *J* = 7.7 Hz, 6H), 0.04 (d, *J* = 7.8 Hz, 6H); ^{13}C NMR (101 MHz, CDCl$_3$) δ 174.3, 140.9, 139.3, 134.2, 131.9, 128.7, 125.4, 124.4, 110.7, 96.4, 83.2, 72.9, 69.6, 51.6, 43.0, 36.4, 34.2, 30.6, 29.4, 29.0, 27.4, 26.0, 25.0, 21.0, 18.4, 14.4, 7.2, 6.3, -4.3, -4.6; HRESTOFMS *m/z* 639.4232 [M + Na]$^+$ (calcd for C$_{36}$H$_{64}$NaO$_4$Si$_2$, 639.4235); TLC (heptane:EtOAc 95:5, CAM stain) R_f = 0.51.

4.2.11   Synthesis of methyl (7*Z*,10*R*,11*E*,13*E*,19*Z*)-10,17-dihydroxy-17-methyldocosa-7,11,13,19-tetraen-15-ynoate
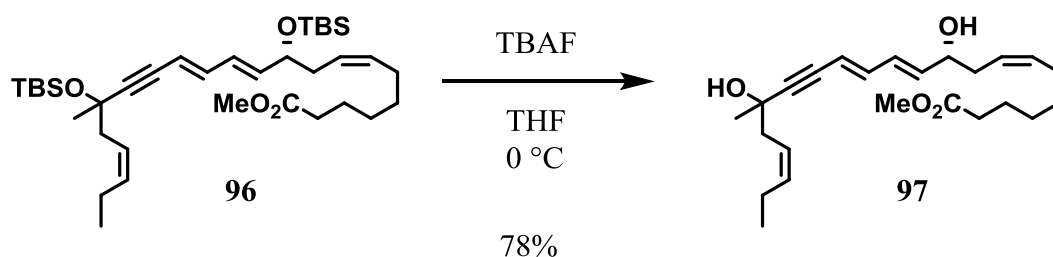
The silyl ether protecting groups were removed with TBAF according to the procedure of Aursnes *et al.*[54] Silyl ether-protected alcohol **96** (41 mg, 0.066 mmol, 1.0 equiv) was dissolved in dry THF (0.90 mL) and cooled to 0 °C. TBAF (86 mg, 0.033 mmol, 5.0 equiv) was added to this solution, and the reaction mixture was stirred for 7 h. Phosphate buffer (pH = 7.2, 0.40 mL) was then added to quench to reaction. Brine (4.0 mL) and EtOAc (4.0 mL) was added to dilute the mixture, and the phases were separated. The aq. phase was extracted with EtOAc (2 x 4 mL), and the combined organic layers were dried (Na$_2$SO$_4$), filtered and concentrated *in vacuo*. The crude product was purified by flash chromatography on silica (heptane:EtOAc 8:2) to afford the title compound **97** as a pale yellow oil. Yield: 21 mg (78%).^{1}H NMR (600 MHz, MeOH-*d*$_4$) δ 6.53 (dd, *J* = 15.5, 10.8 Hz, 1H), 6.28 (dd, *J* = 15.8, 11.0 Hz, 1H), 5.81 (dd, *J* = 15.2, 6.3 Hz, 1H), 5.66 (d, *J* = 15.5 Hz, 1H), 5.59 − 5.37 (m, 4H), 4.16 − 4.09 (m, 1H), 3.66 (s, 3H), 2.48 − 2.39 (m, 2H), 2.33 (t, *J* = 7.4 Hz, 2H), 2.32 − 2.23 (m, 2H), 2.15 − 2.04 (m, 5H), 1.70 (bs, *J* = 4.4 Hz, 1H), 1.62 (p, *J* = 7.4 Hz, 2H), 1.43 (s, 3H),

1.40 – 1.30 (m, 4H), 0.99 (t, J = 7.6 Hz, 3H). ^{13}C NMR (151 MHz, MeOH-d_4) δ 176.0, 142.3, 139.7, 135.4, 132.9, 130.3, 126.1, 124.9, 111.8, 96.7, 83.0, 72.8, 68.9, 52.0, 42.3, 36.3, 34.8, 30.3, 29.4, 28.2, 25.9, 24.8, 21.8, 13.9; HRESTOFMS m/z 411.2508 [M + Na]$^+$ (calcd for $C_{24}H_{36}NaO_4$, 411.2506). TLC (heptane:EtOAc 7:3, CAM stain) R_f = 0.23.

4.2.12 Synthesis of methyl (7*Z*,10*R*,11*E*,13*E*,15*Z*,19*Z*)-10,17-dihydroxy-17-methyldocosa-7,11,13,15,19-pentaenoate
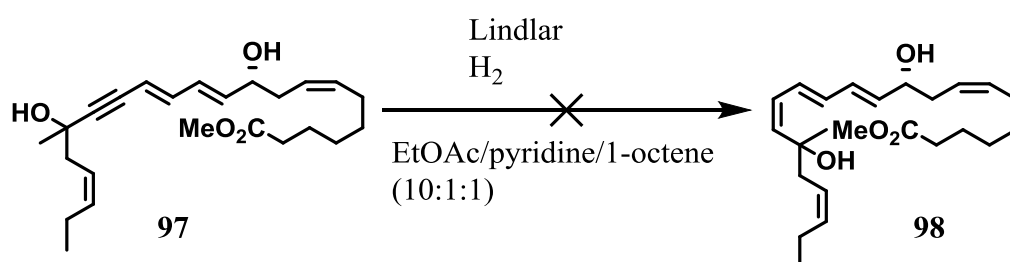
Alkyne **97** was attempted to be reduced to the Z-alkene **98** by a Lindlar reduction according to the procedure of Aursnes *et al.*[54] Alkyne **97** (11 mg, 0.031 mmol) was dissolved in EtOAc/pyridine/1-octene (0.80 mL, 10:1:1) and stirred under argon. Lindlar's catalyst (18 mg) was added to the solution. The reaction mixture was stirred under a balloon of hydrogen gas at room temperature for 7 h. The mixture was then directly purified by chromatography on silica (heptane:EtOAc 9:1) to afford a pale yellow oil. Yield: 7 mg. TLC (heptane:EtOAc 7:3, CAM stain) R_f = 0.35.

4.2.13 Synthesis of methyl (7*Z*,10*R*,11*E*,13*E*,15*Z*,19*Z*)-10,17-dihydroxy-17-methyldocosa-7,11,13,15,19-pentaenoate
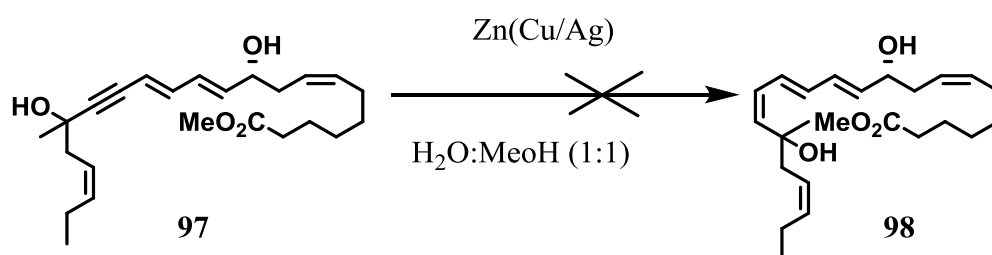
Alkyne **97** was attempted to be reduced to the *Z*-alkene **98** according to the procedure of Boland *et al.*[75] Activated zinc complex was prepared as previously reported by stirring zinc dust (0.5 g) under argon for 15 min, before adding $Cu(OAc)_2$ (0.05 g) and stirring for another 15 min. Then, $AgNO_3$ (0.05 g) was added and the mixture was stirred for an additional 30 min. The mixture was filtered under argon and washed successively with H_2O, MeOH, acetone and Et_2O. This wet mixture was then added to a flask with a solution of alkyne **97** (5 mg, 0.014 mmol) in the reaction solvents (MeOH:H_2O 1:1, 2 mL), which was stirred in the dark at room temperature for 2.5 h. Then the reaction mixture was filtered through a pad of Celite and washed with Et_2O (10 mL). H_2O (10 mL) was added, the phases separated and the aq. layer was extracted with Et_2O (2 x 10 mL). Combined organic layers were dried (Na_2SO_4) and concentrated *in vacuo*. The crude product was purified by column chromatography on silica (heptane:EtOAc 9:1) to afford a pale yellow oil. Yield: 3 mg. TLC (heptane:EtOAc 7:3, CAM stain) $R_f = 0.25$.

5 References

(1)   Webb, G. *Br. J. Nutr.* **1999**, *82*, 134.
(2)   Radimer, K.; Bindewald, B.; Hughes, J.; Ervin, B.; Swanson, C.; Picciano, M. F. *Am. J. Epidemiol.* **2004**, *160*, 339.
(3)   Fetterman, J. W., Jr.; Zdanowicz, M. M. *Am. J. Health-Syst. Pharm.* **2009**, *66*, 1169.
(4)   Simopoulos, A. P. *J. Am. Coll. Nutr.* **2002**, *21*, 495.
(5)   Harper, C. R.; Jacobson, T. A. *Arch. Intern. Med.* **2001**, *161*, 2185.
(6)   Breslow, J. L. *Am. J. Clin. Nutr.* **2006**, *83*, 1477S.
(7)   Thomas, J.; Thomas, C. J.; Radcliffe, J.; Itsiopoulos, C. *BioMed Res. Int.* **2015**, 1.
(8)   Nettleton, J. A.; Katz, R. *J. Am. Diet. Assoc.* **2005**, *105*, 428.
(9)   Larsson, S. C.; Kumlin, M.; Ingelman-Sundberg, M.; Wolk, A. *Am. J. Clin. Nutr.* **2004**, *79*, 935.
(10)   BASF. *Baden Aniline and Soda Factory*; www.basf.com (accessed 10.02.2016)
(11)   Legemiddelverk, S. *SPC for Omacor®*; http://www.legemiddelverket.no/_layouts/Preparatomtaler/Spc/0000-08041.pdf?id=05042016094728 (accessed 12.02.2016)
(12)   Serhan, C. N. *Prostaglandins Leukot. Essent. Fatty Acids* **2005**, *73*, 141.
(13)   Serhan, C. N.; Chiang, N.; Van Dyke, T. E. *Nat. Rev. Immunol.* **2008**, *8*, 349.
(14)   Serhan, C. N.; Hong, S.; Gronert, K.; Colgan, S. P.; Devchand, P. R.; Mirick, G.; Moussignac, R.-L. *J. Exp. Med.* **2002**, *196*, 1025.
(15)   Serhan, C. N.; Petasis, N. A. *Chem. Rev.* **2011**, *111*, 5922.
(16)   Serhan, C. N.; Ward, P. A.; Gilroy, D. W.; Ayoub, S. S. *Fundamentals of Inflammation*; Cambridge University Press New York, 2010. Chapter 1-2.
(17)   Kumar, V.; Abbas, A. K.; Fausto, N.; Aster, J. C. *Robbins & Cotran Pathologic Basis of Disease*; 8th edition ed.; Elsevier - Health Sciences Division 2009. Chapter 2.
(18)   Sugimoto, M. A.; Sousa, L. P.; Pinho, V.; Perretti, M.; Teixeira, M. M. *Frontiers in Immunology* **2016**, *7*. Ahead of print.
(19)   Libby, P. *Sci. Am.* **2002**, *286*, 46.
(20)   Hansson, G. K.; Libby, P. *Nat. Rev. Immunol.* **2006**, *6*, 508.
(21)   Serhan, C. N.; Brain, S. D.; Buckley, C. D.; Gilroy, D. W.; Haslett, C.; O'Neill, L. A. J.; Perretti, M.; Rossi, A. G.; Wallace, J. L. *FASEB J.* **2007**, *21*, 325.
(22)   Levy, B. D.; Clish, C. B.; Schmidt, B.; Gronert, K.; Serhan, C. N. *Nat. Immunol.* **2001**, *2*, 612.
(23)   Serhan, C. N.; Clish, C. B.; Brannon, J.; Colgan, S. P.; Chiang, N.; Gronert, K. *J. Exp. Med.* **2000**, *192*, 1197.
(24)   Needleman, P.; Turk, J.; Jakschik, B. A.; Morrison, A. R.; Lefkowith, J. B. *Annu. Rev. Biochem.* **1986**, *55*, 69.
(25)   FitzGerald, G. A. *Nat. Rev. Drug Discovery* **2003**, *2*, 879.
(26)   Marnett, L. J. *Annu. Rev. Pharmacol. Toxicol.* **2009**, *49*, 265.
(27)   Rajakariar, R.; Yaqoob, M. M.; Gilroy, D. W. *Mol. Interventions* **2006**, *6*, 199.
(28)   Norel, X.; Brink, C. *Pharmacol. Ther.* **2004**, *103*, 81.
(29)   Steinhilber, D.; Hofmann, B. *Basic Clin. Pharmacol. Toxicol.* **2014**, *114*, 70.
(30)   Serhan, C. N. *Prostaglandins Leukot. Essent. Fatty Acids* **2005**, *73*, 141.
(31)   Bannenberg, G.; Serhan, C. N. *Biochim. Biophys. Acta, Mol. Cell Biol. Lipids* **2010**, *1801*, 1260.

(32) Dalli, J.; Colas, R. A.; Serhan, C. N. *Sci. Rep.* **2013**, *3*, 1940. doi:10.1038/srep01940.

(33) Arita, M.; Bianchini, F.; Aliberti, J.; Sher, A.; Chiang, N.; Hong, S.; Yang, R.; Petasis, N. A.; Serhan, C. N. *J. Exp. Med.* **2005**, *201*, 713.

(34) Hong, S.; Porter, T. F.; Lu, Y.; Oh, S. F.; Pillai, P. S.; Serhan, C. N. *J. Immunol.* **2008**, *180*, 3512.

(35) Dalli, J.; Zhu, M.; Vlasenko, N. A.; Deng, B.; Haeggstrom, J. Z.; Petasis, N. A.; Serhan, C. N. *FASEB J.* **2013**, *27*, 2573.

(36) Serhan, C. N.; Yang, R.; Martinod, K.; Kasuga, K.; Pillai, P. S.; Porter, T. F.; Oh, S. F.; Spite, M. *J. Exp. Med.* **2009**, *206*, 15.

(37) Serhan, C. N.; Dalli, J.; Karamnov, S.; Choi, A.; Park, C.-K.; Xu, Z.-Z.; Ji, R.-R.; Zhu, M.; Petasis, N. A. *FASEB J.* **2012**, *26*, 1755.

(38) Petasis, N. A.; Akritopoulou-Zanze, I.; Fokin, V. V.; Bernasconi, G.; Keledjian, R.; Yang, R.; Uddin, J.; Nagulapalli, K. C.; Serhan, C. N. *Prostaglandins Leukot. Essent. Fatty Acids* **2005**, *73*, 301.

(39) Samuelsson, B.; Dahlen, S. E.; Lindgren, J. A.; Rouzer, C. A.; Serhan, C. N. *Science* **1987**, *237*, 1171.

(40) Ariel, A.; Li, P.-L.; Wang, W.; Tang, W.-X.; Fredman, G.; Hong, S.; Gotlinger, K. H.; Serhan, C. N. *J. Biol. Chem.* **2005**, *280*, 43079.

(41) Aursnes, M.; Tungen, J. E.; Colas, R. A.; Vlasakov, I.; Dalli, J.; Serhan, C. N.; Hansen, T. V. *J. Nat. Prod.* **2015**, *78*, 2924.

(42) Serhan, C. N.; Gotlinger, K.; Hong, S.; Lu, Y.; Siegelman, J.; Baer, T.; Yang, R.; Colgan, S. P.; Petasis, N. A. *J. Immunol.* **2006**, *176*, 3843.

(43) Duffield, J. S.; Hong, S.; Vaidya, V. S.; Lu, Y.; Fredman, G.; Serhan, C. N.; Bonventre, J. V. *J. Immunol.* **2006**, *177*, 5902.

(44) Blaho, V. A.; Buczynski, M. W.; Brown, C. R.; Dennis, E. A. *J. Biol. Chem.* **2009**, *284*, 21599.

(45) Bazan, N. G.; Calandria, J. M.; Serhan, C. N. *J. Lipid Res.* **2010**, *51*, 2018.

(46) Calandria, J. M.; Marcheselli, V. L.; Mukherjee, P. K.; Uddin, J.; Winkler, J. W.; Petasis, N. A.; Bazan, N. G. *J. Biol. Chem.* **2009**, *284*, 17877.

(47) Mukherjee, P. K.; Marcheselli, V. L.; Serhan, C. N.; Bazan, N. G. *Proc. Natl. Acad. Sci. U. S. A.* **2004**, *101*, 8491.

(48) Gonzalez-Periz, A.; Horrillo, R.; Ferre, N.; Gronert, K.; Dong, B.; Moran-Salvador, E.; Titos, E.; Martinez-Clemente, M.; Lopez-Parra, M.; Arroyo, V.; Claria, J. *FASEB J.* **2009**, *23*, 1946.

(49) Lukiw, W. J.; Cui, J.-G.; Marcheselli, V. L.; Bodker, M.; Botkjaer, A.; Gotlinger, K.; Serhan, C. N.; Bazan, N. G. *J. Clin. Invest.* **2005**, *115*, 2774.

(50) Zhao, Y.; Calon, F.; Julien, C.; Winkler, J. W.; Petasis, N. A.; Lukiw, W. J.; Bazan, N. G. *PLoS One* **2011**, *6*, e15816.

(51) Chen, P.; Fenet, B.; Michaud, S.; Tomczyk, N.; Vericel, E.; Lagarde, M.; Guichardant, M. *FEBS Lett.* **2009**, *583*, 3478.

(52) Hong, S.; Gronert, K.; Devchand, P. R.; Moussignac, R.-L.; Serhan, C. N. *J Biol Chem* **2003**, *278*, 14677.

(53) Tungen, J. E.; Aursnes, M.; Vik, A.; Ramon, S.; Colas, R. A.; Dalli, J.; Serhan, C. N.; Hansen, T. V. *J. Nat. Prod.* **2014**, *77*, 2241.

(54) Aursnes, M.; Tungen, J. E.; Vik, A.; Colas, R.; Cheng, C.-Y. C.; Dalli, J.; Serhan, C. N.; Hansen, T. V. *J. Nat. Prod.* **2014**, *77*, 910.

(55) Corey, E. J.; Mehrotra, M. M. *Tetrahedron Lett.* **1986**, *27*, 5173.

(56) Aursnes, M.; Tungen, J. E.; Vik, A.; Dalli, J.; Hansen, T. V. *Org. Biomol. Chem.*

2014, *12*, 432.

(57) Lucet, D.; Heyse, P.; Gissot, A.; Le Gall, T.; Mioskowski, C. *Eur. J. Org. Chem.* **2000**, 3575.

(58) Maryanoff, B. E.; Reitz, A. B. *Chem. Rev.* **1989**, *89*, 863.

(59) Vedejs, E.; Peterson, M. J. *Top. Stereochem.* **1994**, *21*, 1.

(60) Wurtz, C. A. *Soc. Chim. Fr.* **1987**, *17*, 436.

(61) Gryko, D.; Walaszek, D. *C-C formation by aldol reaction*; John Wiley & Sons, Inc.: New Jersey, 2013. 81-127.

(62) Nielsen, A. T.; Houlihan, W. J. *Org. React.* **1968**, *16*, 438.

(63) Zhang, J. *Evans aldol reaction*; John Wiley & Sons, Inc.: New Jersey, 2009. 532-553.

(64) Evans, D. A.; Bartroli, J.; Shih, T. L. *Journal of the American Chemical Society* **1981**, *103*, 2127.

(65) Nagao, Y.; Dai, W. M.; Ochiai, M.; Shiro, M. *J. Org. Chem.* **1989**, *54*, 5211.

(66) Tungen, J. E.; Aursnes, M.; Hansen, T. V. *Tetrahedron Lett.* **2015**, *56*, 1843.

(67) Primdahl, K. G.; Tungen, J. E.; Aursnes, M.; Hansen, T. V.; Vik, A. *Org. Biomol. Chem.* **2015**, *13*, 5412.

(68) Chinchilla, R.; Najera, C. *Chem. Rev.* **2007**, *107*, 874.

(69) Dieck, H. A.; Heck, F. R. *J. Organomet. Chem.* **1975**, *93*, 259.

(70) Cassar, L. *J. Organomet. Chem.* **1975**, *93*, 253.

(71) Sonogashira, K.; Tohda, Y.; Hagihara, N. *Tetrahedron Lett.* **1975**, 4467.

(72) Nishihara, Y.; Springer, Berlin Heidelberg: 2013; Vol. 80.

(73) Nolsøe, J. M. J.; Hansen, T. V. *Unpublished protocols*

(74) Gottlieb, H. E.; Kotlyar, V.; Nudelman, A. *J. Org. Chem.* **1997**, *62*, 7512.

(75) Boland, W.; Schroer, N.; Sieler, C.; Feigel, M. *Helv. Chim. Acta* **1987**, *70*, 1025.

(76) Dalli, J.; Chiang, N.; Serhan, C. N. *Proc. Natl. Acad. Sci. U. S. A.* **2014**, *111*, E4753.

(77) Dalli, J.; Ramon, S.; Norris, P. C.; Colas, R. A.; Serhan, C. N. *FASEB J.* **2015**, *29*, 2120.

(78) Rodriguez, A. R.; Spur, B. W. *Tetrahedron Lett.* **2015**, *56*, 5811.

(79) Ramon, S.; Dalli, J.; Sanger, J. M.; Winkler, J. W.; Aursnes, M.; Tungen, J. E.; Hansen, T. V.; Serhan, C. N. *Am. J. Pathol.* **2016**, *186*, 962.

6 Appendix

6.1 NMR spectra of the synthesized compounds

^{1}H NMR (400 MHz, CDCl$_3$) δ 4.12 – 3.82 (m, 2H), 2.48 (s, 1H), 2.02 – 1.67 (m, 2H), 1.48 (s, 3H).
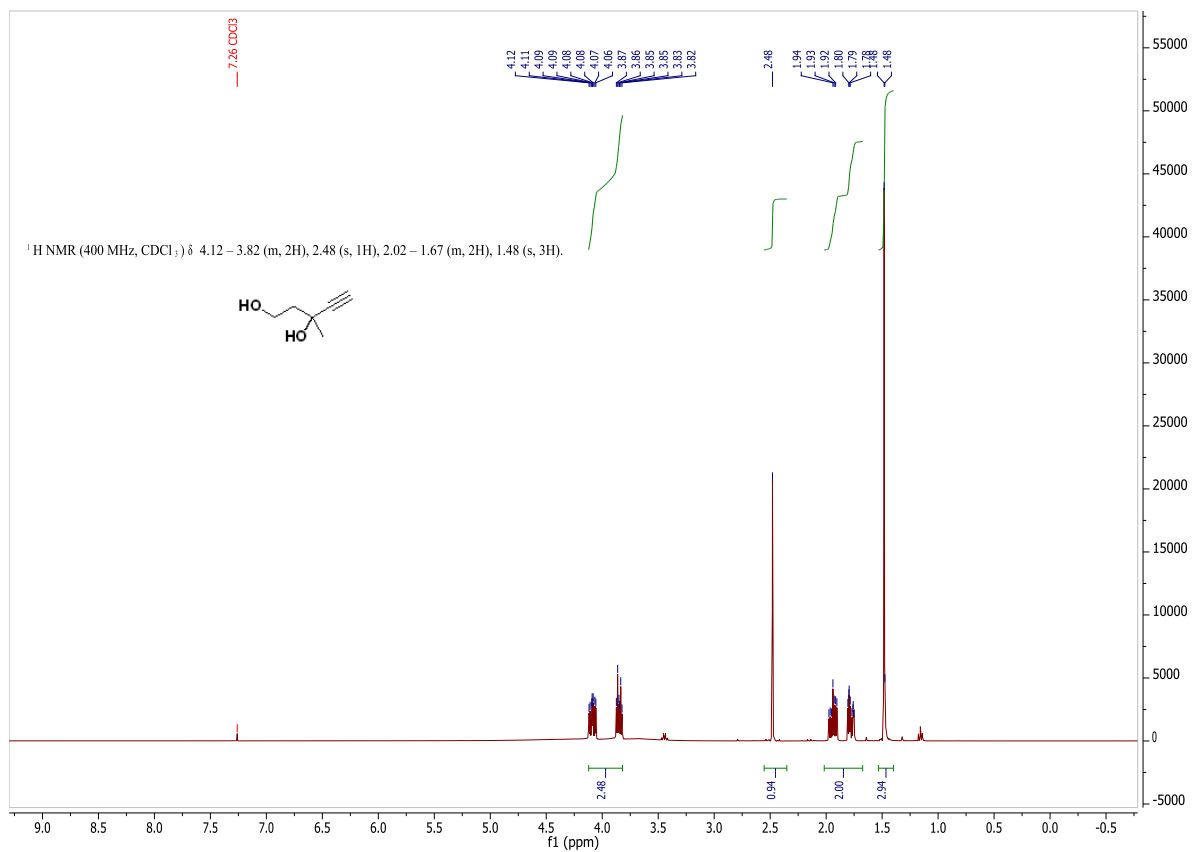
Figure A-1. ^{1}H NMR spectrum of compound **87**.

^{13}C NMR (101 MHz, CDCl$_3$) δ 87.0, 72.1, 68.5, 60.3, 43.4, 30.5.
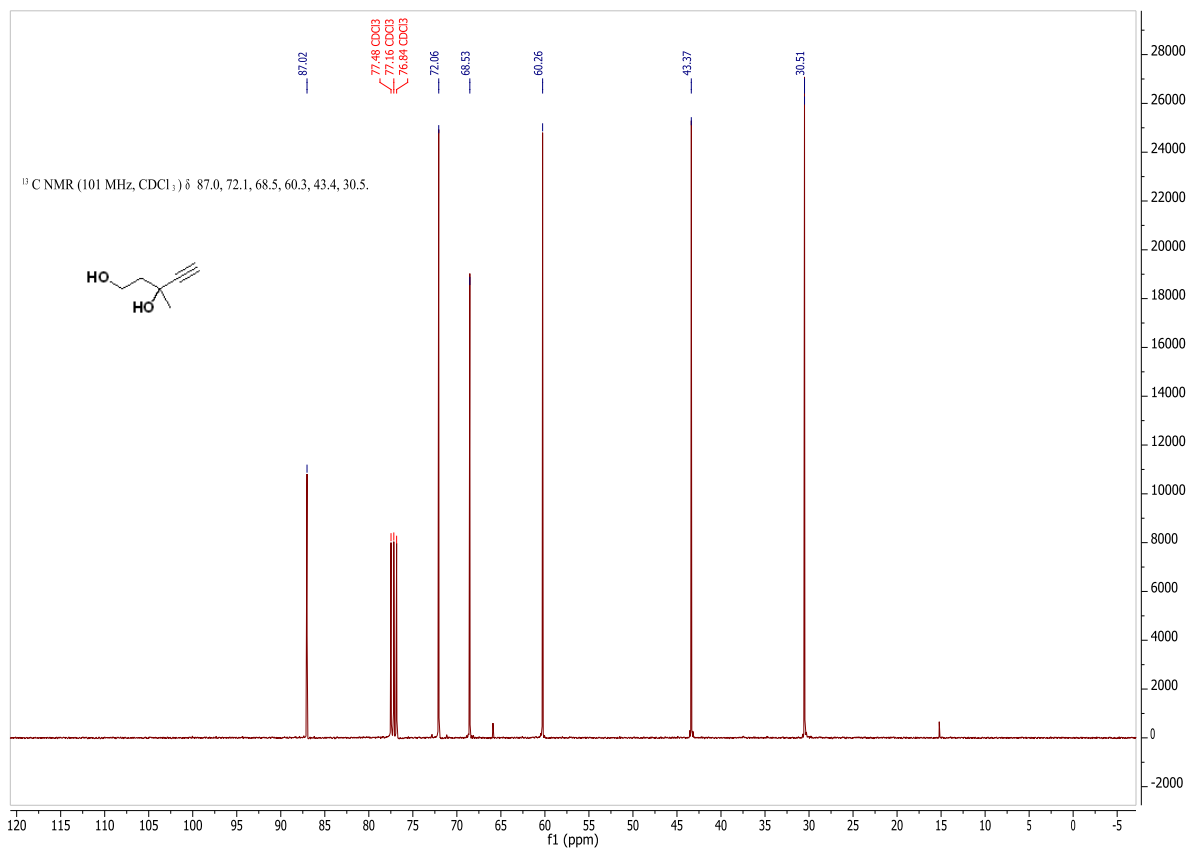
Figure A-2. ^{13}C NMR spectrum of compound **87**.
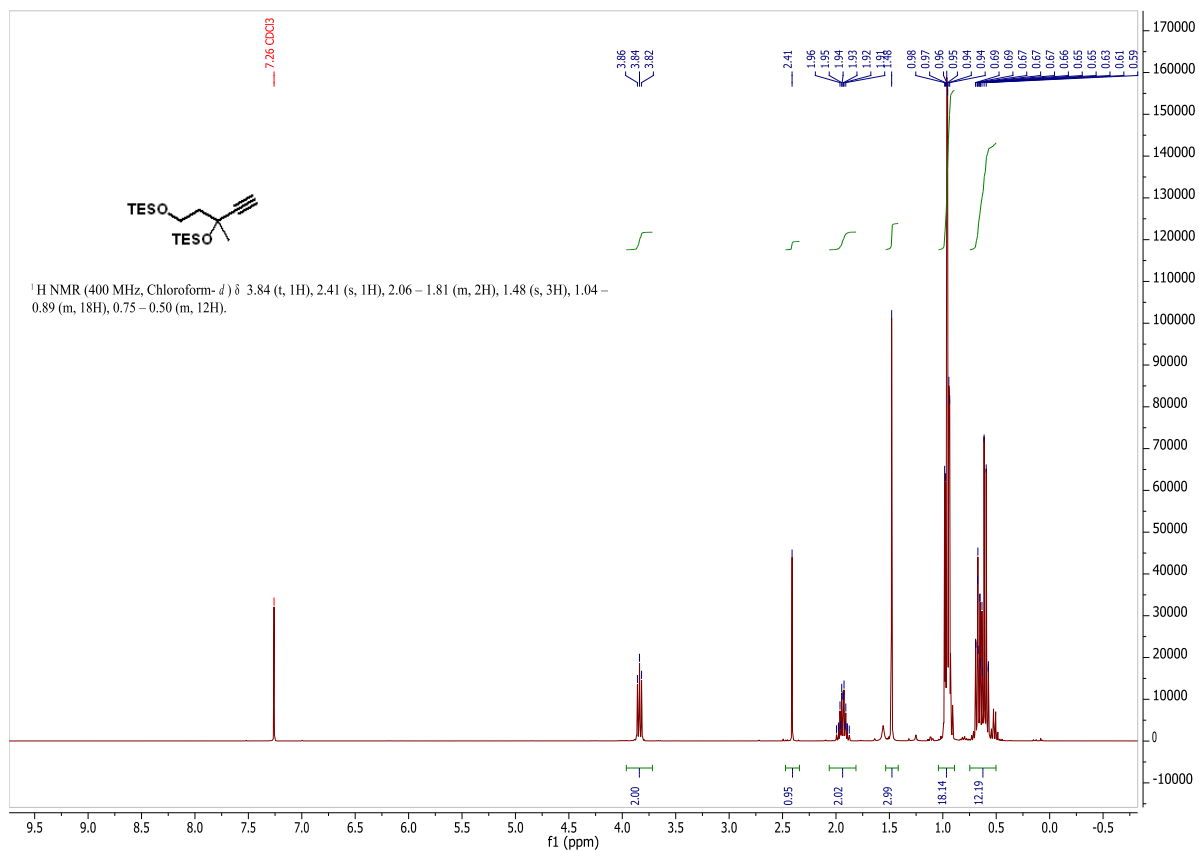
Figure A-3. ^{1}H NMR spectrum of compound **88**.

^{1}H NMR (400 MHz, Chloroform-*d*) δ 3.84 (t, 1H), 2.41 (s, 1H), 2.06 – 1.81 (m, 2H), 1.48 (s, 3H), 1.04 – 0.89 (m, 18H), 0.75 – 0.50 (m, 12H).

^{13}C NMR (101 MHz, CDCl$_3$) δ 88.0, 72.1, 67.6, 59.7, 47.8, 31.6, 7.1, 6.9, 6.2, 4.6.
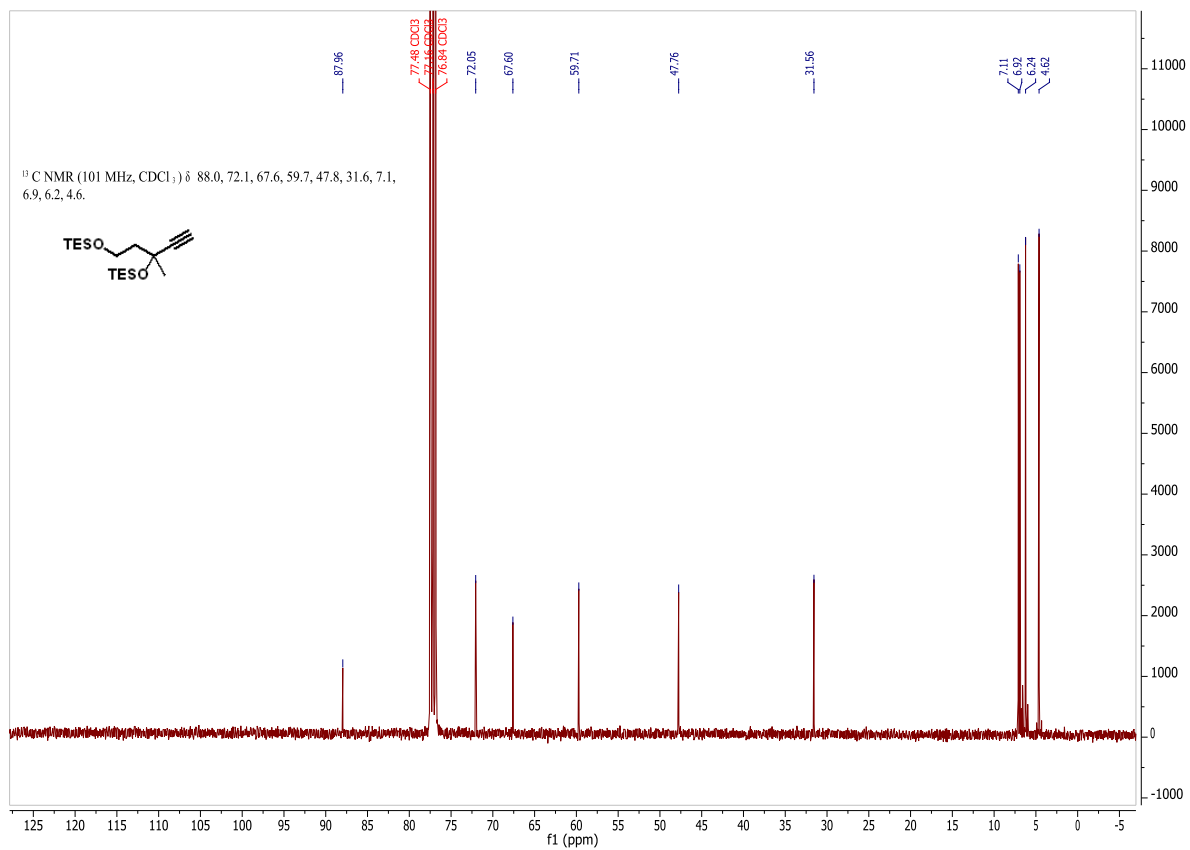
Figure A-4. ^{13}C NMR spectrum of compound **88**.

^{1}H NMR (400 MHz, CDCl$_3$) δ 9.89 (t, J = 2.8 Hz, 1H), 2.62 (d, J = 2.8 Hz, 2H), 2.57 (s, 1H), 1.58 (s, 3H), 0.96 (t, J = 7.9 Hz, 9H), 0.770 (qd, J = 7.8, 2.2 Hz, 6H).
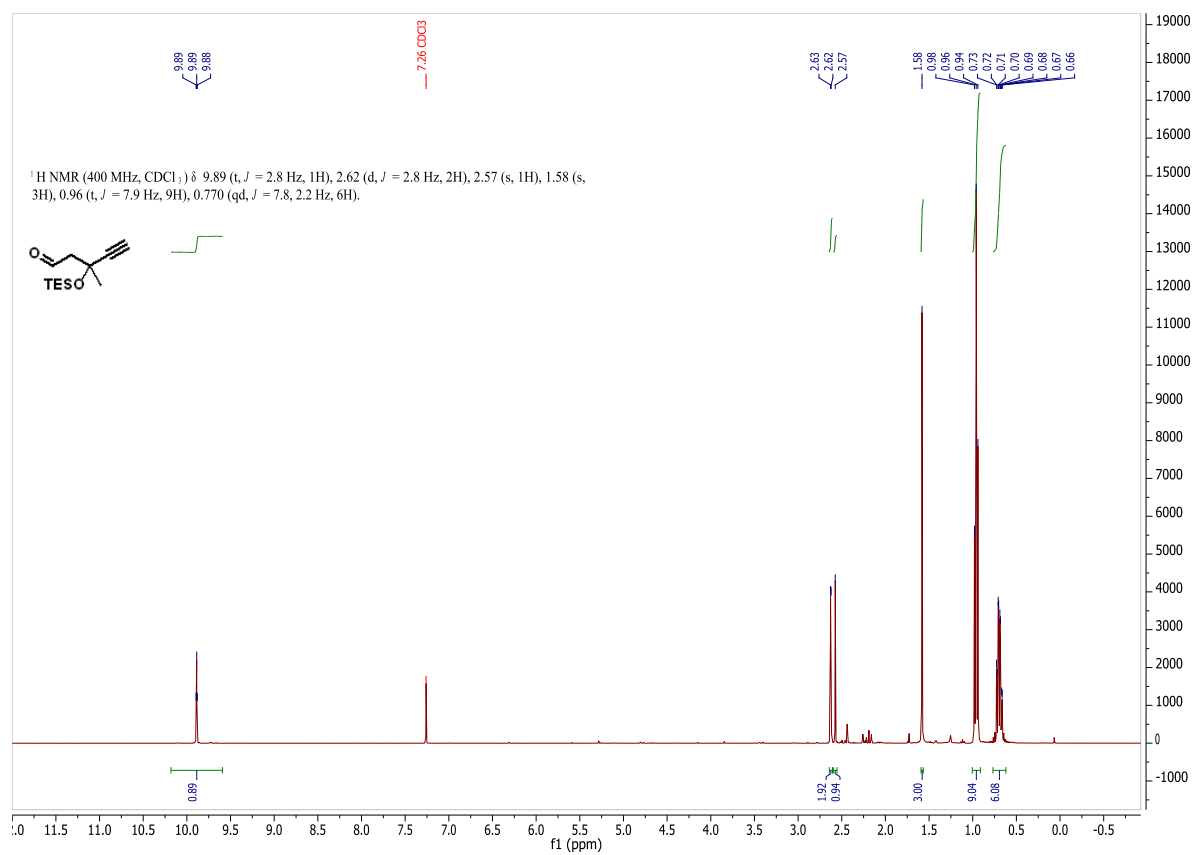
Figure A-5. ^{1}H NMR spectrum of compound **89**.

^{13}C NMR (101 MHz, CDCl$_3$) δ 201.7, 86.6, 73.9, 66.4, 57.3, 31.6, 7.0, 6.1.
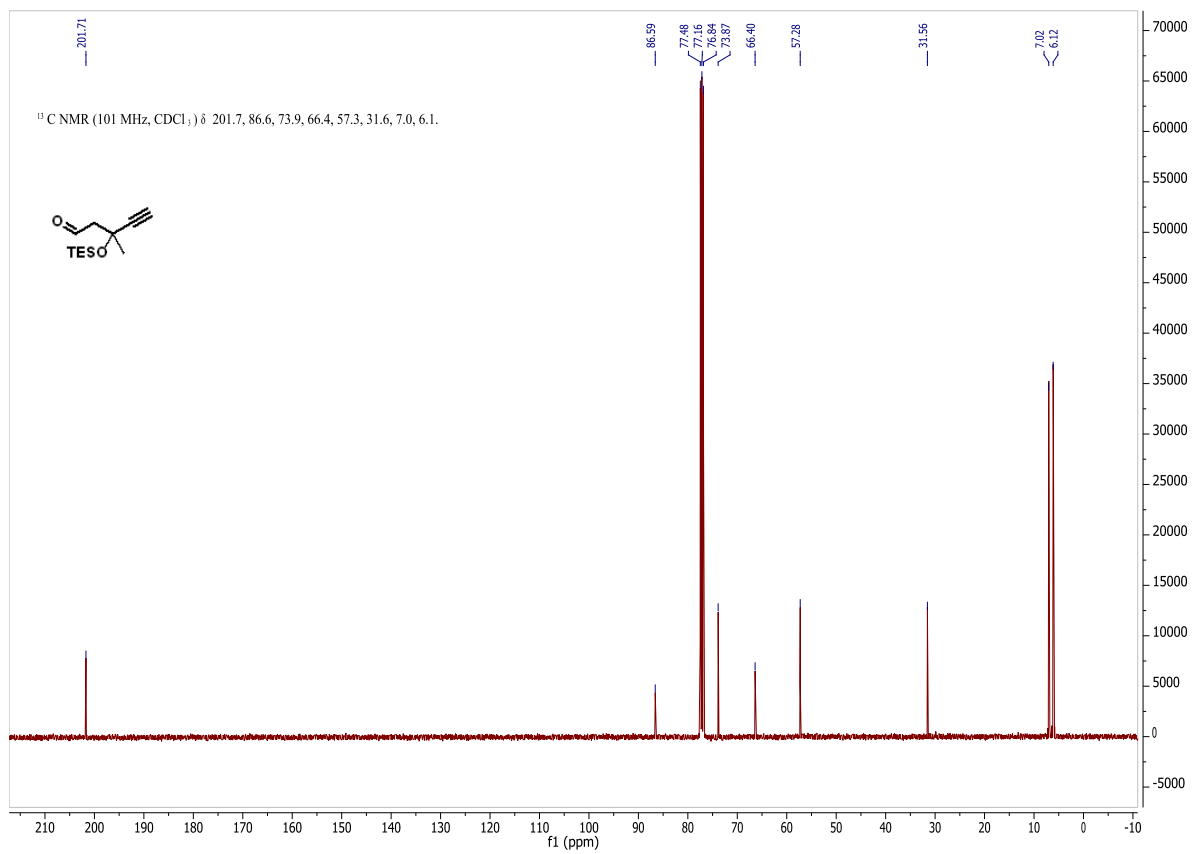
Figure A-6. ^{13}C NMR spectrum of compound **89**.

¹H NMR (400 MHz, Chloroform-*d*) δ 5.62 – 5.40 (m, *J* = 11.9 Hz, 2H), 2.51 – 2.33 (m, 3H), 2.15 – 1.97 (m, 2H), 1.44 (s, 3H), 0.97 (t, *J* = 7.9 Hz, 12H), 0.74 – 0.64 (m, 6H).
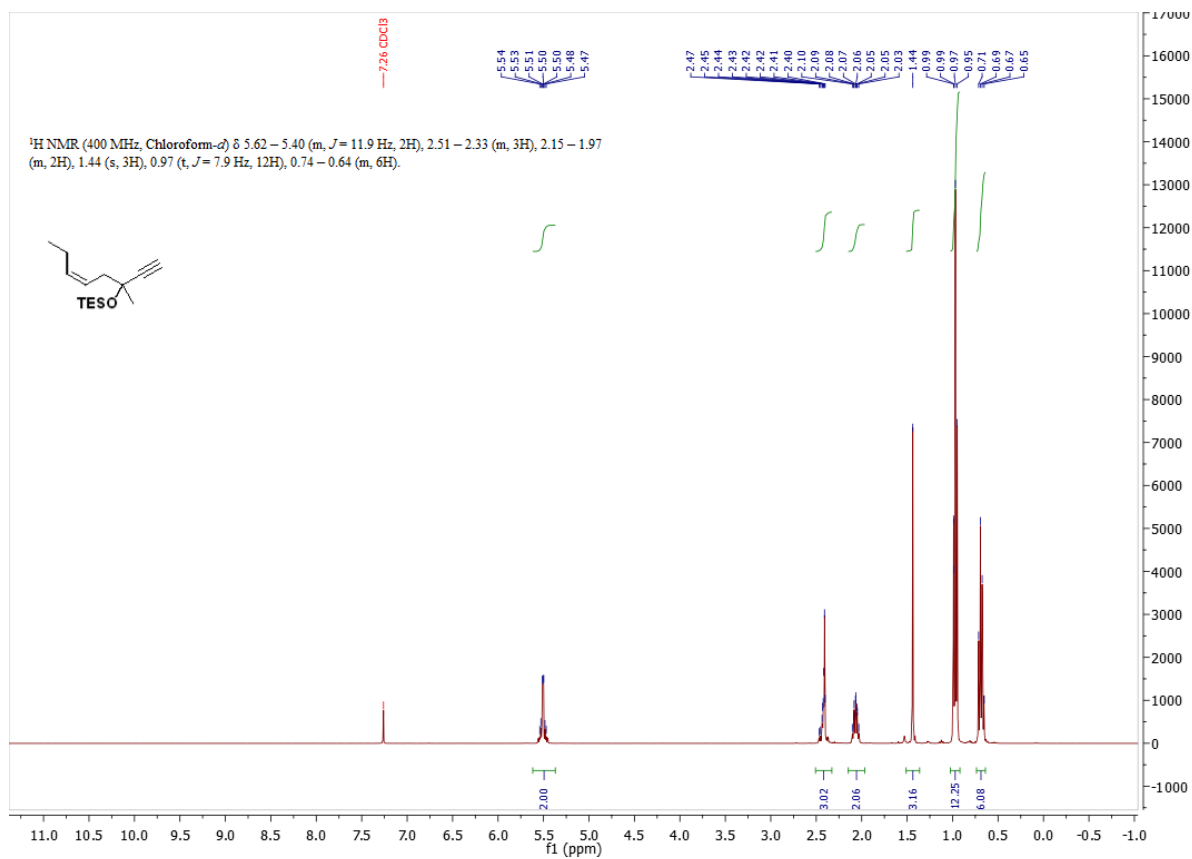
Figure A-7. ¹H NMR spectrum of compound **85**.

^{13}C NMR (101 MHz, CDCl$_3$) δ 134.3, 124.1, 88.5, 72.0, 69.0, 42.9, 30.6, 21.0, 14.3, 7.1, 6.3.
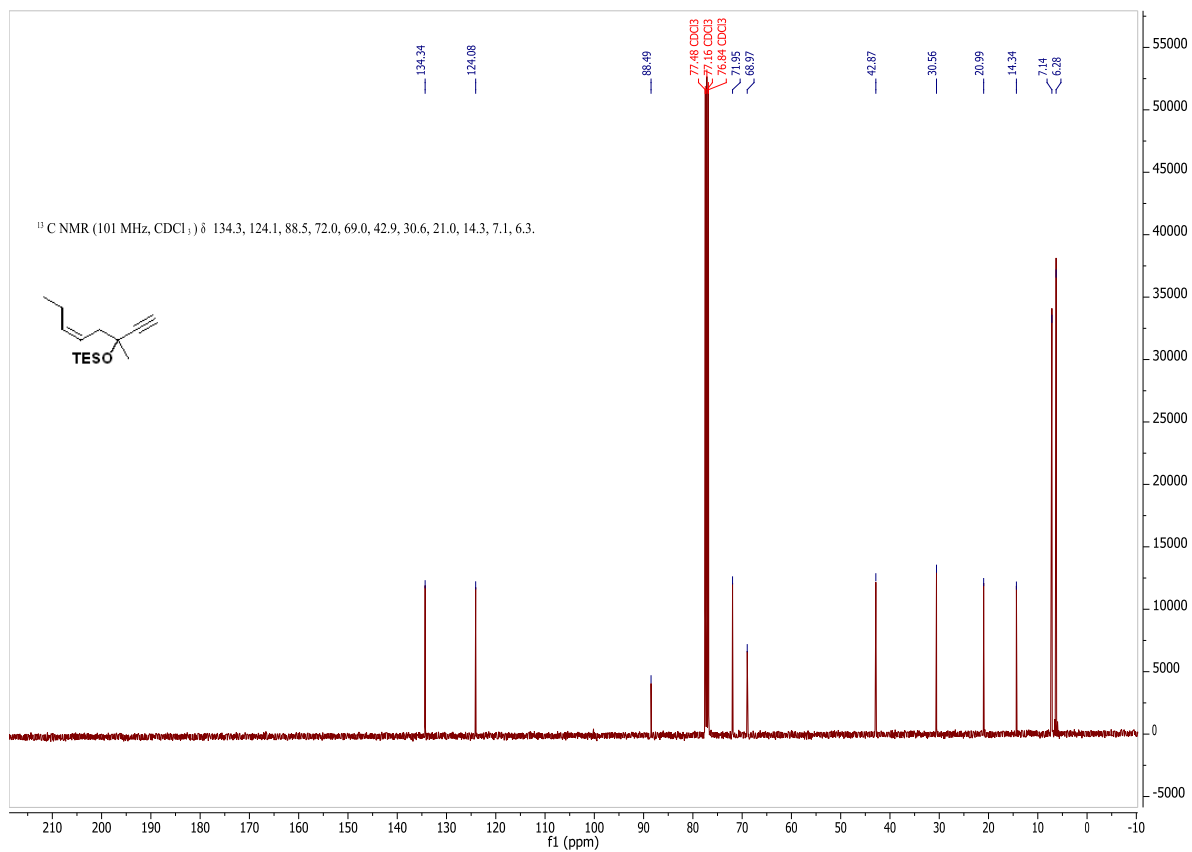
Figure A-8. ^{13}C NMR spectrum of compound **85**.

¹H NMR (400 MHz, Chloroform-*d*) δ 3.66 (s, 3H), 3.63 (t, *J* = 6.5 Hz, 2H), 2.31 (t, *J* = 7.5 Hz, 2H), 1.99 (bs, 1H), 1.68 – 1.52 (m, 4H), 1.43 – 1.30 (m, 4H).
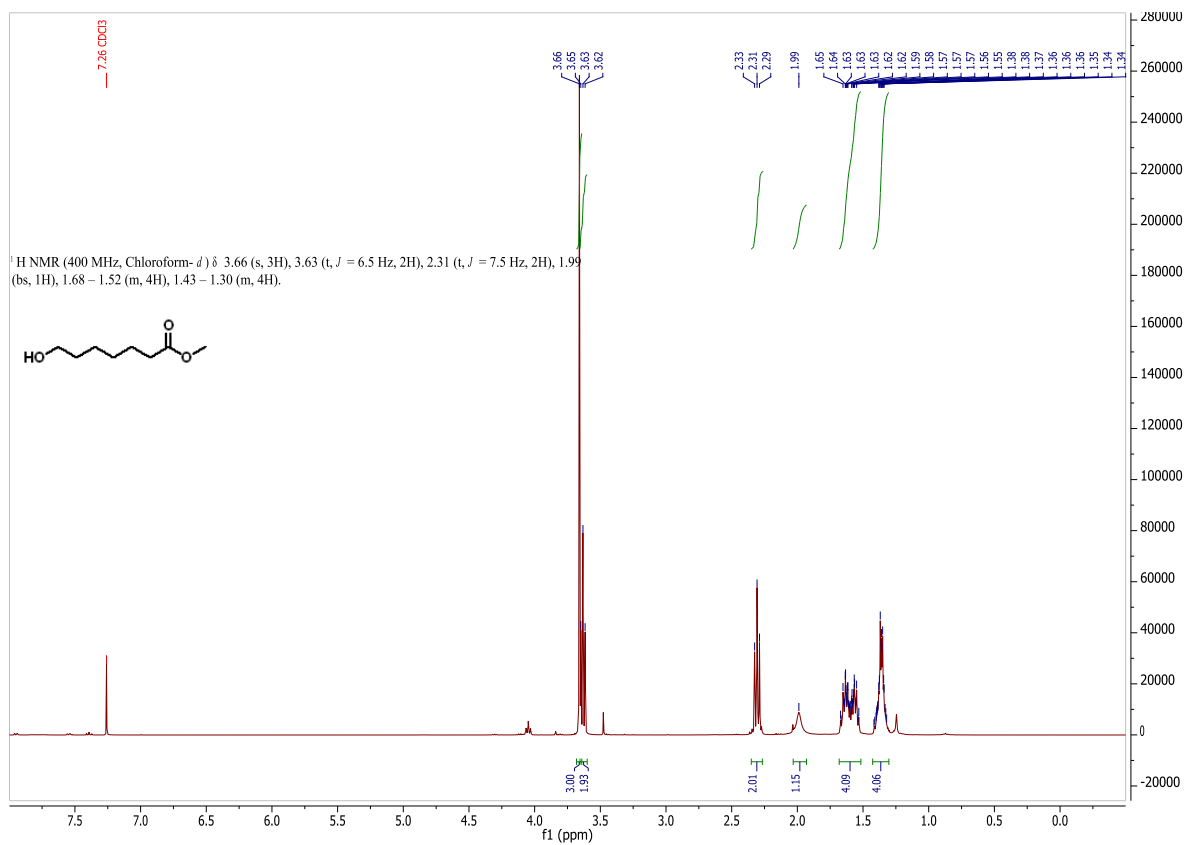
Figure A-9. ¹H NMR spectrum of compound **92**.

^{13}C NMR (101 MHz, CDCl$_3$) δ 174.4, 63.0, 51.6, 34.1, 32.7, 29.0, 25.5, 25.0.
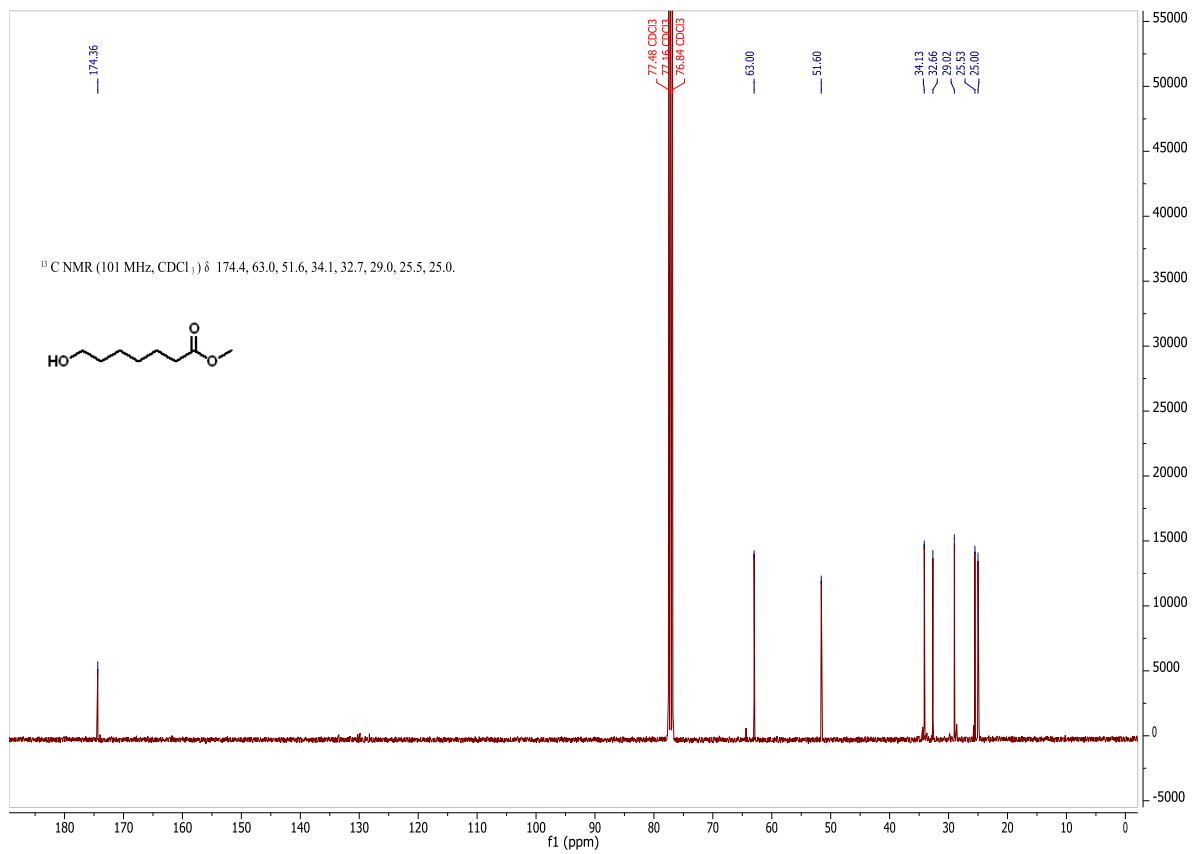
Figure A-10. ^{13}C NMR spectrum of compound **92**.

¹H NMR (400 MHz, Chloroform-*d*) δ 3.66 (s, 3H), 3.17 (t, *J* = 7.0 Hz, 2H), 2.30 (t, *J* = 7.5 Hz, 2H), 1.81 (p, *J* = 7.0 Hz, 2H), 1.63 (p, *J* = 7.6 Hz, 2H), 1.47 – 1.26 (m, 4H).
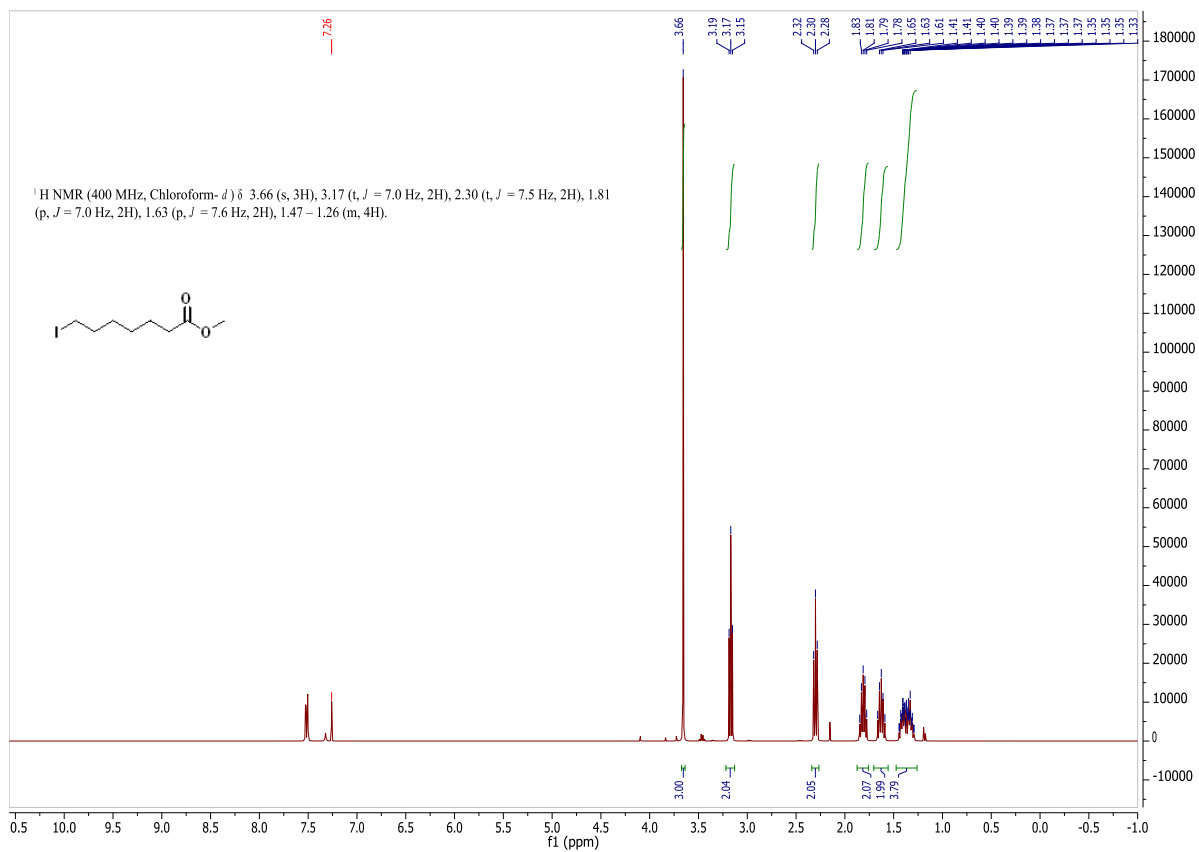
Figure A-11. ¹H NMR spectrum of compound **93**.

^{13}C NMR (101 MHz, CDCl$_3$) δ 174.1, 51.6, 34.0, 33.4, 30.2, 28.1, 24.8, 7.0.
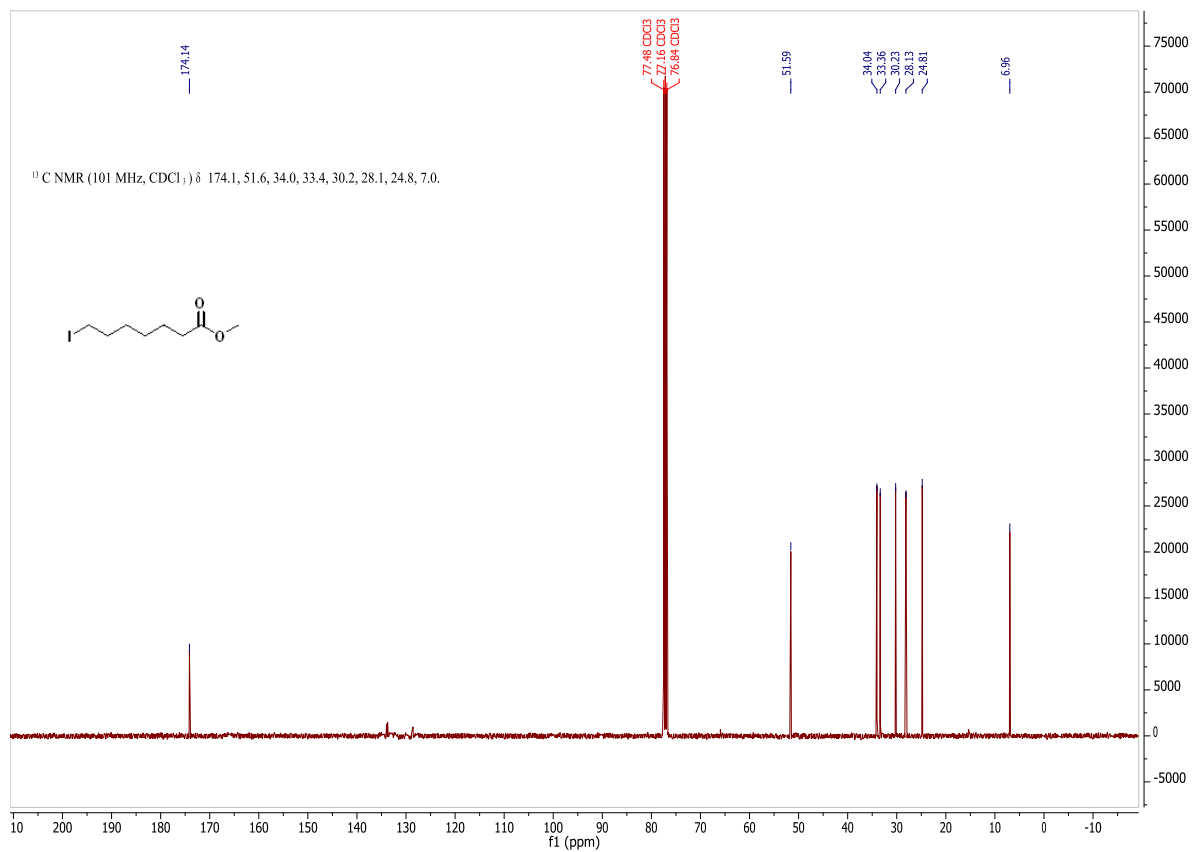
Figure A-12. ^{13}C NMR spectrum of compound **93**.

^{1}H NMR (400 MHz, CDCl$_3$) δ 7.91 – 7.58 (m, 15H), 3.69 – 3.62 (m, 2H), 3.60 (s, 3H), 2.24 (t, J = 7.3 Hz, 2H), 1.72 – 1.47 (m, 6H), 1.37 – 1.22 (m, 2H).
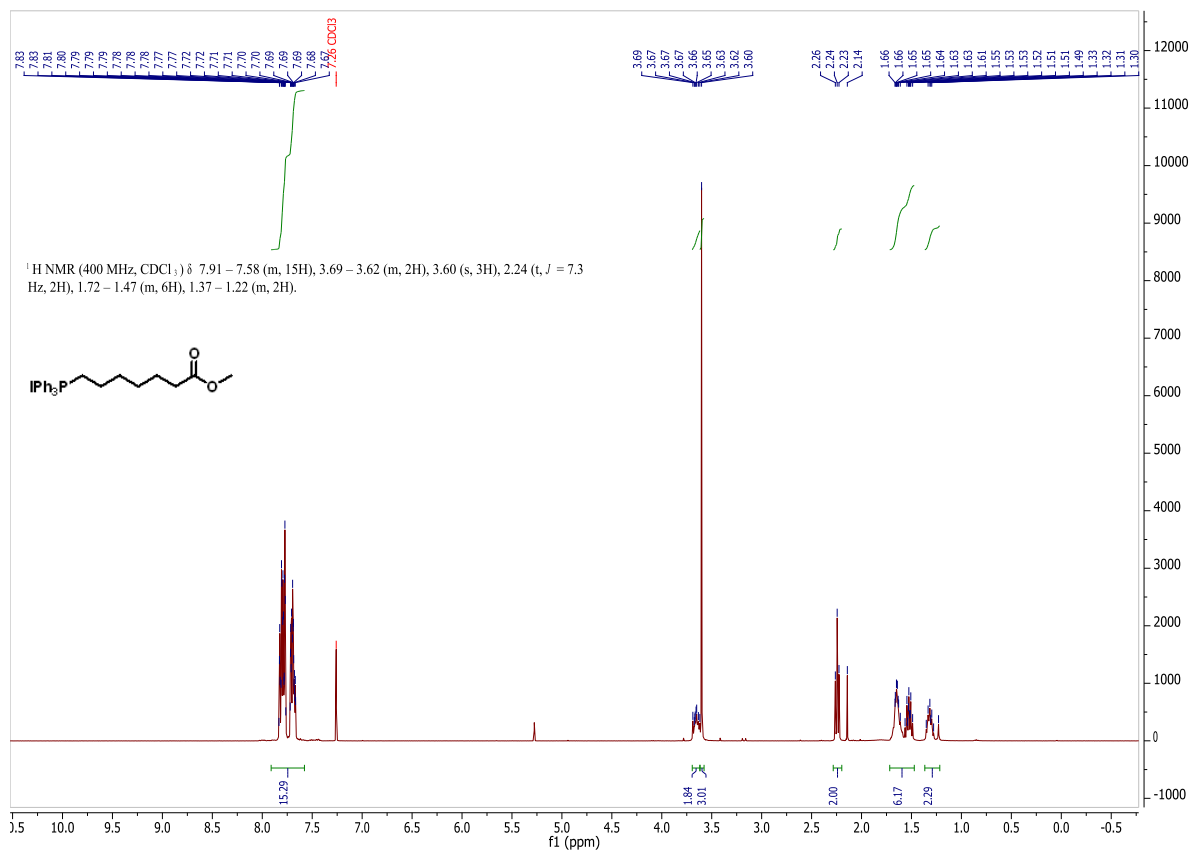
Figure A-13. ^{1}H NMR spectrum of compound **58**.

^{13}C NMR (101 MHz, Chloroform-d) δ 174.2 , 135.2 (d, J = 3.1 Hz), 133.8 (d, J = 10.0 Hz), 130.7 (d, J = 12.5 Hz), 118.2 (d, J = 86.0 Hz), 51.5, 33.9, 30.1 (d, J = 15.8 Hz), 24.4, 23.2 (d, J = 50.1 Hz), 22.5 (d, J = 4.5 Hz).
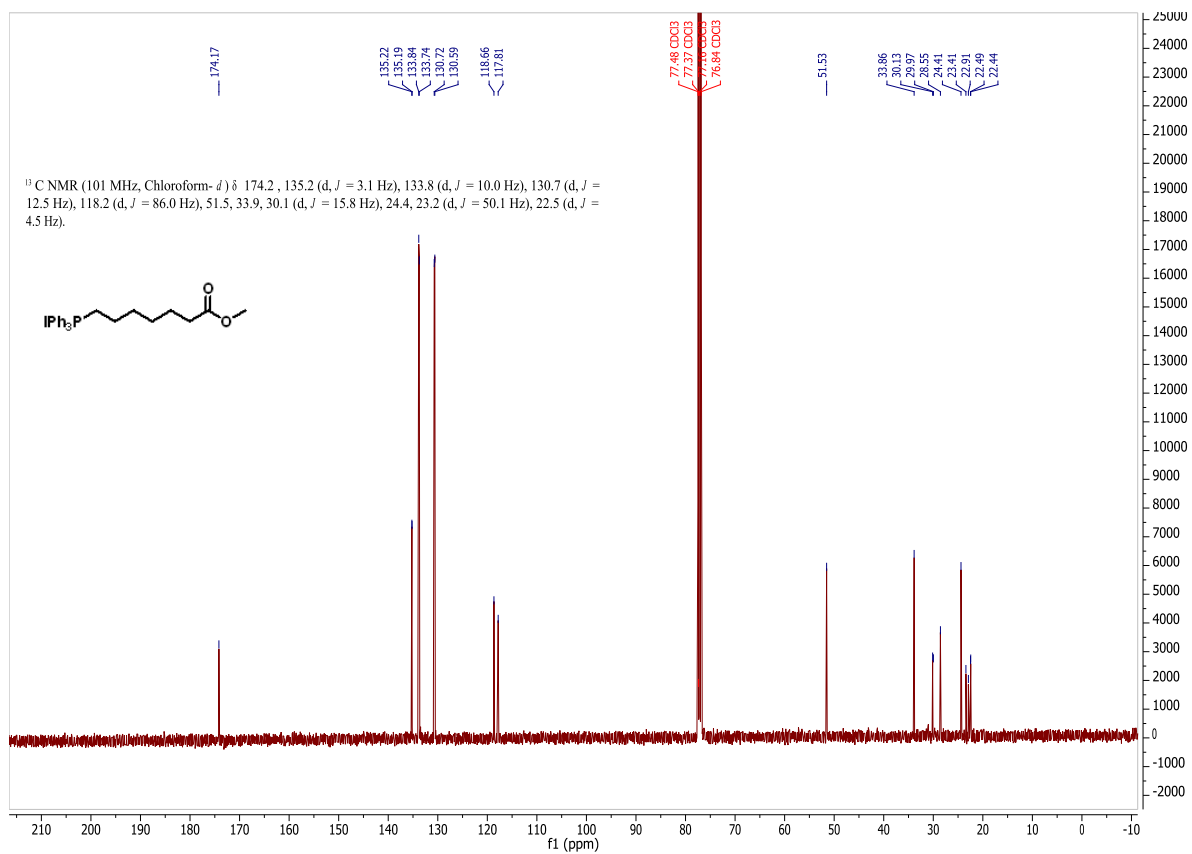
Figure A-14. ^{13}C NMR spectrum of compound **58**.

^{1}H NMR (400 MHz, Chloroform-d) δ 9.76 (t, J = 2.3 Hz, 1H), 6.70 (dd, J = 13.5, 10.9 Hz, 1H), 6.34 (d, J = 13.5 Hz, 1H), 6.17 (ddd, J = 15.0, 10.7, 1.5 Hz, 1H), 5.76 (ddd, J = 15.2, 6.0, 0.9 Hz, 1H), 4.67 (dd, J = 6.8, 5.5 Hz, 1H), 2.76 – 2.42 (m, 2H), 0.88 (s, 9H), 0.07 (s, 3H), 0.04 (s, 3H).
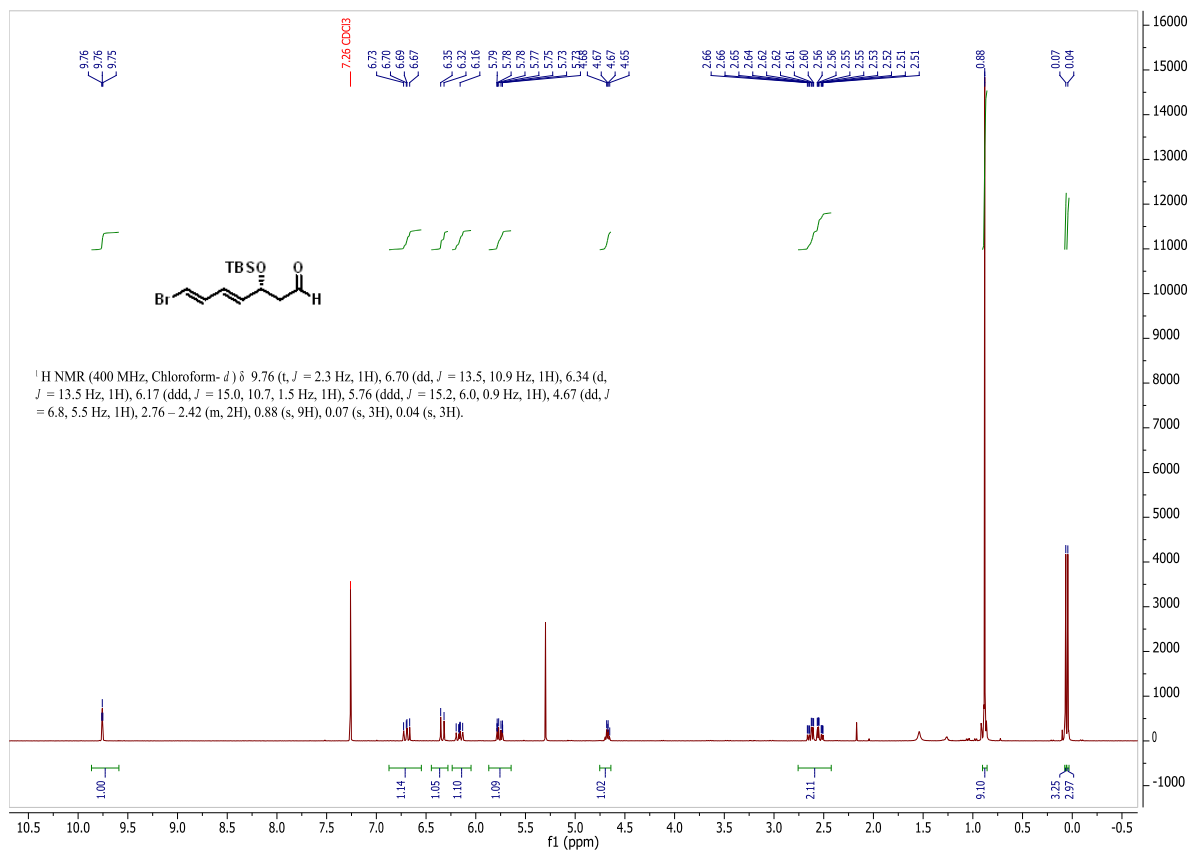
Figure A-15. ^{1}H NMR spectrum of compound **57**.
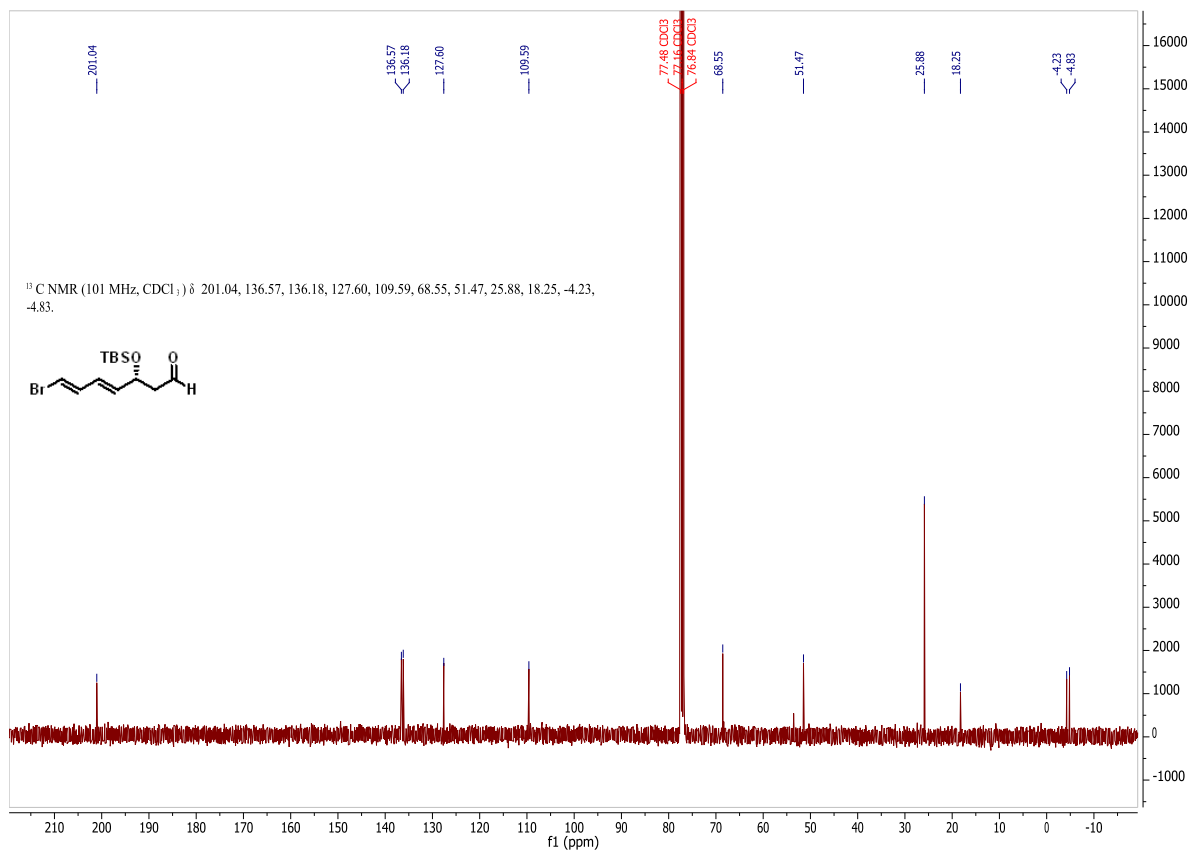
Figure A-16. ^{13}C NMR spectrum of compound **57**.

^{1}H NMR (400 MHz, Chloroform-d) δ 6.68 (dd, J = 13.5, 10.8 Hz, 1H), 6.27 (d, J = 13.6 Hz, 1H), 6.08 (dd, J = 15.2, 10.8 Hz, 1H), 5.72 (dd, J = 15.2, 9.3 Hz, 1H), 5.50 – 5.28 (m, J = 12.3 Hz ,2H), 4.14 (dd, J = 6.1, 1.6 Hz, 1H), 3.67 (s, 3H), 2.30 (t, J = 7.6 Hz, 2H), 2.37 – 2.15 (m, 2H), 2.01 (q, J = 7.0 Hz, 2H), 1.62 (p, J = 7.4 Hz, 2H), 1.42 – 1.30 (m, 4H), 0.89 (s, 9H), 0.05 (s, 3H), 0.02 (s, 3H).
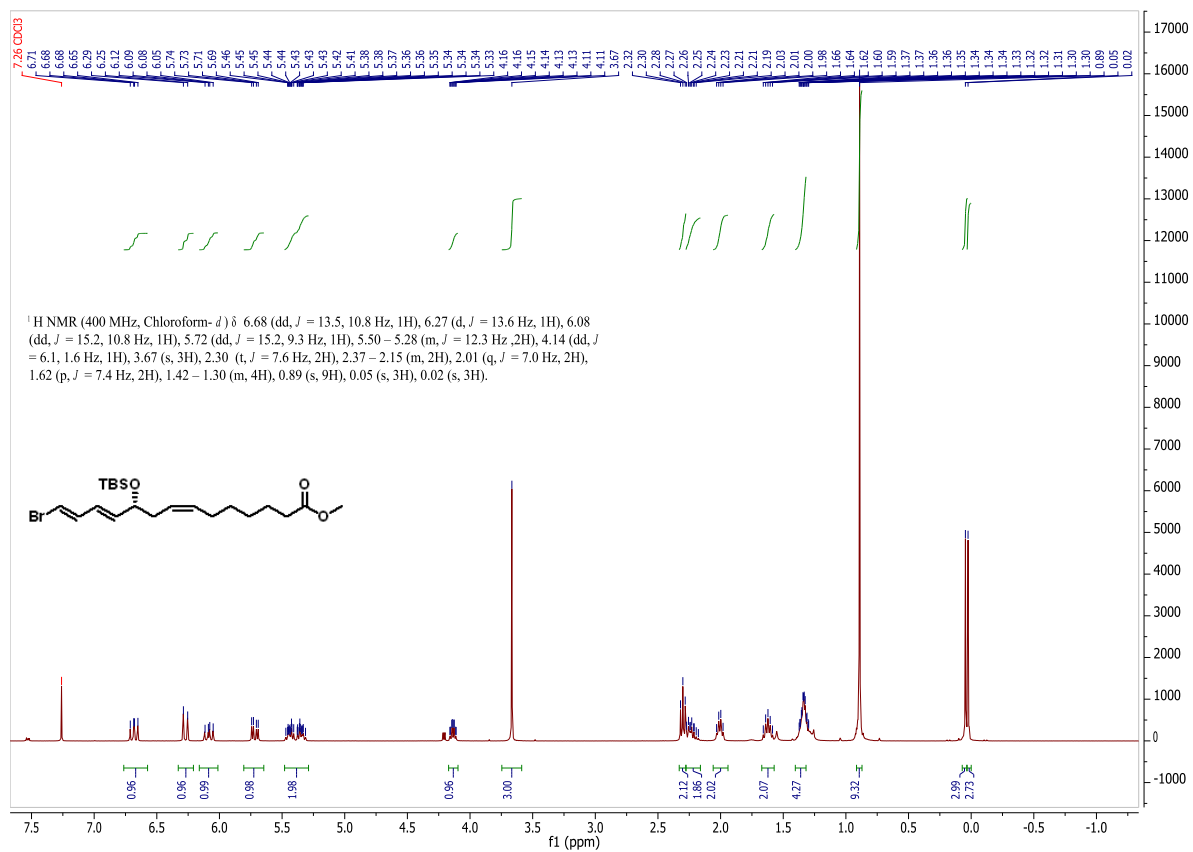
Figure A-17. ^{1}H NMR spectrum of compound **95**.

^{13}C NMR (101 MHz, CDCl$_3$) δ 174.33, 138.10, 137.17, 131.93, 126.59, 125.20, 108.23, 72.71, 51.59, 36.31, 34.21, 29.37, 28.98, 27.42, 26.01, 25.02, 18.41, -4.36, -4.60.
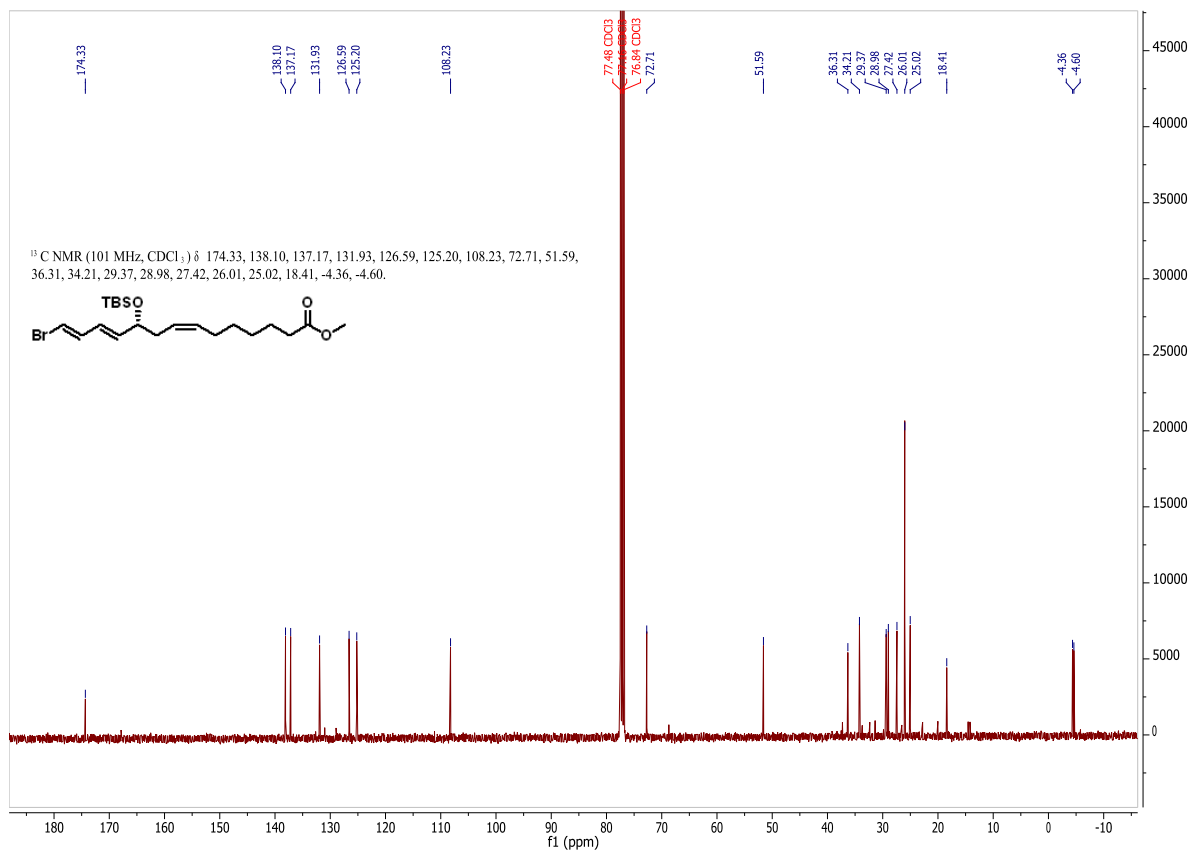
Figure A-18. ^{13}C NMR spectrum of compound **95**.

¹H NMR (400 MHz, Chloroform-*d*) δ 6.49 (dd, *J* = 15.5, 10.9 Hz, 1H), 6.19 (dd, *J* = 15.2, 11.4 Hz, 1H), 5.76 (dd, *J* = 15.0, 5.8 Hz, 1H), 5.64 – 5.28 (m, 5H), 4.25 – 4.12 (m, 1H), 3.67 (s, 3H), 2.42 (t, *J* = 5.7 Hz, 2H), 2.30 (t, *J* = 7.4 Hz, 2H), 2.31 – 2.15 (m, 2H), 2.13 – 1.96 (m, 4H), 1.62 (p, *J* = 6.7, 6.2 Hz, 2H), 1.43 (s, 3H), 1.38 – 1.23 (m, 4H), 1.03 – 0.92 (m, 12H), 0.89 (s, 9H), 0.67 (q, *J* = 7.7 Hz, 6H), 0.04 (d, *J* = 7.8 Hz, 6H).
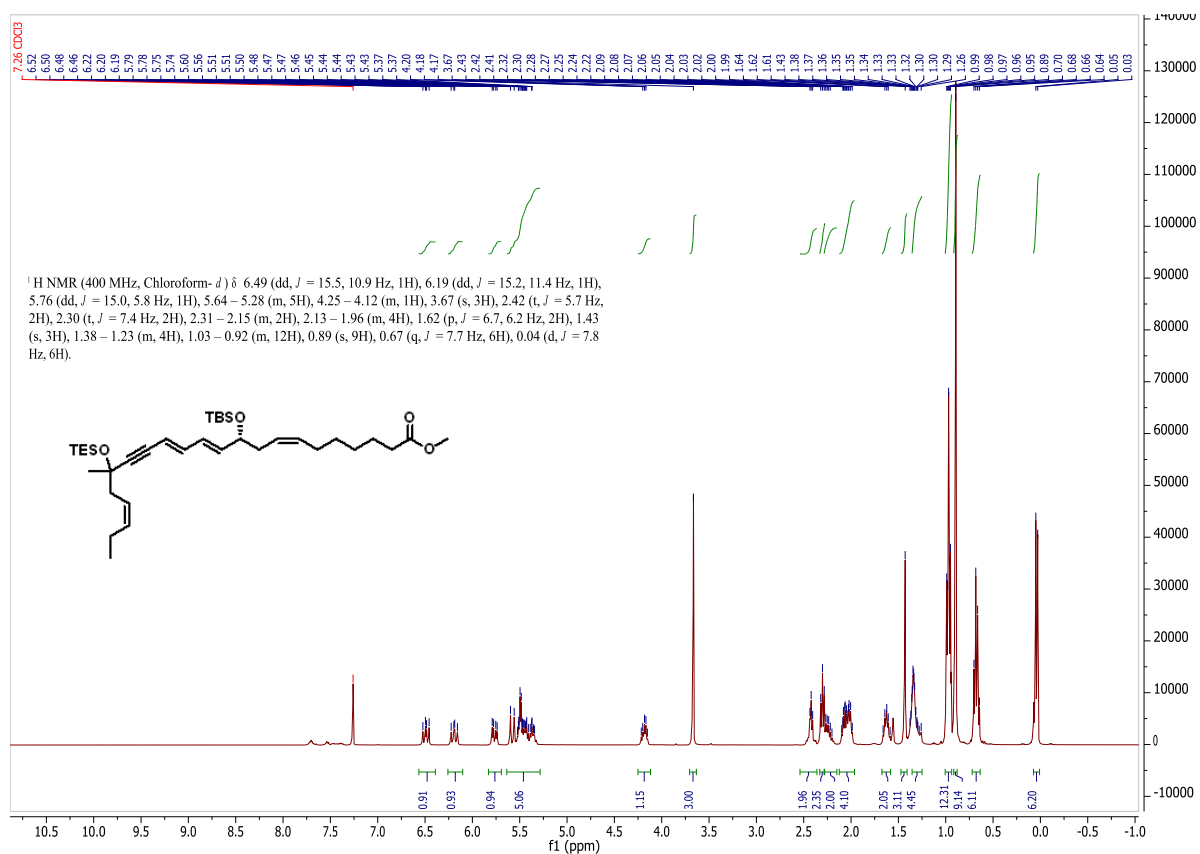
Figure A-19. ¹H NMR spectrum of compound **96**.

^{13}C NMR (101 MHz, CDCl$_3$) δ 174.33, 140.93, 139.28, 134.16, 131.85, 128.65, 125.36, 124.36, 110.72, 96.42, 83.15, 72.92, 69.56, 51.58, 42.99, 36.42, 34.21, 30.60, 29.37, 28.97, 27.43, 26.03, 25.02, 20.98, 18.42, 14.35, 7.19, 6.27, -4.32, -4.59.
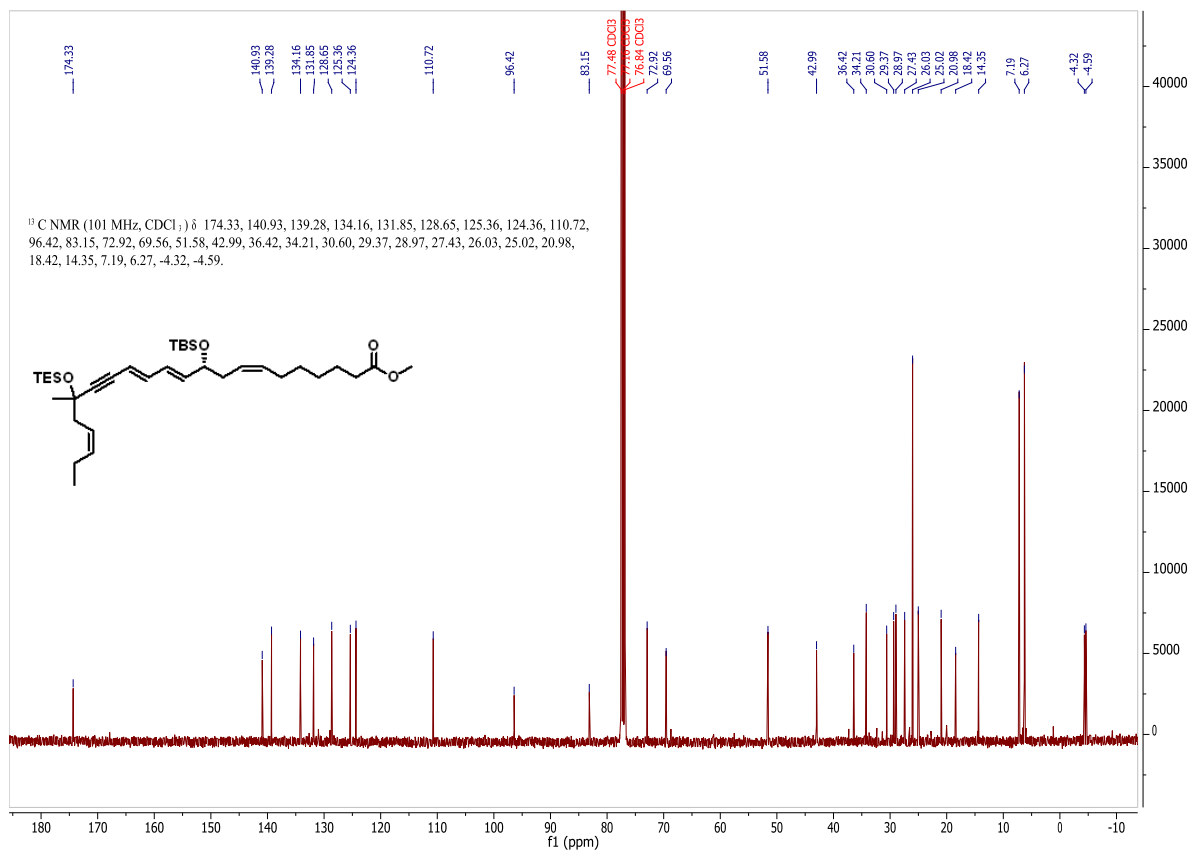
Figure A-20. ^{13}C NMR spectrum of compound **96**.

¹H NMR (600 MHz, MeOH- d_4) δ 6.53 (dd, J = 15.5, 10.8 Hz, 1H), 6.28 (dd, J = 15.8, 11.0 Hz, 1H), 5.81 (dd, J = 15.2, 6.3 Hz, 1H), 5.66 (d, J = 15.5 Hz, 1H), 5.59 – 5.37 (m, 4H), 4.16 – 4.09 (m, 1H), 3.66 (s, 3H), 2.48 – 2.39 (m, 2H), 2.33 (t, J = 7.4 Hz, 2H), 2.32 – 2.23 (m, 2H), 2.15 – 2.04 (m, 5H), 1.70 (bs, J = 4.4 Hz, 1H), 1.62 (p, J = 7.4 Hz, 2H), 1.43 (s, 3H), 1.40 – 1.30 (m, 4H), 0.99 (t, J = 7.6 Hz, 3H).

Figure A-21. ¹H NMR spectrum of compound **97**

^{13}C NMR (151 MHz, MeOH-d_4) δ 176.0, 142.3, 139.7, 135.4, 132.9, 130.3, 126.1, 124.9, 111.8, 96.7, 83.0, 72.8, 68.9, 52.0, 42.3, 36.3, 34.8, 30.3, 29.4, 28.2, 25.9, 24.8, 21.8, 13.9.

Figure A-22. ^{13}C NMR spectrum of compound **97**

^{1}H NMR (400 MHz, Chloroform-d) δ 3.60 (s, 3H), 2.26 (dq, J = 11.8, 7.5 Hz, 5H), 2.10 (s, 19H), 1.98 (q, J = 5.2, 4.7 Hz, 5H), 1.19 (s, 71H), 1.04 (s, 10H), 0.84 – 0.79 (m, 30H).
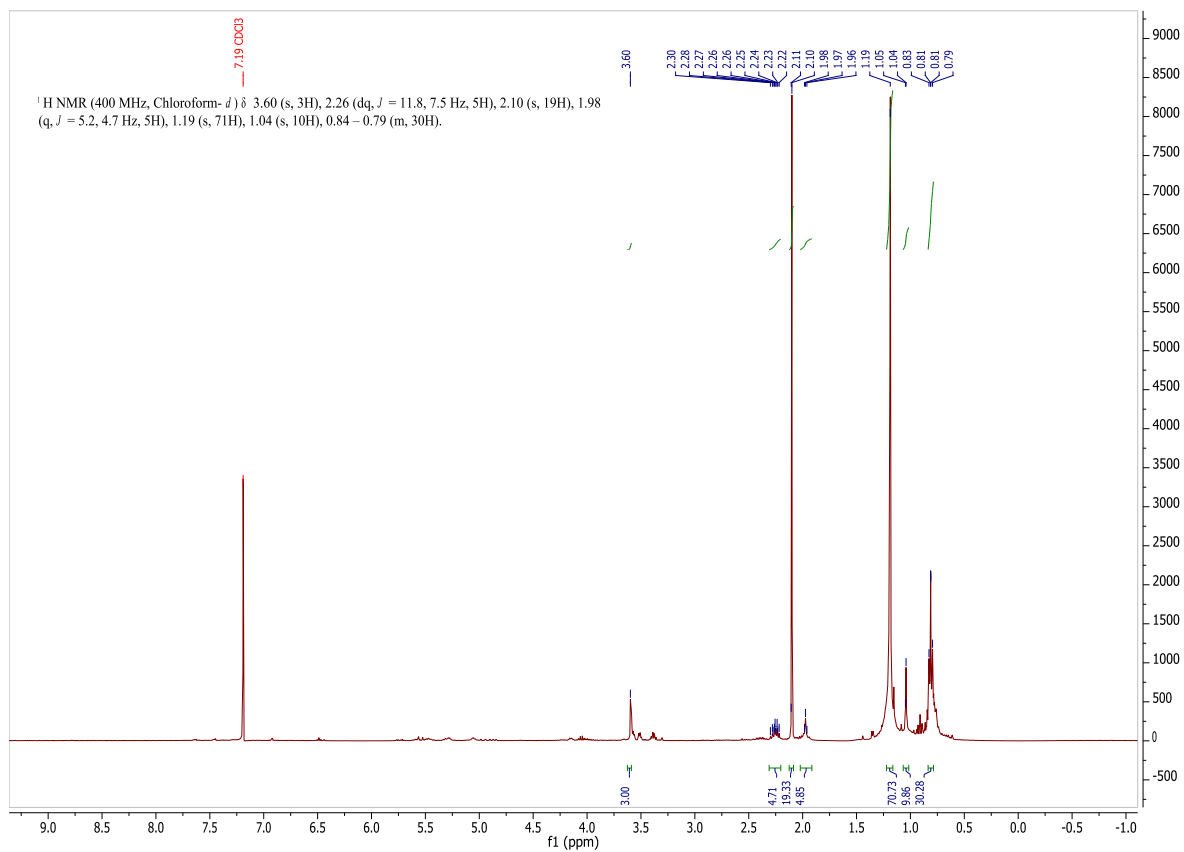
Figure A-23. ^{1}H NMR spectrum of compound from synthesis 4.2.12.

^{13}C NMR (101 MHz, CDCl$_3$) δ 51.98, 42.32, 36.26, 34.79, 30.79, 30.48, 30.29, 29.80, 29.40, 28.20, 25.94, 24.79, 23.75, 21.75, 20.95, 20.71, 15.44, 14.55, 13.93.
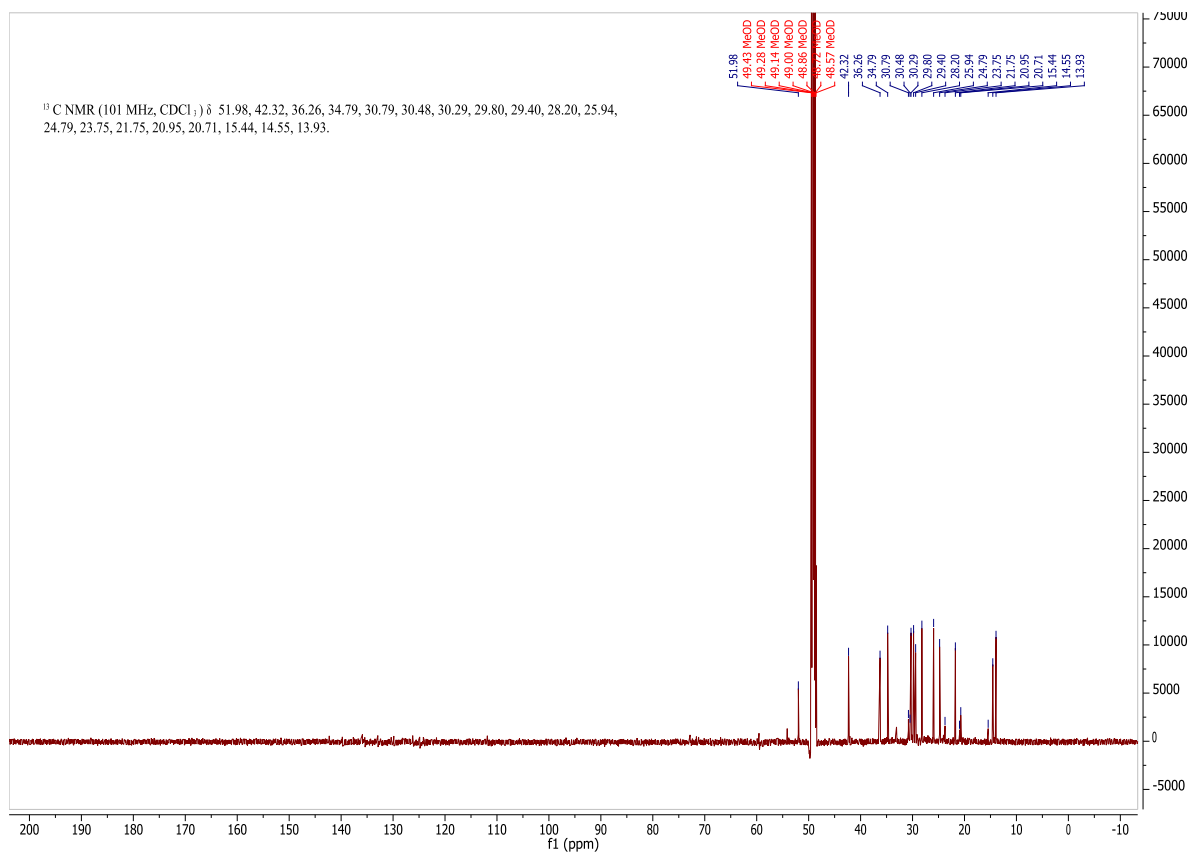
Figure A-24. ^{13}C NMR spectrum of compound from synthesis 4.2.12.

¹H NMR (400 MHz, Chloroform-*d*) δ 4.18 – 4.04 (m, 4H), 3.49 (s, 3H), 2.04 (s, 5H), 1.37 – 1.11 (m, 15H), 0.94 – 0.76 (m, 18H).
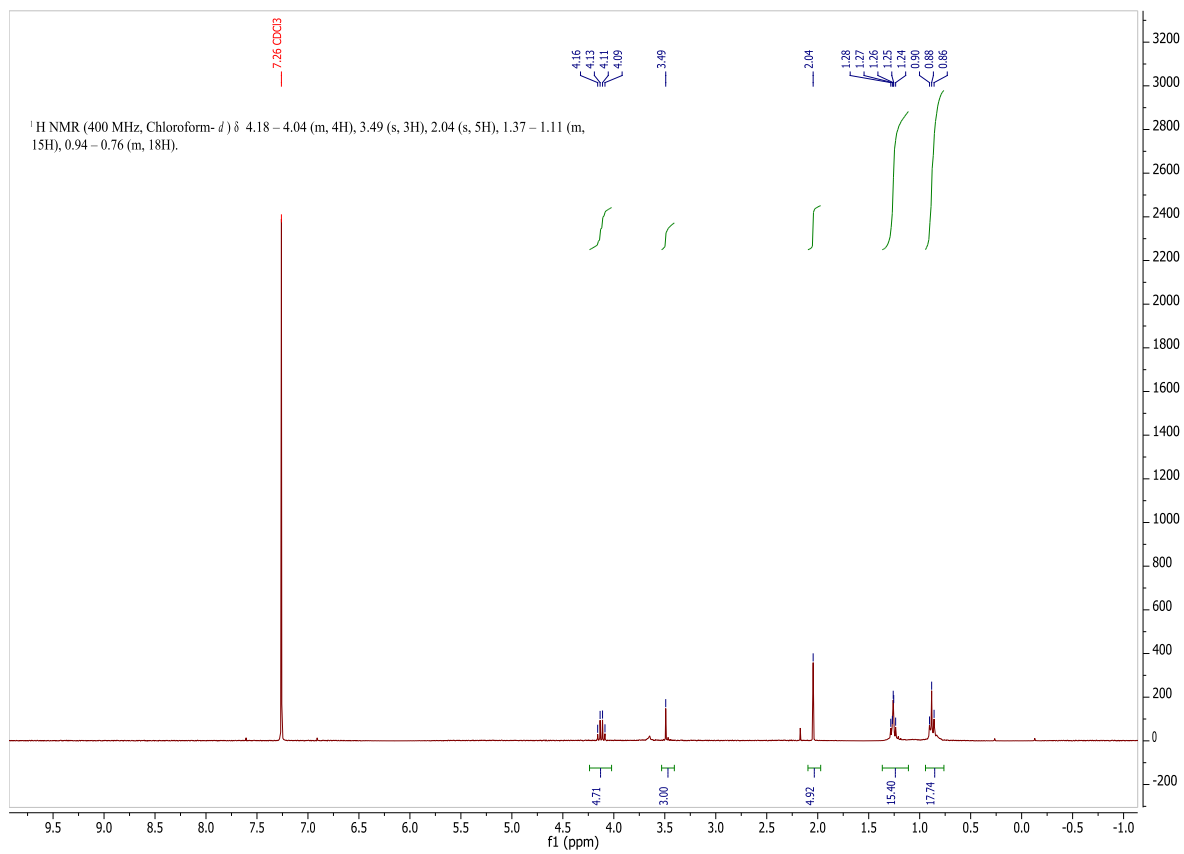
Figure A-25. ¹H NMR spectrum of compound from synthesis 4.2.13.

^{13}C NMR (101 MHz, CDCl$_3$) δ 32.09, 31.06, 29.86, 29.82, 29.52, 22.85, 14.26.
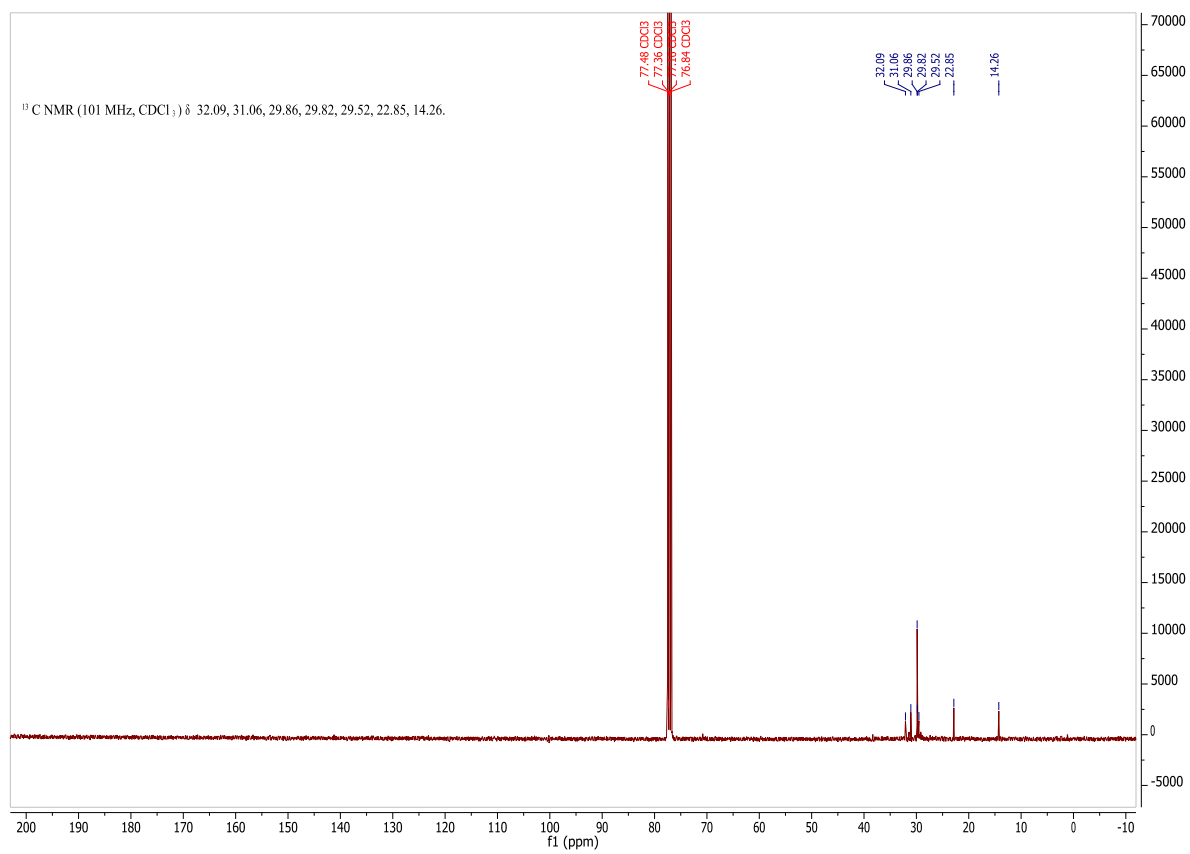
Figure A-26. ^{13}C NMR spectrum of compound from synthesis 4.2.13.

6.2 GC chromatograms

```
Data File C:\CHEM32\1\DATA\TEST\STD TEST278.D
Sample Name:

=====================================================================
Acq. Operator   : SYSTEM
Sample Operator : SYSTEM
Acq. Instrument : 7820 GC                        Location : Vial 1
Injection Date  : 3/21/2016 12:27:09
                                                 Inj Volume : Manually
Acq. Method     : C:\CHEM32\1\METHODS\ANDERS METODER\MARIUS WITTIG.M
Last changed    : 3/21/2016 12:26:10 by SYSTEM
                  (modified after loading)
Analysis Method : C:\CHEM32\1\METHODS\ANDERS METODER\MARIUS WITTIG.M
Last changed    : 2/3/2015 09:03:48 by SYSTEM
Additional Info : Peak(s) manually integrated
```


FID1 B, Back Signal (TEST\STD TEST278.D)
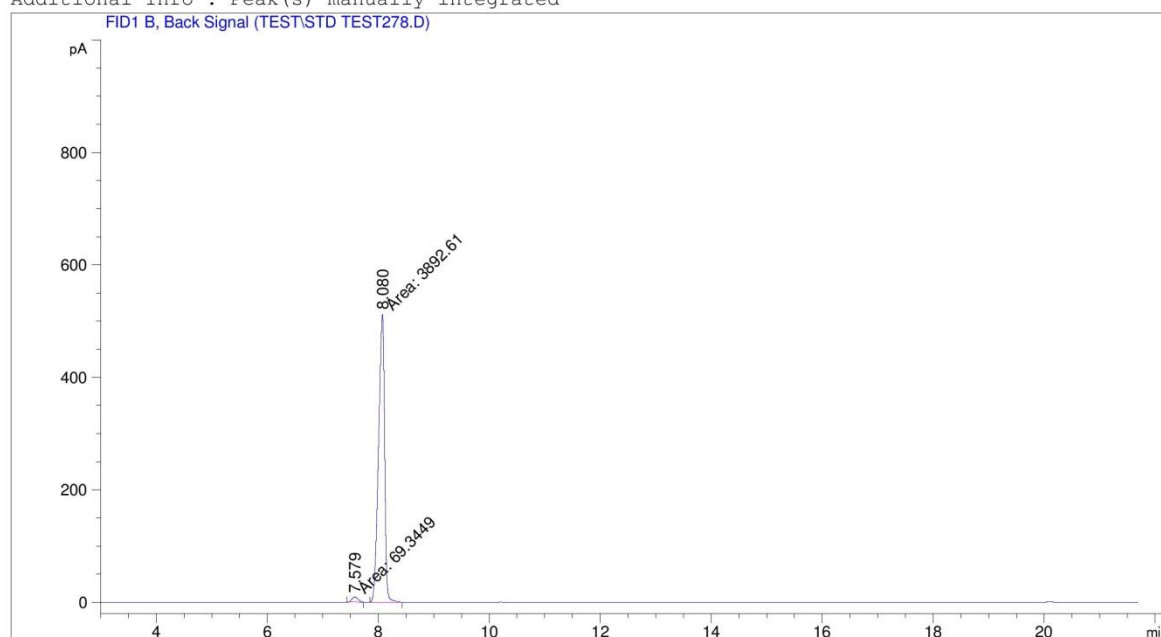
```
=====================================================================
                    External Standard Report
=====================================================================

Sorted By             :      Signal
Multiplier            :      1.0000
Dilution              :      1.0000
Do not use Multiplier & Dilution Factor with ISTDs


Signal 1: FID1 B, Back Signal


=====================================================================
=====================================================================
                    Area Percent Report
=====================================================================

Sorted By             :      Signal
Multiplier            :      1.0000
Dilution              :      1.0000
Do not use Multiplier & Dilution Factor with ISTDs
```

```
Data File C:\CHEM32\1\DATA\TEST\STD TEST278.D
Sample Name:


   Signal 1: FID1 B, Back Signal

   Peak RetTime Type  Width     Area        Height      Area
    #   [min]         [min]    [pA*s]       [pA]         %
   ----|-------|----|-------|----------|----------|--------|
      1   7.579 MM    0.1270   69.34486     9.10218  1.75027
      2   8.080 MM    0.1265 3892.60938   513.01422 98.24973

   Totals :                  3961.95424   522.11641


   =====================================================================
                      *** End of Report ***
```

Figure A-27. GC chromatogram of compound **85**.

6.3 MS spectra of synthesized compounds

MS Spectrum Report

Acquisition Parameter

Source Type	ESI	Ion Polarity	Positive	Set Nebulizer	0.4 Bar
Focus	Not active	Set Capillary	3500 V	Set Dry Heater	200 °C
Scan Begin	50 m/z	Set End Plate Offset	-500 V	Set Dry Gas	4.0 l/min
Scan End	1500 m/z	Set Charging Voltage	2000 V	Set Divert Valve	Waste
		Set Corona	0 nA	Set APCI Heater	0 °C

#	m/z	I %
1	121.0	14.7
2	133.0	13.9
3	135.0	13.9
4	147.0	8.7
5	157.1	19.1
6	164.9	43.1
7	199.0	7.5
8	206.9	11.9
9	216.9	14.6
10	230.9	9.8
11	257.0	14.2
12	271.0	11.6
13	275.2	100.0
14	276.2	19.0
15	298.3	18.8
16	301.1	10.3
17	304.3	14.0
18	326.4	17.6
19	332.3	7.8
20	413.3	10.7

Figure A-28. MS spectrum of compound **85**.
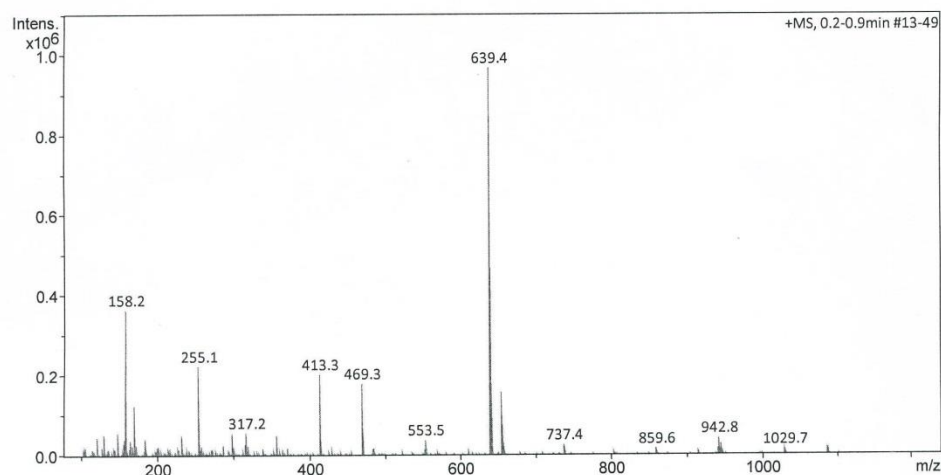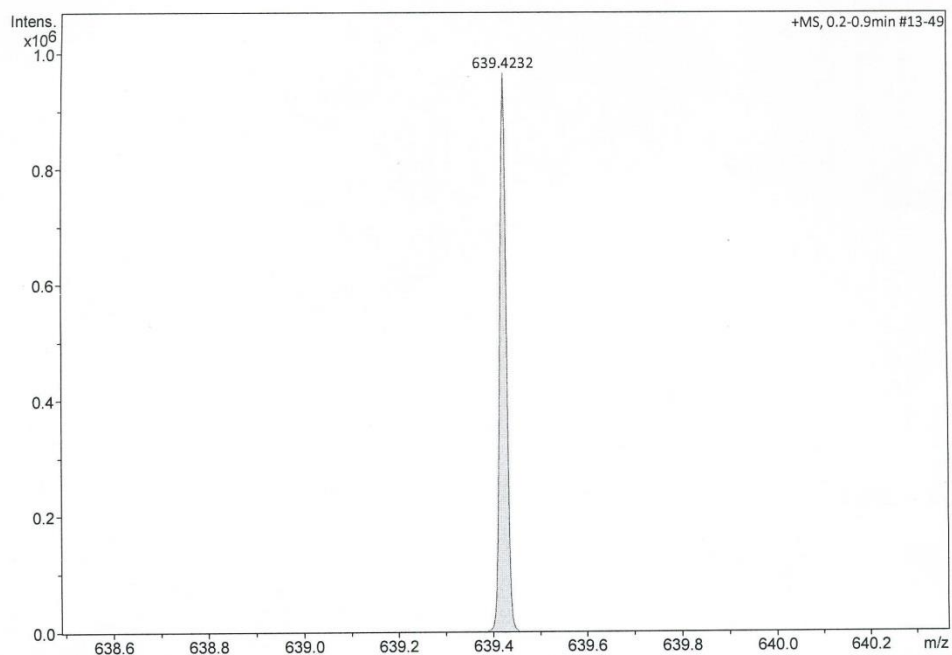
Elemental Analysis Report

Analysis Info
Sample Name

Method   ESI_pos_50_1500.m

Acquisition Date   3/11/2016 8:02:23 AM
Analysis Name   D:\Data\maxis2016\11109.d

Acquisition Parameter

Source Type	ESI	Ion Polarity	Positive	Set Nebulizer	0.4 Bar
Focus	Not active	Set Capillary	3500 V	Set Dry Heater	200 °C
Scan Begin	50 m/z	Set End Plate Offset	-500 V	Set Dry Gas	4.0 l/min
Scan End	1500 m/z	Set Charging Voltage	2000 V	Set Divert Valve	Waste
		Set Corona	0 nA	Set APCI Heater	0 °C
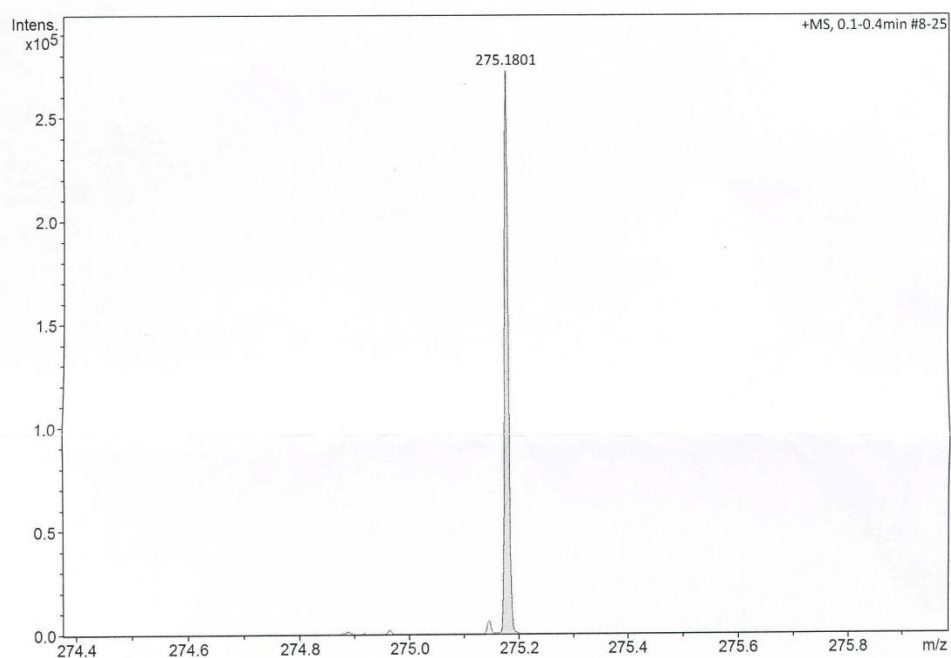
Meas. m/z	Ion Formula	m/z	err [ppm]
275.1801	C12H27N2O3Si	275.1785	-5.6
	C15H28NaOSi	275.1802	0.3
	C21H23	275.1794	-2.4
	C17H27OSi	275.1826	9.0

11109.d
Bruker Compass DataAnalysis 4.3   printed: 3/11/2016 8:11:47 AM   Page 1 of 1

Figure A-29. HRMS spectrum of compound **85**.

MS Spectrum Report

Acquisition Parameter

Source Type	ESI	Ion Polarity	Positive	Set Nebulizer	0.4 Bar
Focus	Not active	Set Capillary	3500 V	Set Dry Heater	200 °C
Scan Begin	50 m/z	Set End Plate Offset	-500 V	Set Dry Gas	4.0 l/min
Scan End	1500 m/z	Set Charging Voltage	2000 V	Set Divert Valve	Waste
		Set Corona	0 nA	Set APCI Heater	0 °C

#	m/z	I %
1	121.0	4.9
2	130.1	5.4
3	148.1	6.0
4	158.2	37.7
5	170.1	12.9
6	185.1	4.3
7	233.1	5.1
8	255.1	23.0
9	299.2	5.8
10	317.2	5.9
11	357.0	5.1
12	413.3	20.9
13	414.3	5.3
14	469.3	18.6
15	470.3	5.8
16	639.4	100.0
17	640.4	48.3
18	641.4	15.3
19	655.4	16.2
20	656.4	7.8

Figure A-30. MS spectrum of compound **96**.

Figure A-31. HRMS spectrum of compound **96**.

MS Spectrum Report

#	m/z	I %
1	135.0	1.2
2	142.2	2.7
3	184.2	0.9
4	186.2	2.5
5	242.3	100.0
6	243.3	18.6
7	244.3	1.5
8	273.2	0.7
9	311.3	0.6
10	353.3	0.7
11	360.3	1.2
12	393.3	0.8
13	397.3	0.7
14	408.3	1.1
15	411.3	1.5
16	413.3	2.5
17	414.3	0.7
18	441.3	1.9
19	442.3	0.6
20	469.3	0.7

Figure A-32. MS spectrum of compound **97**.

Elemental Analysis Report

Meas. m/z	Ion Formula	m/z	err [ppm]
411.2508	C21H35N2O6	411.2490	-4.5
	C24H36NaO4	411.2506	-0.5
	C22H31N6O2	411.2503	-1.2
	C25H32N4Na	411.2519	2.7

Figure A-33. HRMS spectrum of compound **97**.